

**A Proposed Methodology for Estimating Wind Damage to
Residential Slab-Only Claims Resulting from a Hurricane
Impacting the Texas Coastline**

Presented to

**David Mattax
Commissioner
Texas Department of Insurance**

By

TDI Expert Panel

Presiding Officer: James R. (Bob) Bailey, Ph.D., P.E., F. ASCE, Exponent, Inc.

Members: Samuel D. Amoroso, Ph.D., P.E., S.E., M. ASCE, Forte and Tablada, Inc.

William (Bill) Coulbourne, P.E., F. ASCE, Coulbourne Consulting

Andrew Kennedy, Ph.D., M. ASCE, University of Notre Dame

Douglas A. Smith, Ph.D., P.E., F. ASCE, Texas Tech University

April 18, 2016

Table of Contents

Section 1	Executive Summary	1-1
Section 2	Introduction	2-1
Section 3	Overall Methodology.....	3-1
Section 4	Hazard Module – Wind	4-1
	4.1 Background	4-4
	4.2 Hurricane Wind Field Model	4-5
	4.3 Physical Measurements of Wind.....	4-6
Section 5	Hazard Module – Surge and Wave	5-1
	5.1 Background	5-1
	5.2 Surge and Wave Modeling Specifications.....	5-3
	5.3 Physical Measurements of Waves and Surge.....	5-5
	5.4 Surge and Wave Computations and Observations	5-6
Section 6	Damage Estimation Module.....	6-1
	6.1 Introduction.....	6-5
	6.2 Wind Load Development	6-9
	6.2.1 Internal Pressure.....	6-11
	6.2.2 Roof Component and Cladding External Pressures	6-12
	6.2.3 Wall Component and Cladding External Pressures	6-17
	6.2.4 Roof Main Wind Force Resisting System (MWFRS) External Pressures.....	6-21
	6.2.5 Wall Main Wind Force Resisting System (MWFRS) External Pressures.....	6-27
	6.2.6 Gust Effect Factor	6-30

6.3	Performance Functions	6-30
6.3.1	Cladding Element Performance Functions	6-31
6.3.2	Wall Stud Bending Performance Function.....	6-32
6.3.3	Wall Stud to Plate Connection Performance Function	6-33
6.3.4	Roof Frame to Wall Connection Performance Function..	6-33
6.3.5	Shear Wall Performance Function	6-34
6.4	Determination of Component Resistance to Wind Damage	6-35
6.4.1	Roof Cover.....	6-36
6.4.2	Roof Panel.....	6-38
6.4.3	Wall Cover	6-39
6.4.4	Wall Sheathing.....	6-40
6.4.5	Windows	6-40
6.4.6	Doors	6-41
6.4.7	Garage Door	6-42
6.4.8	Wood Stud Bending.....	6-42
6.4.9	Wall Stud Plate Connection	6-44
6.4.10	Roof-to-wall Connection.....	6-44
6.4.11	Shear Wall Capacity	6-46
6.4.12	Summary Resistances	6-47
6.5	Modifications to Resistance Values	6-48
6.5.1	Construction Variability Applicable to All Building Systems.....	6-49
6.5.2	Installation Variability Appropriate for Individual Building Components.....	6-51
6.5.3	Component Variability Associated with Age and Deterioration	6-54
6.6	Interior Damage Predictions	6-56
6.7	Identification of Limitations	6-60
6.8	Example Calculations	6-64

Section 7	Validation of Methodology	7-1
7.1	Qualitative Analysis	7-3
7.1.1	Review of Select Coastal Properties	7-3
7.1.2	Exploratory Analysis of Select Properties Subjected to Hurricanes Katrina (2005) and Ike (2008)	7-5
7.2	Quantitative Analysis	7-10
7.2.1	Hurricanes Charley and Ivan (2004).....	7-10
7.2.2	Hurricanes Rita (2005).....	7-18
7.2.3	Hurricanes Ike (2008).....	7-26
Section 8	Economic Loss Module	8-1
Section 9	Report Generation Module	9-1
Section 10	Summary	10-1
Section 11	Recommendations	11-1
11.1	Proposed Methodology.....	11-1
11.1.1	Essential	11-1
11.1.2	Beneficial	11-2
11.2	Pre-storm Actions.....	11-2
11.3	Post-storm Actions	11-3
11.4	Ongoing Model Validation.....	11-3
Section 12	References	12-1
Section 13	Appendices	13-1
A	Example Calculations	13-2
B	Expert Panel CVs	13-19
C	Sensitivity Analysis of Failure Probability Calculation Techniques.....	13-30

Figures

<u>Figure</u>		<u>Page</u>
2-1	Illustration of “Slab-only” Property versus Surviving Structures	2-2
3-1	Overall Methodology Flowchart.....	3-4
4-1	Hazard Module Flowchart	4-2
4-2	Typical Wind and Water Hazard Time Histories	4-3
4-3	Wind Field Measurements	4-9
5-1	Definition Sketch for Wave and Surge Properties around Buildings	5-2
5-2	Output from a High Resolution Surge and Wave Model	5-5
5-3	Collapse Failure Probabilities from Variant 5 of Tomiczek et al. (2014)...	5-7
6-1	Damage Estimation Module Flowchart.....	6-2
6-2	Roof Component and Cladding Areas and Wind Sectors for a Gable Roof.....	6-13
6-3	Roof Component and Cladding Areas and Wind Sectors for a Hip Roof.....	6-14
6-4	Wall Component and Cladding Areas and Wind Sectors.....	6-19
6-5	Gable Roof Wind Direction Sectors, A through D for MWRFS Loads.....	6-22
6-6	Hip Roof Wind Direction Sectors, A through D, for MWRFS Loads	6-23
6-7a	Nominal MWFRS Windward Roof Pressure Coefficients, Uplift Case, Wind Perpendicular to Ridge	6-25
6-7b	Nominal MWFRS Windward Roof Pressure Coefficients, Gravity Case, Wind Perpendicular to Ridge	6-25
6-8a	Nominal MWFRS Leeward Roof Pressure Coefficients, Uplift Case, Wind Perpendicular to Ridge	6-26
6-8b	Nominal MWFRS Leeward Roof Pressure Coefficients, Gravity Case, Wind Perpendicular to Ridge	6-26
6-9	Variation of Leeward Wall MWFRS C_p with Building Plan Aspect Ratio, L/B	6-28

6-10	MWFRS Wall Numbers, 1 – 4, with respect to Four Wind Direction Sectors, A – D.....	6-29
6-11	Illustration of Relative Roof Cover Damage to Residential Structures	6-61
6-12	Residential Structural Features	6-64
6-13	Hazard Time History	6-65
6-14	Estimation of Wind Damage.....	6-66
7-1	Damaged Properties following Hurricane Ike in 2008.....	7-1
7-2	Surviving and Slab-only Structures along Lake Pontchartrain	7-4
7-3	Representative Surviving and Slab-only Structures.....	7-6
7-4	Florida Citizens Policy Sampling	7-11
7-5	Variability of Modeled Wind Damage Results over a Variety of Wind Speeds	7-12
7-6	Locations of Randomly Sampled TWIA Hurricane Ike Property Claims...	7-26
7-7	Rate of TWIA Property Insurance Claims versus Wind Speed for Hurricane Ike	7-27
7-8	Observed versus Predicted Roof Cover Damage.....	7-29
7-9	Observed versus Predicted Roof Panel Damage	7-29
7-10	Observed versus Predicted Wall Cover Damage	7-30
7-11	Observed versus Predicted Wall Panel Damage.....	7-30
7-12	Observed versus Predicted Window Damage	7-31
7-13	Observed versus Predicted Door Damage.....	7-31
7-14	Observed versus Predicted Garage Door Damage	7-32
7-15	Observed versus Predicted Interior Finish Damage	7-32
8-1	Economic Loss Module Flowchart.....	8-2
9-1	Report Generation Module Flowchart.....	9-1

Tables

<u>Table</u>	<u>Page</u>
6-1	EXPOSURE FACTOR STATISTICS 6-10
6-2	INTERNAL PRESSURE COEFFICIENT STATISTICS..... 6-12
6-3	GABLE ROOF COMPONENT AND CLADDING PRESSURE ZONE ASSIGNMENTS AS A FUNCTION OF WIND ANGLE OF ATTACK..... 6-15
6-4	HIP ROOF COMPONENT AND CLADDING PRESSURE ZONE ASSIGNMENTS AS A FUNCTION OF WIND ANGLE OF ATTACK..... 6-16
6-5	ROOF COMPONENT AND CLADDING EXTERNAL PRESSURE COEFFICIENT STATISTICS 6-17
6-6	WALL COMPONENT AND CLADDING PRESSURE ZONE ASSIGNMENTS AS A FUNCTION OF WIND ANGLE OF ATTACK (AOA)..... 6-19
6-7	WALL COMPONENT AND CLADDING EXTERNAL PRESSURE COEFFICIENT STATISTICS 6-20
6-8	GABLE ROOF MWFRS SURFACE CLASSIFICATIONS FOR FRAME LINES WITH RESPECT TO WIND ANGLE OF ATTACK (AOA)..... 6-24
6-9	HIP ROOF MWFRS SURFACE CLASSIFICATIONS FOR FRAME LINES WITH RESPECT TO WIND ANGLE OF ATTACK (AOA)..... 6-24
6-10	NOMINAL MWFRS ROOF PRESSURE COEFFICIENTS FOR SLOPE LESS THAN 10 DEGREES OR WIND PARALLEL TO RIDGE 6-27
6-11	ROOF MWFRS EXTERNAL PRESSURE COEFFICIENT STATISTICS . 6-27
6-12	MWFRS WALL CLASSIFICATIONS AS WINDWARD (WW), SIDE (SW), OR LEEWARD (LW) WITH RESPECT TO WIND DIRECTION SECTOR 6-29
6-13	WALL MWFRS EXTERNAL PRESSURE COEFFICIENT (C_p) STATISTICS 6-29
6-14	GUST EFFECT FACTOR, G, STATISTICS 6-30
6-15	F_B DESIGN VALUES 6-43
6-16	ROOF-TO-WALL ULTIMATE RESISTANCE VALUES (LBS)..... 6-46
6-17	SUMMARY OF RESISTANCES AND COVs USED IN TWIA DAMAGE ESTIMATION MODULE..... 6-47
6-18	CONSTRUCTION VARIABILITY..... 6-50

6-19	INSTALLATION VARIABILITY APPROPRIATE FOR INDIVIDUAL BUILDING COMPONENTS	6-52
6-20	INSTALLATION COMPONENT VARIABILITY RESULTS.....	6-54
6-21	INSTALLATION COMPONENT VARIABILITY RESULTS FOR AGE INTERVALS.....	6-55
6-22	WIND DAMAGE TO COMPONENTS FOR SURVIVING STRUCTURE..	6-59
6-23	WIND DAMAGE TO COMPONENTS FOR SLAB-ONLY STRUCTURE..	6-59
6-24	ESTIMATED ROOF COVER DAMAGE FOR ILLUSTRATIVE EXAMPLE	6-62
7-1	VALIDATION SUMMARY	7-2
7-2	DAMAGE ESTIMATION MODULE COLLAPSE PROBABILITY RESULTS FOR 21 SELECTED PROPERTIES	7-9
7-3	CLAIMS FILE REVIEW RESULTS: ROOF COVER	7-13
7-4	CLAIMS FILE REVIEW RESULTS: ROOF PANEL	7-14
7-5	CLAIMS FILE REVIEW RESULTS: WALL COVER.....	7-14
7-6	CLAIMS FILE REVIEW RESULTS: WALL SHEATHING.....	7-15
7-7	CLAIMS FILE REVIEW RESULTS: WINDOWS.....	7-15
7-8	CLAIMS FILE REVIEW RESULTS: DOORS.....	7-16
7-9	CLAIMS FILE REVIEW RESULTS: GARAGE DOORS.....	7-16
7-10	CLAIMS FILE REVIEW RESULTS: ROOF FRAMING	7-17
7-11	CLAIMS FILE REVIEW RESULTS: INTERIOR FINISHES.....	7-17
7-12	SELECT TWIA POLICIES.....	7-18
7-13	RITA CLAIMS FILE REVIEW RESULTS: ROOF COVER.....	7-21
7-14	RITA CLAIMS FILE REVIEW RESULTS: ROOF PANEL	7-22
7-15	RITA CLAIMS FILE REVIEW RESULTS: WALL COVER.....	7-22
7-16	RITA CLAIMS FILE REVIEW RESULTS: WALL SHEATHING.....	7-23
7-17	RITA CLAIMS FILE REVIEW RESULTS: WINDOWS.....	7-23
7-18	RITA CLAIMS FILE REVIEW RESULTS: DOORS.....	7-24
7-19	RITA CLAIMS FILE REVIEW RESULTS: GARAGE DOORS.....	7-24
7-20	RITA CLAIMS FILE REVIEW RESULTS: ROOF FRAMING	7-25
7-21	RITA CLAIMS FILE REVIEW RESULTS: INTERIOR FINISHES.....	7-25
7-22	OBSERVED DAMAGE RATIOS FROM TWIA HURRICANE IKE CLAIMS	7-28

1 Executive Summary

In 2013 the Texas Department of Insurance (TDI) assembled an Expert Panel under Insurance Code §2210.578 and 28 Texas Administrative Code §§5.4260-5.4268. The purpose of the Panel is “to advise TWIA concerning the extent to which a loss to insurable property was incurred as a result of wind, waves, tidal surges, or rising waters not caused by waves or surges.

The Panel subsequently recommended a methodology to the Commissioner for predicting the portion of damage sustained by residential properties due to wind for cases where only the foundation or a portion thereof remains after a hurricane. These properties, sometimes referred to as “slab” or “slab-only” claims, arise when forces caused by a tropical cyclone are sufficient to destroy a residential superstructure. For cases where partial buildings remain, the Panel recommends that an adjuster or engineer be sent to the site for purposes of determining building damage by hazard type. The predicted damage is the result of wind, waves, and tidal surge effects. Damage resulting from rising waters not caused by waves or surges (i.e., riverine or localized flooding) is not addressed at this time as such a scenario does not typically result in a slab-only claim.

Two key components of the proposed methodology are a Hazard Module and a Damage Estimation Module. The Hazard Module provides information about the highest wind speeds and the greatest storm surge depths along with time histories of the event, including the times when the peaks were experienced. The Damage Estimation Module calculates the probability of failure of various building components and structural systems during the progress of the storm.

The storm surge vulnerability is represented as a probability of total collapse based on the hazard, site, and building properties. The proposed methodology also enables development of more accurate damage estimates by including refinement of model results with observational results, or with building-specific component information regarding resistance to wind failure. The model results for wind provide percent damage estimates for the building components using probability theory to construct failure

probabilities based on ultimate calculated wind pressures and researched ultimate component or connection resistances. TWIA or its insurance adjustment professionals are then able to use the percent damage estimates to determine financial losses and insurance policy payouts.

Use of the proposed methodology, as with any potential method for estimating damage caused by a natural hazard, comes with several limitations regarding its application to various building types and configurations, and also regarding model configuration which can influence error in the results. An effort was made to validate the model results using claims data from Hurricanes Ike and Rita in Texas, Hurricane Katrina in Louisiana and Mississippi, and Hurricanes Charley and Ivan in Florida. Recommendations are also provided for model data needs, on how to obtain such data, and for long term model enhancements.



2 Introduction

In 2013 the Texas Department of Insurance (TDI) assembled an Expert Panel under Insurance Code §2210.578 and 28 Texas Administrative Code §§5.4260-5.4268. The purpose of the Panel is to advise TWIA concerning the extent to which a loss to insurable property was incurred as a result of wind, waves, tidal surges, or rising waters not caused by waves or surges. The Texas Insurance Commissioner will consider the recommended methodology of the Panel prior to publishing guidelines for TWIA to use in the adjustment of claims.

This document describes a methodology that the Panel recommends to the Commissioner for predicting the portion of damage sustained by residential properties due to wind for cases where only the foundation or a portion thereof remains after a hurricane. As illustrated in Figure 2-1, these properties are sometimes referred to as “slab” or “slab-only” claims. They arise when forces caused by a tropical cyclone are sufficient to destroy a residential superstructure.

For cases where the residential superstructure survives, the Panel recommends that an on-site assessment by a field adjuster or engineer be the preferred method for adjusting the claim. It is the opinion of the Panel that, when physical evidence of the structure remains, the judgment of a field adjuster or engineer will far exceed the ability of the recommended methodology (which is based on probabilistic methods and accompanying statistics) to determine the cause and extent of storm damage.

The methodology combines existing technologies and procedures to: (1) establish the hazard levels for any tropical storm affecting the Texas coast in future hurricane seasons; (2) consider how any property’s construction characteristics affect the vulnerability of subject properties to damage; and, (3) estimate the consequences of the event in terms of percent damage to specific components and structural systems of the property. Each of these steps requires substantial planning, careful preparation, and the mobilization of significant resources on the part of the Texas Windstorm Insurance Association (TWIA) to effectively execute the Panel’s recommendations after a tropical cyclone impacts the Texas Coastline.

It is assumed that the reader has some background in wind engineering, as it would be beyond the scope of this document to describe the concepts contributing to the methodology by starting from fundamental principles (see Peraza et al, 2014). Panel member curriculum vitae (CVs) are provided in the Appendices.



Figure 2-1: Illustration of “Slab-only” Property versus Surviving Structures
(Photograph courtesy of Andrew Kennedy)

3 Overall Methodology

Figure 3-1 is a flowchart illustrating the overall structure of the methodology recommended by the Panel. The principal modules of the flowchart are (1) Property Database; (2) Hazard; (3) Damage; (4) Economic Loss; and (5) Report Generation. While there is some allowance for recursion within the process illustrated by the flowchart, acquiring results from the methodology requires a more or less step-by-step progression through each of the modules.

The Property Database must be developed and populated prior to a storm. This database will include structure characteristics pertinent to the performance of each subject property in a tropical cyclone. The Hazard Module includes a blend of up-front and operational activities that yield time histories of gust wind speed, wind direction, storm surge elevation, significant wave height, and wave period at each property considered by the model. The Damage Estimation Module combines the information housed in the Property Database with the hazard time histories to produce corresponding time histories of component wind damage and the probability of structural collapse due to the effects of wind and storm surge and waves. The Economic Loss Module transforms the physical damage estimates into monetary losses. The Report Module summarizes the results of the analysis.

The Panel recommends that probabilistic methods for predicting damage to a residential property be used for cases in which only the foundation, or a portion of the foundation, remains after a storm. Mentioned earlier, such cases are sometimes referred to as “slab” or “slab-only” claims. The proposed methodology should be applied only when a competent engineer cannot determine the extent of water versus wind damage based on what is left of the surviving superstructure. For cases in which there is a surviving superstructure, the Panel recommends that an assessment by a field adjuster or engineer be the method for adjusting the claim. Figure 2-1 shows the distinction between these two damage states.

The preference for field adjustments of surviving structures is based on the Panel's familiarity with current methods for predictive modeling of storm damage, including the method recommended in this report. For cases in which there is a surviving superstructure, the Panel is confident that on a case-by-case basis, the training, experience, and judgment of a field adjuster or engineer will be more accurate than a predictive model. The predictive approach to modeling storm losses is best applied when there is limited physical evidence on which to base an assessment of the cause and timing of damage.

The Panel may eventually produce a parallel set of recommendations to guide field damage assessments of surviving structures. Over time, the range of application of predictive damage models could be extended as research in this field advances. However, the recommended method will still produce information such as property-specific data and hazard time histories that will be helpful in the field assessment and adjustment of surviving structures. At this time, the Panel has not developed or proposed methods for estimating damage to ancillary structures such as fences and outbuildings.

The Panel understands that TWIA insures commercial properties in addition to residential structures. However, commercial construction is not addressed in the present recommendations. Another potential limitation on the appropriate use of a predictive model is the apparent cause of damage. If it is clear by the evidence that a structure was only damaged by wind and not by storm surge or waves, then the use of a model may not be required or helpful. Examples include a residence located outside of the surge zone.

In an effort to determine the reliability of the recommended methodology, the Panel reviewed individual claim files from recent hurricanes that affected the U.S. Gulf Coast. Damage to individual components and structural systems was estimated based on photographs and adjustment reports included in the files. While comparing model results to actual claim data would appear to be a straightforward way to measure model reliability, claim data itself has variability, especially if they are represented as the aggregate of the loss and do not represent component-level damage. For example, developers of the Florida Public Hurricane Loss Model found significant variation in

claims data across insurance companies when controlling for wind speed and general construction type. Though an undisputed insurance adjustment can accurately reflect the economic loss incurred by an insurer, it may not be a true representation of the physical damage.

In summary, limitations on the use of the model may be based on whether or how much of a structure remains; how many hazard types affected the structure; whether it is a commercial or residential structure; or the construction type. Predictive models are recommended in circumstances in which it is the Panel's professional opinion that they are more reliable than field adjustments or assessments. Otherwise, field adjustments or assessments are recommended.

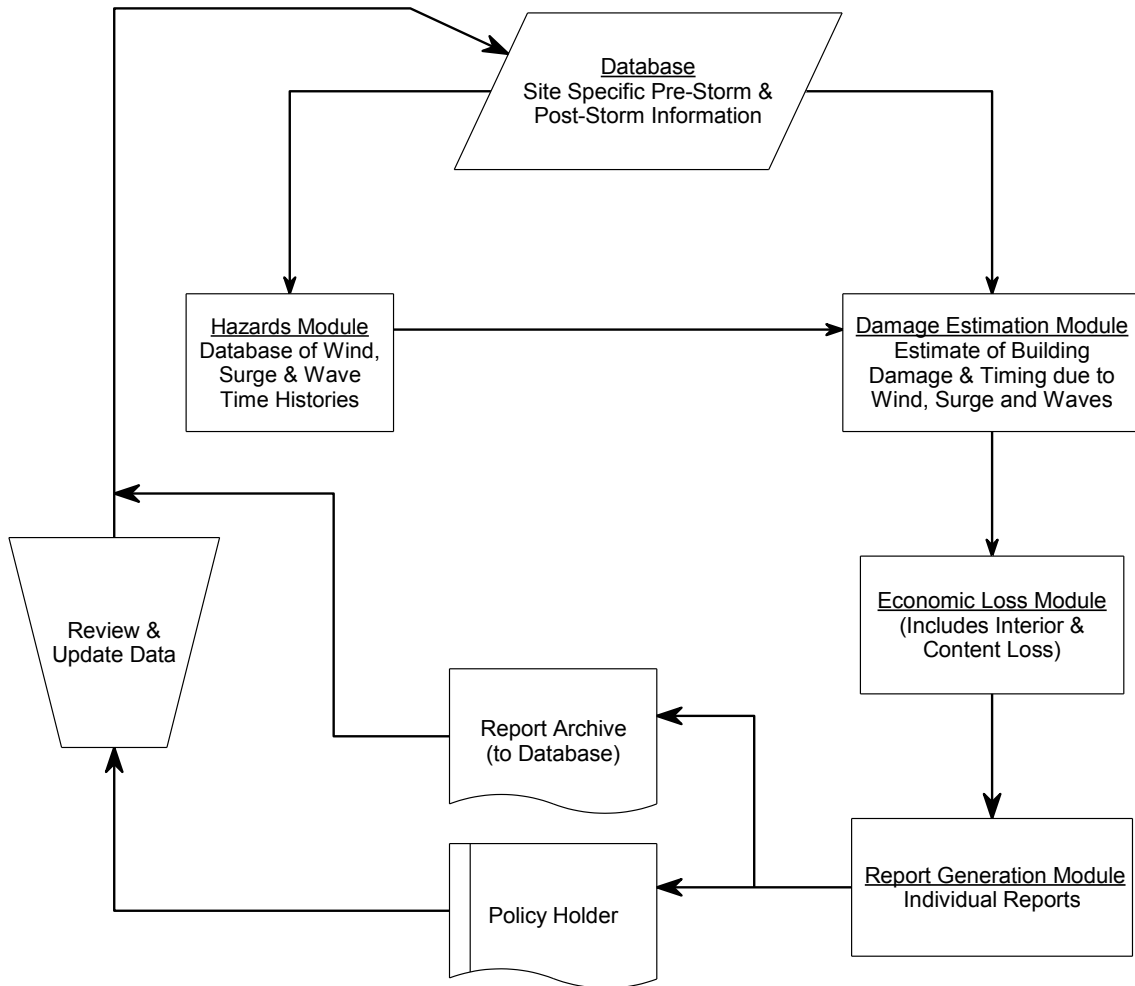


Figure 3-1: Overall Methodology Flowchart

4 Hazard Module – Wind

The Hazard Module shown in Figure 4-1 is designed to generate site specific wind speed and direction time histories along with storm surge and wave time histories. These histories are synchronous for a specific property insured by TWIA. As illustrated in Figure 4-1, the two main components of the Hazard Module are a hurricane wind field model, and storm surge and wave model. A key feature of the two models is that they must work together, meaning the wind field model is used to drive the storm surge and wave model. The data requirements and results from these two models must therefore be compatible and consistent.

The two models produce their estimates of the hazard intensities and timing based on a combination of numerical simulation, actual measurements of storm-related data from field instrumentation, and post-event observations. The time histories should have a minimum of error as compared to physical measurements collected during the hurricane. An exemplar time history of the two model components is shown in Figure 4-2.

This section of the report addresses the wind hazard component of the Hazard Module. Section 5 addresses the surge and wave hazard component. Once generated, the time histories are then used to estimate damage to the property. Discussed in Section 6, this Damage Estimation Module establishes both the timing of individual building component damage, and the time that the structure was likely destroyed and by which hazard.

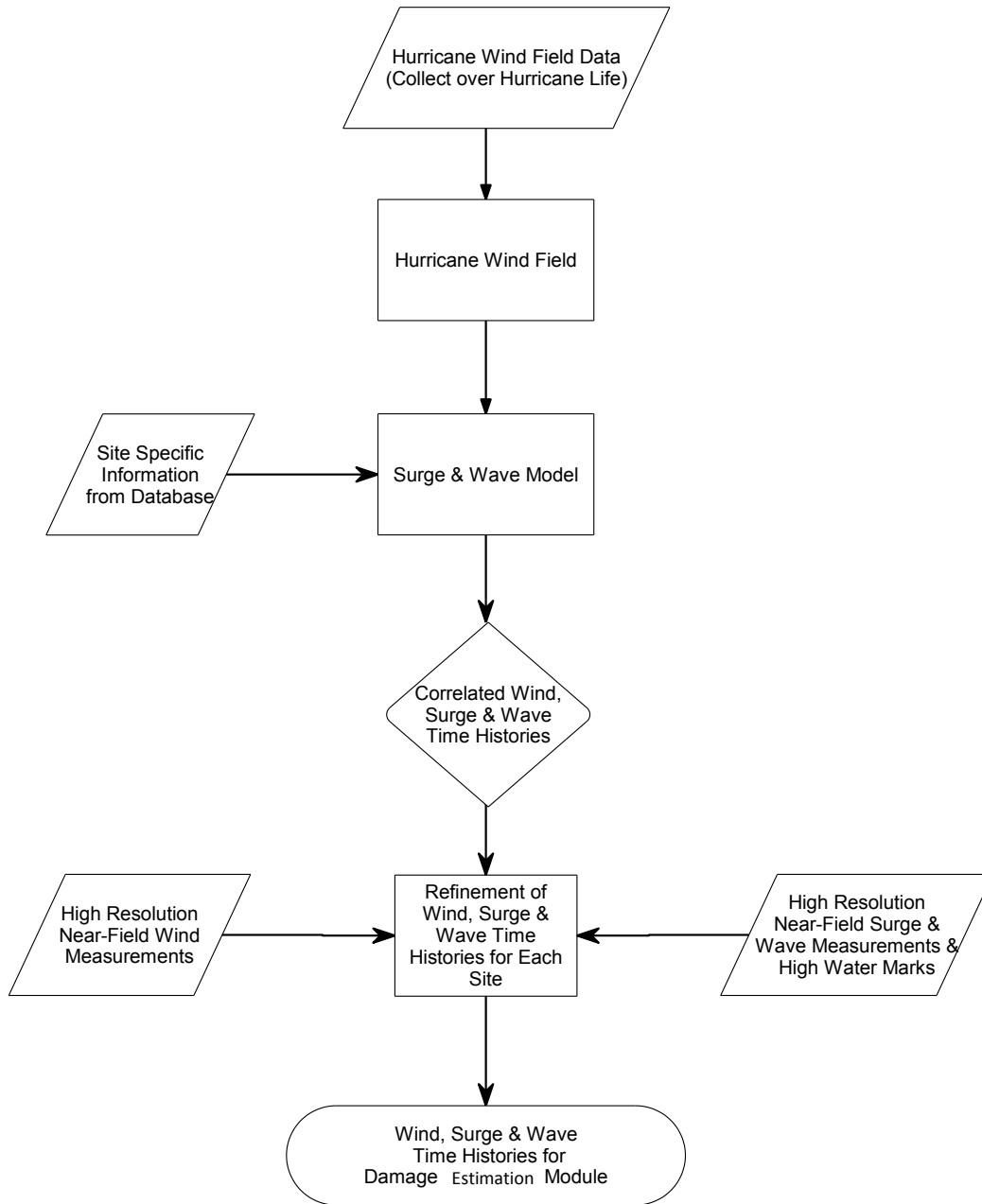


Figure 4-1: Hazard Module Flowchart

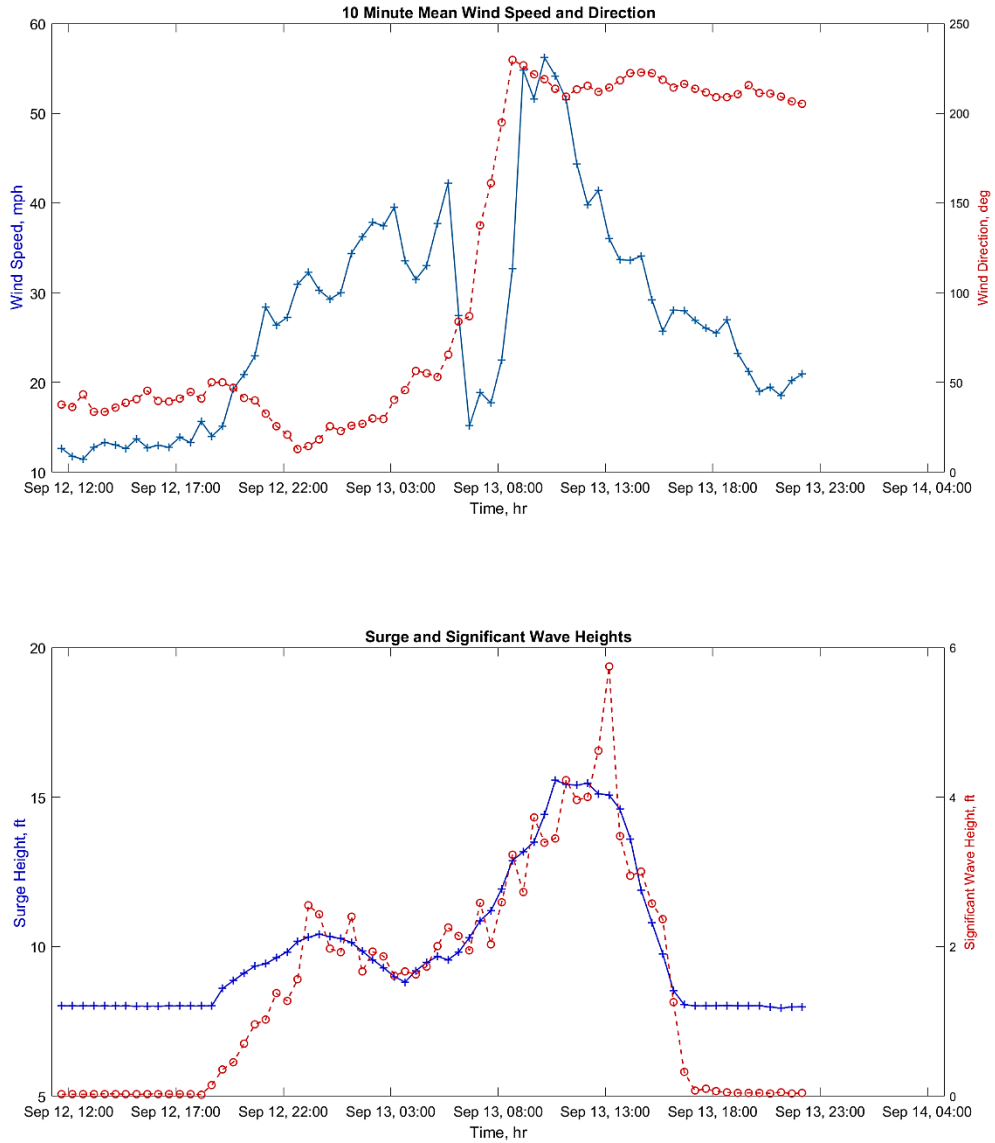


Figure 4-2: Typical Wind and Water Hazard Time Histories

4.1 Background

The wind field model serves two purposes: (1) provide site specific wind speed and wind direction time histories that are used for wind damage prediction; and, (2) provide a wind field that can be used as input for a surge and wave model that outputs time histories for surge and wave damage prediction. These time histories are produced as a hindcast (as opposed to a forecast) and thus can use all of the post-storm validated data that is available.

The required scales of the wind field for these two purposes can be vastly different. The wind field required for accurate surge modeling requires a description of the wind field over a time period of many days before hurricane landfall and a spatial scale the size of the Gulf of Mexico. Site specific wind speeds and directions can also be developed using a shorter temporal scale and a smaller spatial scale (possibly defined only over an area of interest limited to the area encompassing where total destruction of structures exists). Although a single wind field model to achieve both purposes simplifies logistics in the overall methodology, two separate models can be used, one for each purpose.

The overarching goal in the Hazard Module is to produce spatially and temporally correlated wind and surge time histories that have minimum error at each specific slab site. In this case, error is defined as the difference between values predicted from models and values measured during the hurricane (e.g., wind speeds predicted by the model at a point in space and time minus the wind speed measured at the same point in space and time).

Wind field models can be classified as: Parametric, Observational, and Dynamical Numerical Weather Prediction (NWP). Parametric models are relatively easy to use and require minimal computational power. These models project radial wind profiles based on various input parameters relating to the size and strength of a given storm. Examples of parametric models include the Holland Model (Holland, 1980), the modified Holland Models (Holland, 2008), and the Willoughby Model (Willoughby 2006).

Observational models directly incorporate surface wind speed measurements to construct wind fields often through the use of objective analysis schemes. Large scale observational models include proprietary models offered by HWind Scientific,

Oceanweather, Inc., and Weatherflow. Small scale models like the one produced by NSS (NSS Wind Field Analysis) to model the wind field produced by Hurricane Ike over a small region where houses were completely destroyed is also an observational model. Observational models can be embedded in larger models for the purposes of storm surge modeling, if necessary.

Dynamical NWP models utilize sophisticated equation sets representing the underlying physics to construct hurricane wind fields over a broad range of domain sizes, but also require significant computational resources. These models include: the Hurricane Weather Research and Forecasting (HWRF) model that uses a nested grid system and the Global Forecasting System global model as its initial conditions; and the Geophysical Fluid Dynamics (GFDL) Hurricane model, a regional triply-nested model that also uses the Global Forecasting System to provide its global boundary conditions.

4.2 Hurricane Wind Field Model

Three model classes were considered by this review. Parametric models can be run very quickly and with any desired spatial resolution. However, a wind field developed by these models is dictated by parameters governing the radial wind speed profile shape, which is subject to large error for tropical cyclones with asymmetric or atypical wind fields, or that contain multiple wind maxima. Observational models utilize atmospheric observations to drive their wind field analyses. As long as adequate observations exist, these models can account for tropical cyclone asymmetries and concentric wind maxima with the spatial and temporal resolution desired with acceptable computational requirements. Dynamical NWP models provide sophisticated, three-dimensional wind fields, but lack the desired spatial and temporal resolution at this time and require significant computational capability.

After reviewing the details of several models used to construct tropical cyclone wind fields, the Panel concluded that an observational model provides the best option for constructing a wind field to drive a storm surge model for the desired application. The observational model chosen must minimize errors between: (a) the observed wind speeds and directions measured during the storm; and, (b) the observed storm surge and wave heights measured during the hurricane.

An increase in available surface wind and surge measurements is vital to producing more accurate wind and water assessments for coastal regions directly impacted by landfalling tropical cyclones. Should a more robust network of surface observations become available, a localized wind field (such as the NSS WFA) is recommended for the damage prediction portion of the methodology. The localized wind field must focus on the most relevant areas at the coastal interface. The localized wind field thus complements the broader observational model wind field with a more detailed, higher-resolution (spatial and temporal) wind field.

The Panel recommends that TWIA procure a contract with a private firm, a university, a government agency, or some partnership thereof to provide the hazard time histories. It would be preferable that multiple organizations compete for this contract. For TWIA to select the team, the wind speeds and directions estimated by the various competing observational models should be compared to field measurements. This process would include the reproduction of the wind fields using the various models/methodologies, and a comparison of the generated data fields (wind speed, wind direction) with available measurements at several locations where they are available (e.g. surface observation platforms). This comparison will highlight the strengths and weaknesses of the various models while providing an example of the errors that can be expected in the generated wind fields. As mentioned earlier, the wind field model must be compatible with the surge and wave model described in Section 5.

4.3 Physical Measurements of Wind

The physical measurements of wind can be categorized into direct measurement and indirect measurement. Direct measurements of wind speed and wind direction are made by anemometers and wind vanes or sonic anemometers. These instruments are mounted on various platforms including mobile platforms (for example StickNet, WEMITE, or Florida Coastal Monitoring Program towers) which are transported and set up in the path of an oncoming hurricane. These measurement platforms provide high quality real-time data that can be used both for forecasting and producing post-storm wind field hindcasts. These datasets are excellent for providing ground truth for the wind field models and for establishing estimates of the errors in the model results.

Fixed surface level assets that provide wind speed and direction measurements include those collected by:

1. NDBC/NOS – National Data Buoy Center/National Ocean Service
<http://www.ndbc.noaa.gov>;
2. ASOS – Automated Surface Observation System
<http://www.nws.noaa.gov/asos/>;
3. TCOON – Texas Coastal Ocean Observation Network
<http://www.cbi.tamucc.edu/TCOON/>; and
4. RAWS – Remote Automatic Weather Stations <http://raws.fam.nwcg.gov>.

These platforms are good auxiliary sources of data for the models. However, they may be subject to a loss of power (and thus their data) during a hurricane. Indirect measurements of wind speed include those made by:

1. Dropsondes which record their GPS coordinates in time from which wind speeds can be computed
<http://www.af.mil/News/ArticleDisplay/tabid/223/Article/601582/tech-report-dropsonde.aspx>; and
2. SFMR – Stepped-Frequency Microwave Radiometer which measures the microwaves generated by the foam on the ocean surface during a hurricane
<http://www.403wg.afrc.af.mil/library/factsheets/factsheet.asp?id=8314>.

Observational models are dependent upon wind speed and direction measurements to produce accurate model results for both the surge and wave models and for the wind field model. As a result of this dependence, the Panel recommends that TWIA commission additional mobile platforms to increase the volume and resolution of the potential measurements. A spacing of three to five miles in the eyewall region is desirable. The spacing can be increased to 10 miles in the outer regions of the hurricane. Two layers of platforms are also desirable, with the first layer in close proximity to the coastline and the second layer about 20 miles inland. Between 40 and 60 mobile platforms are required to make a deployment with this resolution.

Mobile platforms are preferable over fixed platforms since they can be positioned at strategic locations in the storm path when the storm is close to landfall. Fixed platforms may or may not be in the best position relative to the storm path to supply wind speed information for wind field modeling. Relying on fixed platforms for wind data also

requires a much larger number of them being installed along the Texas coastline to provide the same coverage across the width of a hurricane.

If sufficient mobile platforms are deployed along the coast in front of a landfalling hurricane, then a high resolution wind field with small errors (one to two percent of the maximum sustained wind measured in a 30 minute period) can be developed for use in wind damage prediction. If these instruments are co-located with surge sensors, then a robust description of the wind and surge field during hurricane landfall based on direct measurement is possible. Such a combined measured hazard dataset will minimize the errors in estimating the wind speeds, wind directions, surge heights, and wave heights used to predict damage to the structures. It will also improve the prediction of the timing and the amount of damage that occurs. Figure 4-3 shows an example of field instrumentation used to measure wind speeds and the resulting record taken during Hurricane Ike in 2008.

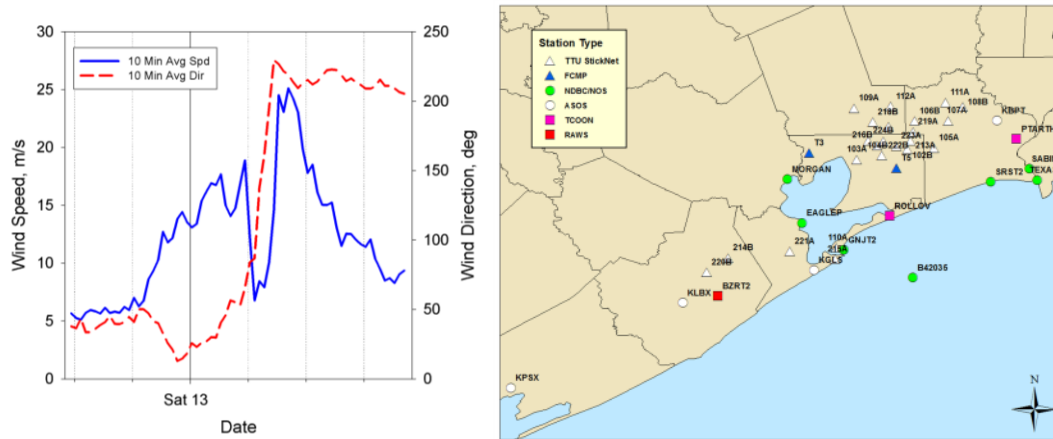
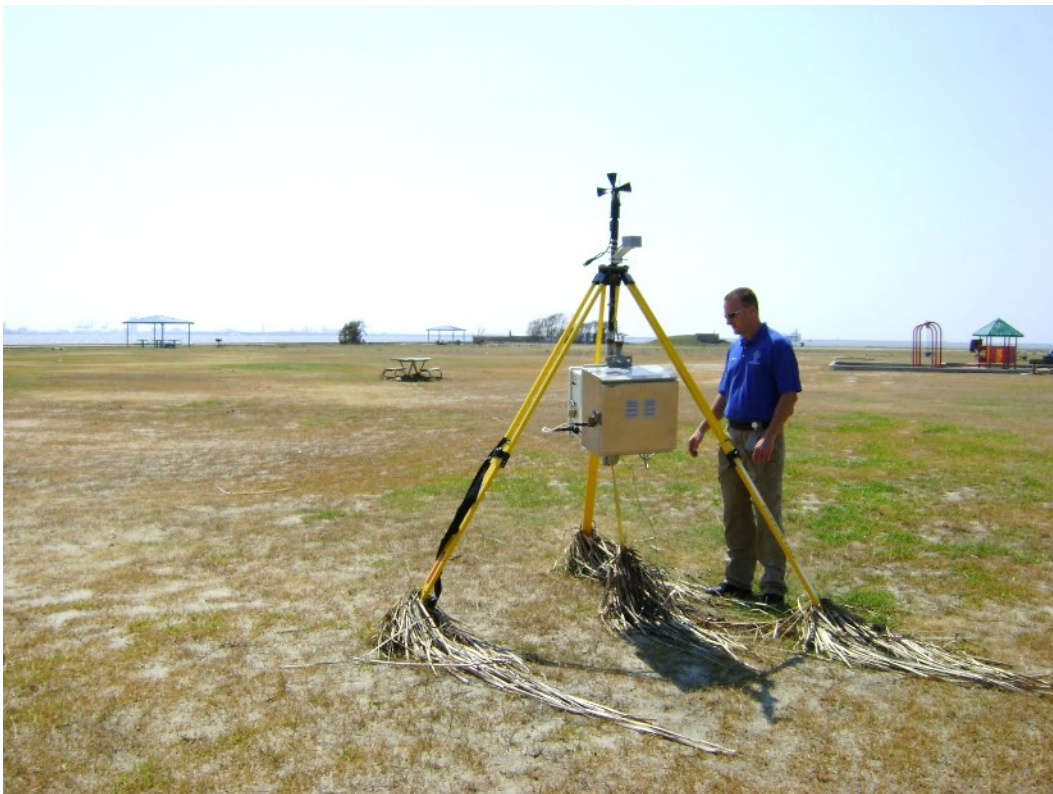


Figure 4-3: Wind Field Measurements
 (Source: Texas Tech University Hurricane Research Team)

5 Hazard Module – Surge and Wave

5.1 Background

Although TWIA insures only against wind damage and not surge damage, disputes over the cause and timing of damage have been the source of much friction, particularly in slab cases where there is little to no structure remaining to provide information regarding the cause and extent of damage. Waves and storm surge are well-known to cause great damage in many coastal regions as seen in Hurricanes Katrina, Ike, and many other tropical cyclones. For this reason, information about the magnitude and timing of storm surge and waves in hurricane-affected regions, and their ability to destroy structures, are vital to the speedy and equitable resolution of claims. Thus, the proposed methodology will include measurements and modeling of waves and surge in affected coastal areas. It will also estimate their potential for complete destruction of coastal residences and compare this estimate to the potential for wind destruction.

To understand storm surge and waves, it is first necessary to define these processes. In a storm-inundated region, the water surface is continuously moving. These movements have different time scales, in that the motion of the water can be separated into relatively quickly-changing motions and slowly-changing motions. During a storm, the slowly varying component of water level over any 10 minute period is the **storm surge** (see Figure 5-1). Storm surge only changes on relatively slow scales: it is defined by the **storm surge elevation**, and has associated **currents**, or water velocities.

All elevations are measured from a zero-elevation, called a datum. Elevations above this datum are positive, and below this datum are negative. For storm surge over flooded terrain, the North American Vertical Datum of 1988 (NAVD88) is usually the appropriate datum. Surge elevations and currents will change slowly over the course of the storm. Measured storm surge elevations will also include some component of the **astronomical tides**, which occur in the absence of storms. The difference between the surge elevation and the ground elevation gives the water depth.

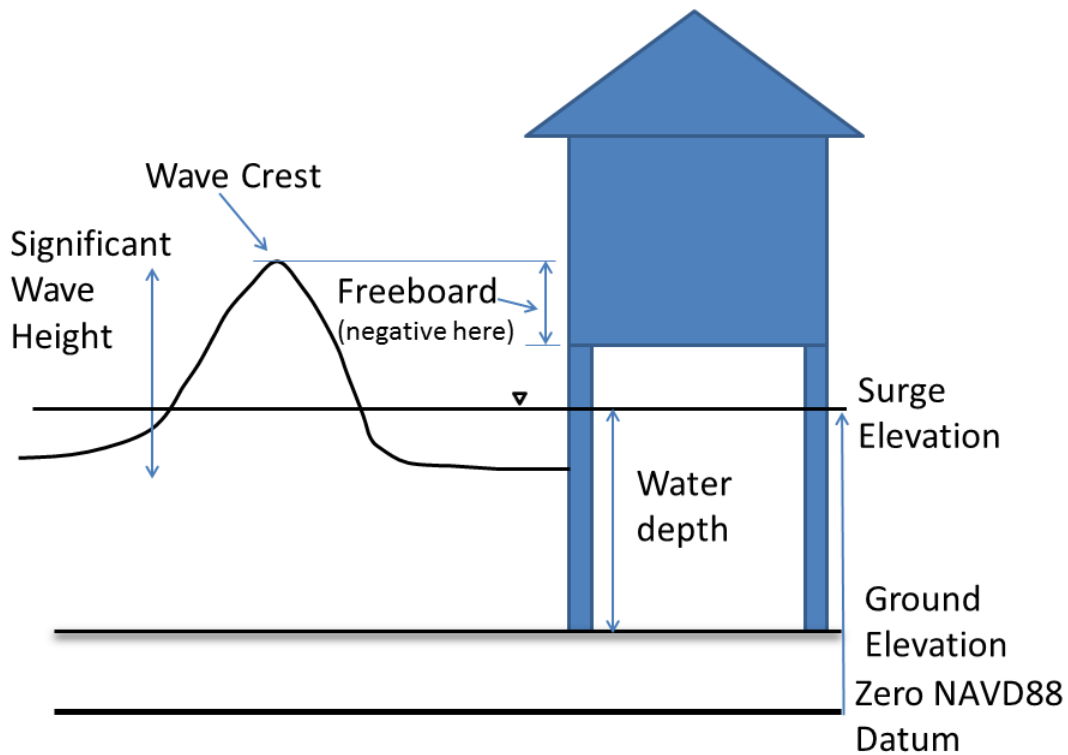


Figure 5-1: Definition Sketch for Wave and Surge Properties around Buildings

Storm surge and astronomical tides also change relatively slowly in space with typical length scales of miles for any significant changes along a shoreline. As surge moves inland, its elevations can change more rapidly in space, with possibly significant changes between the shoreline surge and at a mile or so inland, particularly around barrier islands or peninsulas.

On smaller temporal scales, the difference between the storm surge elevation and the actual water surface will vary quickly with time scales of seconds. These differences over shorter periods of time are called **waves**, which can be seen at any beach. Waves also have surface elevations: a local high point is called a **crest**, while a local low point is called a **trough**. **Wave crest elevations** are quite important, as these are what first reach elevated structures and begin to cause damage.

Waves are defined statistically, with the **significant wave height** (a measure of the crest to trough elevation), **peak period** (a measure of the time between wave crests), and **mean direction** (direction waves are heading) all being basic properties. Waves also force water motion called **orbital velocities** that vary on the same time scales as wave surface elevations. Orbital velocities are largest in the wave crests, and can be much larger than currents from surge in many cases. When orbital velocities are large, waves tend to cause more structural damage than storm surge, although surge by itself can also cause significant damage.

Knowledge of these hazards is important in flooded areas to estimate the level of damage they cause. The proposed methodology for evaluating the wave and surge hazard will feature high resolution wave and surge modeling, supplemented by local measurements of waves and water levels taken during the storm and high water marks taken after the storm. These modeling estimates will be used, in concert with building properties, to compute probabilities of structural collapse or “slabbing” for locations where the cause of destruction is not immediately self-evident.

5.2 Surge and Wave Modeling Specifications

Surge and wave modeling are necessary to provide estimates of hazard timing and magnitude at TWIA-insured properties and, along with on-site measurements, will be a major factor in decreasing disputes post-storm. TWIA must set up contractual arrangements to rapidly model waves and surge post-event. All contracts must be in place well before hurricane season to ensure that models may be run rapidly post-landfall. Technical features of the modeling must include:

- The domain of wave and surge modeling shall extend from at least Pensacola, FL to the Mexican coast at 23°N, and at minimum 500 km offshore of Texas;
- In Texas and parts of Louisiana west of 93.5°W, surge and wave modeling shall feature high resolution (grid with 50m or finer resolution nearshore and overland) models that should be run on the same grid if possible to avoid interpolation errors. Dunes and other significant features impeding flow shall be resolved. The wave and surge grid may either be structured or unstructured, and may or

may not be nested, as long as resolution requirements are met. Resolution may be coarser offshore and in other locations;

- Surge and wave modeling shall use the same wind field as is used to compute wind damage, which shall be a best-available reanalysis wind field that incorporates measurements made during the storm (observational model);
- The drag coefficient shall feature a high wind cutoff that is defensible from observations or the scientific literature;
- Wave computations shall use a third-generation unsteady spectral wave model that has been tested closely against data from Hurricane Ike and other storms in Texas;
- Wave computations must include feedback from velocities and water levels output from the surge model;
- Wave breaking dissipation shall be spectrally-based and shall not use a simple depth-limited cutoff;
- The surge model shall use a shallow water model (either depth-averaged or multi-level) that includes convective processes and bottom friction that varies with substrate and/or vegetation;
- The surge model shall include tides as an integral part of the model;
- The modeling system must be set up to be able to produce initial estimates within 48 hours of landfall;
- The model shall be set up to readily incorporate new Lidar topographical data and wind data as it becomes available post-storm;
- The modeling system must quickly produce updated estimates of waves and surge as additional data becomes available, and pass these to TWIA for use in the Damage Estimation Module; and
- The modeling system shall compare with measured wave and water level data as it becomes available, and shall produce error estimates for each storm.

Figure 5-2 shows an example of the output produced by a high resolution surge and wave model.

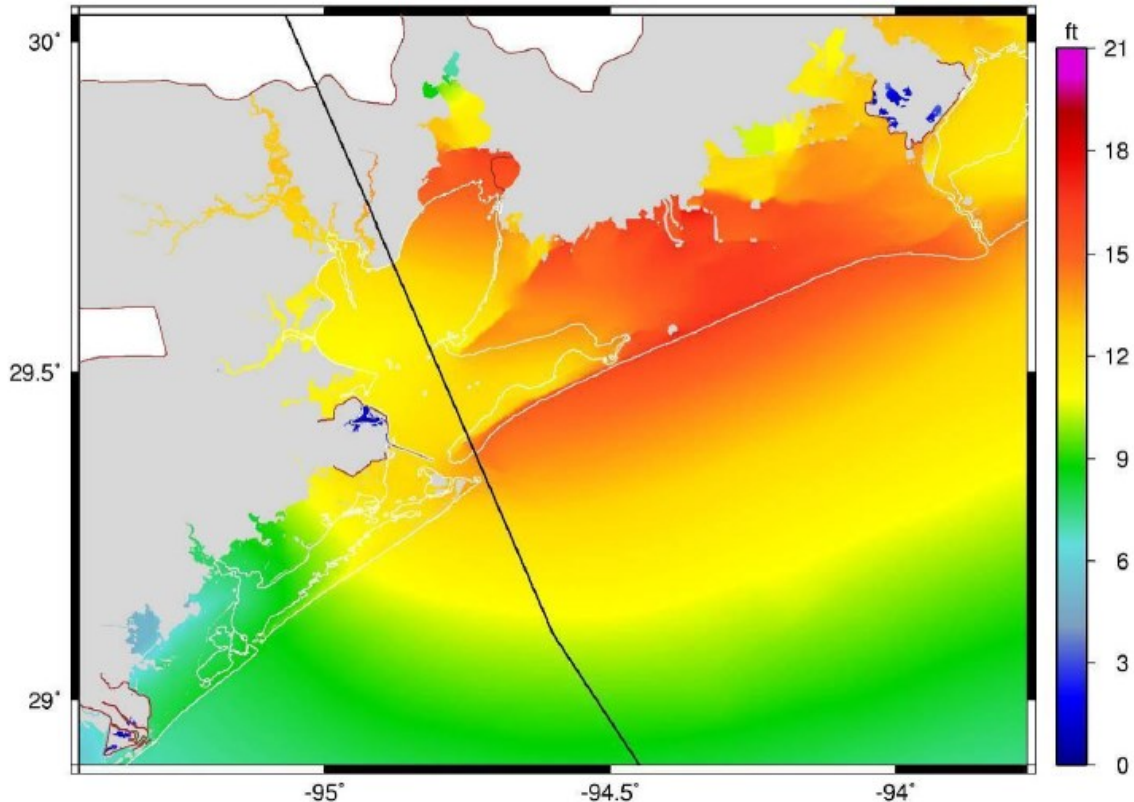


Figure 5-2: Output from a High Resolution Surge Model
(Source: ARCADIS U.S., Inc., Highlands Ranch, Colorado 80129)

5.3 Physical Measurements of Waves and Surge

Observations of surge and waves can be divided into two main groups: direct observations using instruments in place before the storm, and indirect measurements from evidence left after the storm. Both methods are useful in determining the hazard experienced at a given location, and to validate numerical models. Available observations are expected to vary depending on the storm and location. TWIA must make arrangements for coordination with federal and state agencies that take data, and

should ensure that plans are in place for physical measurements either by other parties, or as contracted by TWIA.

It is always best to have wave and surge observations as close to desired property locations as possible, although many times this arrangement is not possible. Physical measurements may include:

- National Oceanic and Atmospheric Administration (NOAA) and other permanent tide gauges;
- Post-storm high water marks;
- Rapidly-deployed wave and surge gauges deployed at sites with the potential to be significantly damaged by waves and surge; and
- Other indications of wave and surge magnitudes at given locations such as elevations of wave/surge damage on buildings.

It will not be possible to obtain either wave or surge observations with sufficient density to resolve all relevant details, but measurements may be used both to evaluate and validate model results, and to improve the computed wave and surge fields. An optimal wave and surge field with error estimates shall be constructed by assimilating observational data. Details of the assimilation will depend strongly on the data taken, but shall be defensible and consistent with best practice.

5.4 Surge and Wave Computations and Observations

One of the most important aspects of claims adjustment for slab cases will be the determination of whether slabbing was caused by wind or waves/surge, if there is no clear evidence remaining at the site. This determination requires estimates of the probability of slabbing both by waves/surge and by wind. Wave/surge estimates are to be driven by large scale hindcasts, and backed up by measurements as described previously.

Once surge and wave fields have been determined, the Panel recommends that TWIA compute the probability of slabbing for residential construction using Variant 5 of the methodology of Tomiczek et al. (2014). This methodology was developed specifically for residential construction in Texas following Hurricane Ike. As an integral part of the Damage Estimation Module, it uses the hindcast significant wave height and surge level,

combined with the elevation of the lowest horizontal structural member and house age, to predict the probability of slab failure using a relatively simple equation. Figure 5-3 gives results for residential structures in four age categories, showing the failure probabilities as a function of significant wave height. Probability of slabbing increases significantly with increasing wave height, increasing structure age, and with decreasing structure elevation (decreasing freeboard). In concert with parallel methods to estimate the probability of wind slabbing, this will help to determine the source of slabbing.

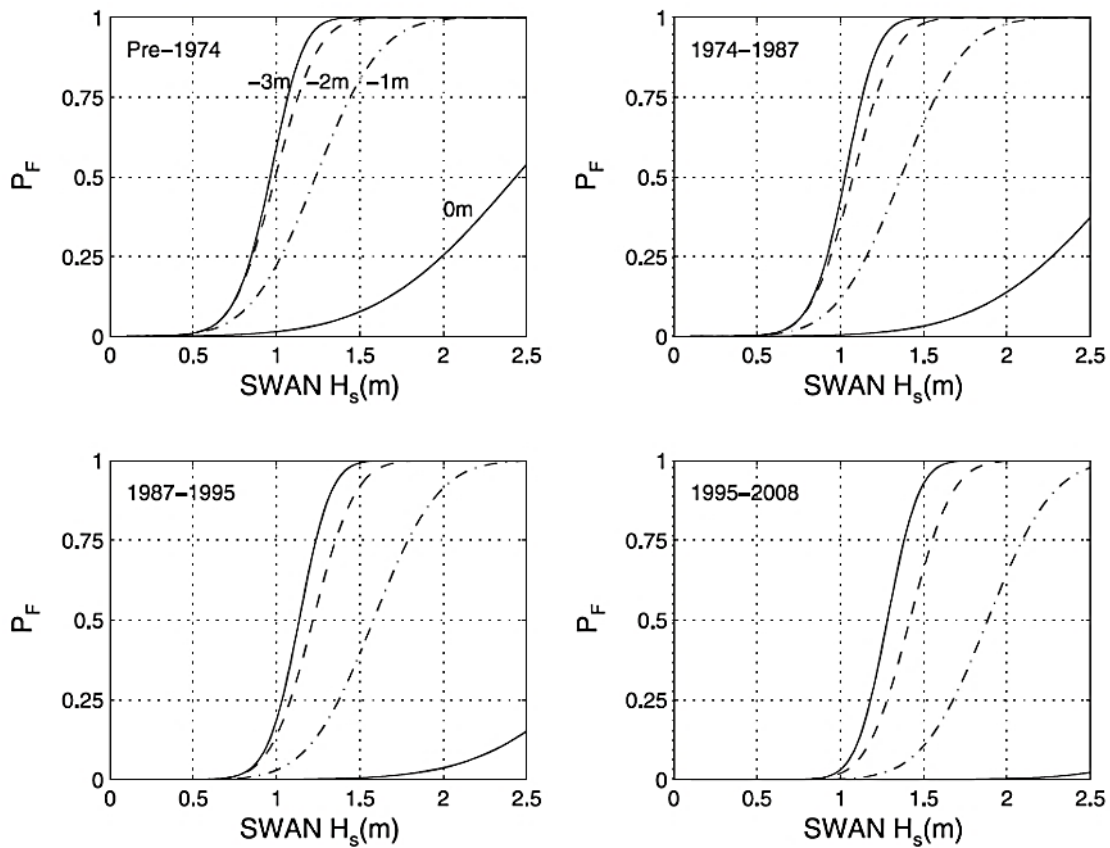


Figure 5-3: Collapse Failure Probabilities from Variant 5 of Tomiczek et al. (2014)
 (This variant uses significant wave height, freeboard, and age groups for age groups 1-4. Lines are (left to right) $FB_{H_s} = (-3, -2, -1, 0)$ m.)

The system of Tomiczek et al was developed to predict the probability of slabbing for residential structures on the Bolivar Peninsula in Texas following Hurricane Ike in 2008. The Bolivar Peninsula saw severe wave and surge damage as almost the entire peninsula was flooded to depths that exceeded 2m above ground in many locations. High resolution hindcasts of waves and surge were made using a system as recommended in this report (Hope et al., 2013). These results were combined with a post-storm damage survey of almost 2,000 houses that included location, house height above grade, and age to arrive at a series of regressions to predict the probability of slabbing during a tropical cyclone.

The most significant factors in the regression were the height of a structure compared to a wave crest (freeboard), the wave height itself, and the structure age. New high elevation buildings in small waves fared best, while old low elevation buildings in large waves had almost no chance of survival. These results mirrored what was seen on Bolivar Peninsula and other locations in Texas, and provide a validated method to estimate the probability of slabbing for locations with surge and waves on the Texas coast.

The system of Tomiczek should not be used for commercial or multifamily structures. It is additionally not able to predict slabbing due to foundation erosion or run-up. In cases where erosion or run-up is suspected of causing wave/surge slabbing at the immediate water edge, these determinations should be made by a qualified professional who will be able to interpret the site.

6 Damage Estimation Module

Damage to a structure caused by the wind and the surge is estimated in this module. The sequence of the methodology is shown in Figure 6-1. A two-pronged approach is used to estimate the damage to the building. The first prong is termed “the model approach” and the second prong “the observational approach.” The model approach is shown in Figure 6-1 using solid lines and represents the default approach. The observational approach is shown using dashed lines. It can be used as a means to: (a) inform the model approach to obtain better damage predictions; (b) validate the model approach; and/or (c) provide an additional methodology to estimate the damage to the building components that can be used in the adjusting process.

The Panel recommends that both model and observational approaches be employed. The reason is that application of the Damage Estimation Module is optimal when all available data are used to estimate damage to individual structures. When applying the observational approach, if nearby surviving structures are very similar to the structure under consideration by the model, then observed damage can be more heavily weighted in consideration of damage estimation. Monetary losses associated with damages are assigned in the Economic Loss Module (Section 8).

The Panel recommends a specific philosophy in computing damage for slab cases: the wind damage used to compute losses should be that which is predicted to have occurred up to the time when the structure is likely to have been destroyed by waves and surge. Of course, if slabbing was caused by wind, then all of this damage will be wind damage. Similarly, if winds were low up to the time of surge destruction, then wind damage will have been very low.

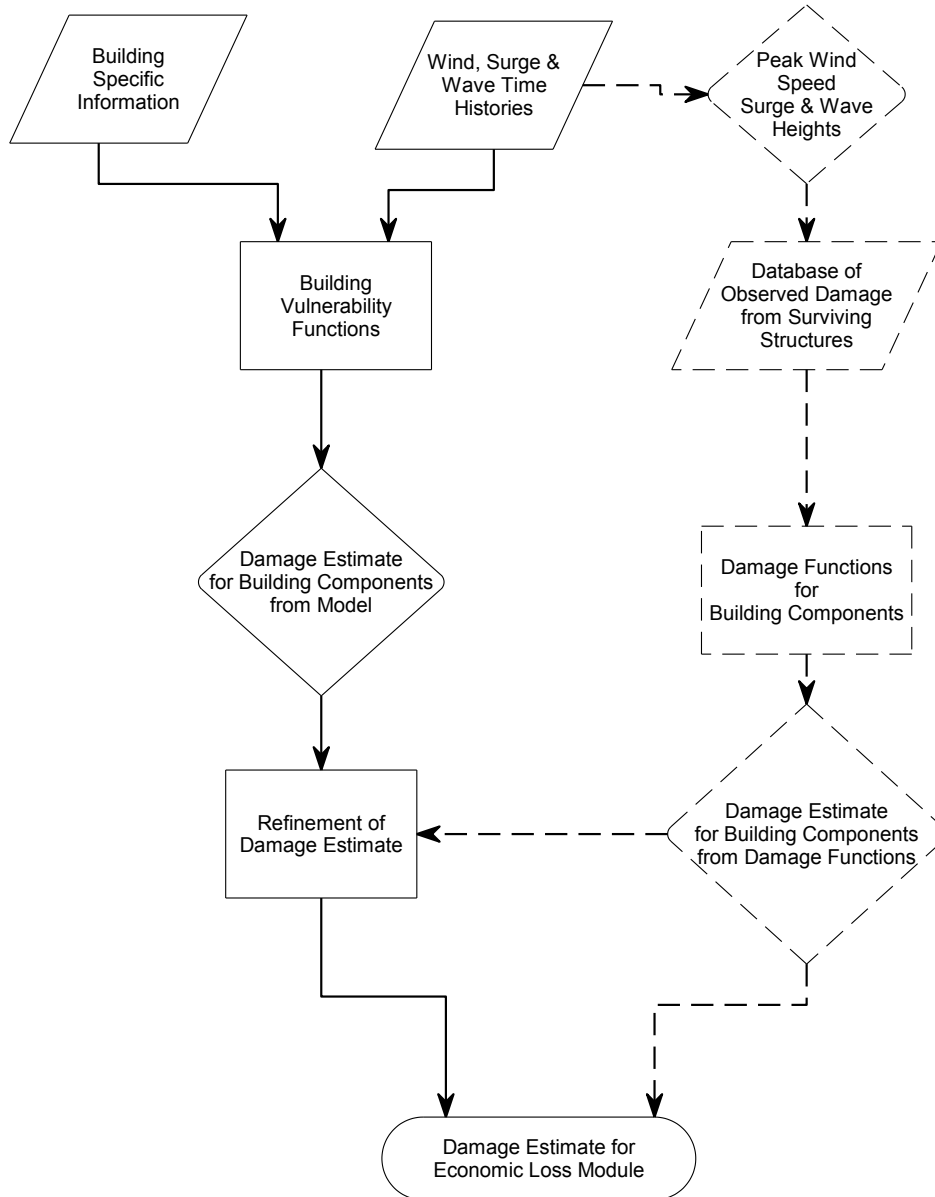


Figure 6-1: Damage Estimation Module Flowchart

(Dashed items indicate components of the observational approach which, although preferred, may not always be possible to accomplish.)

To arrive at an equitable result for wind damage for slab-only cases, the Panel recommends a two-step approach. First, it is necessary to independently estimate the probabilities of slabbing from both wind, P_{wind} , and from waves/surge, P_{surge} . For wind slabbing, the panel recommends that the probability of collapse be taken as the maximum of the probabilities of failure for wall studs in bending, the connections of the wall studs to the wall plates, and the shear walls. For wave/surge slabbing probability, the panel recommends the methodology of Tomiczek et al (2014) as detailed in the Section 5.4.

Computation of wind damage at time of surge slabbing is performed at t_{surge} , which is the earliest time where: (1) the probability of wave/surge collapse, P_{surge} , reaches its maximum; or (2) the probability of wave/surge collapse first reaches 50 percent. The next step of the recommended methodology calculates the wind damage at time t_{surge} as $D_{t_{surge}}$ using the Damage Estimation Module as described in Section 6.1. The recommended physical damage levels to be used for wind damage, $D_{total_component}$, are then recommended to be given as a probability weighted blend of the computed damage at time t_{surge} , $D_{t_{surge}}$, and a total damage. This approach gives:

$$D_{total_component} = \frac{P_{surge} D_{t_{surge}} + P_{wind} D_{100\%}}{P_{surge} + P_{wind}}$$

where $D_{100\%} = 1.0$ represents the damage for total damage. This relation changes smoothly as probabilities and damage levels also change. It also implicitly accounts for timing. Examples are presented below to illustrate these features of the proposed formulation.

Example 1: Strong Surge, Weak Wind

Assume the probability of surge slabbing is $P_{surge} = 0.9$ and the computed wind damage for any component at t_{surge} is $D_{t_{surge}} = 0.1$. The low probability of wind slabbing is taken as $P_{wind} = 0.05$. The probability-weighted wind damage is $D_{total} = 0.1474$.

Example 2: Weak Surge, Strong Wind

Assume the probability of surge slabbing is $P_{surge} = 0.1$ and the computed wind damage for any component at t_{surge} is $D_{t_{surge}} = 0.8$. The high probability of wind slabbing is taken

as $P_{wind} = 0.75$. The probability-weighted wind damage is $D_{total} = 0.9765$, reflecting the high likelihood of wind slabbing.

Example 3: Weak Surge, Weak Wind

The most difficult case is when slabbing occurs with low probabilities of wind and surge slabbing. However, an answer must still be obtained. So, assume the probability of surge slabbing is $P_{surge} = 0.1$ and the computed wind damage for any component at t_{surge} is $D_{t_{surge}} = 0.1$. The low probability of wind slabbing is also taken as $P_{wind} = 0.1$. The probability-weighted wind damage is $D_{total} = 0.55$, reflecting the high uncertainty in this estimate.

Example 4a: Strong Early Surge, Strong Wind

When wind and surge slabbing probabilities are both large, timing becomes important. Assuming a strong early surge occurs before the wind peak, so $P_{surge} = 0.9$ and the computed wind damage for any component at t_{surge} is $D_{t_{surge}} = 0.1$. The high probability of wind slabbing is taken as $P_{wind} = 0.75$. The probability-weighted wind damage is $D_{total} = 0.5091$.

Example 4b: Strong Late Surge, Strong Wind

Assuming a strong late surge occurs after the wind peak, so $P_{surge} = 0.9$ and the computed wind damage for any component at t_{surge} is $D_{t_{surge}} = 0.7$. The high probability of wind slabbing is taken as $P_{wind} = 0.75$. The probability-weighted wind damage is $D_{total} = 0.8364$.

Overall, this approach reasonably balances wind and surge slabbing probabilities, and in assigning damage to each case. Of course, it is sensitive to probabilities of wind and surge slabbing; and to the predicted wind damage for any component at time of maximum surge. Accurate estimates of these quantities are therefore important.

6.1 Introduction

The Hazard Module yields time histories of wind speed and direction. The Damage Estimation Module uses this information to estimate the evolution of loads for several building components and systems at many distinct locations on the building. The Damage Estimation Module also establishes resistances for each of these building components and systems. The estimated loads and resistances are compared at locations on the building and at each time step to determine the probability that each component or system will fail at those locations.

A variety of valid techniques are available to estimate component and system failure probabilities. Among them are the First-Order, Second-Moment reliability index, the Rackwitz-Fiessler procedure, and Monte Carlo Simulation. The proposed methodology can be implemented using any of these methods, each of which has advantages and disadvantages.

The calculation of the probabilities of failure are developed and demonstrated in this report using a First-Order, Second-Moment, Mean Value (FOSM-MV) reliability analysis (Nowak and Collins, 2000). This method is easy to use and does not require knowledge of the distribution types for the random variable under consideration. A discussion of the advantages and disadvantages of some of the available methods and the results of a sensitivity analysis comparing failure probabilities using various approaches are included in Appendix C. The components and systems currently considered in the analysis are:

- Roof Cover
- Roof Panel
- Wall Cover
- Wall Sheathing
- Windows
- Doors
- Garage Door
- Wood Stud Bending
- Wall Stud Plate Connection
- Roof-to-wall Connection
- Shear Wall Capacity
- Interior Finishes

The probability of structural collapse due to wind is taken as the maximum of the probabilities of failure among the wall stud bending, wall stud-to-plate connection, and shear wall failure modes. The computation of the probability of failure for each component and system requires the establishment of a performance function (or limit state function), the generic form of which is shown below in Equation 6.1.

$$g(R, Q) = R - Q \quad (\text{Eq. 6.1})$$

Where,

R = Resistance, and

Q = Load.

The units for each term, R and Q , must be consistent. Failure is considered to occur when the value of g is less than zero. That is, failure occurs when the resistance of the component or system is exceeded by the load. However, the values of resistance and load are not deterministic quantities. They are random variables with mean values, standard deviations, and probability distributions that preclude an absolute prediction of failure. The probability of failure is calculated by first determining a reliability index, β , as shown below in Equation 6.2.

$$\beta = \frac{\mu_R - \mu_Q}{\sqrt{\sigma_R^2 + \sigma_Q^2}} \quad (\text{Eq. 6.2})$$

Where,

μ_R = Mean value of resistance,

μ_Q = Mean value of load,

σ_R = Standard deviation of resistance, and

σ_Q = Standard deviation of load.

Equation 6.2 can be thought of as the ratio of reserve capacity to the combined variability of the load and resistance. Higher values of the reliability index will yield lower values of the probability of failure. The probability of failure is calculated according to Equation 6.3.

$$P_f = \Phi(-\beta) \quad (\text{Eq. 6.3})$$

where Φ is the standard normal cumulative distribution function (Freund and Wilson 2003). As an illustration, reliability indices of 0.0, 1.0, 2.0 and 3.0 yield probabilities of failure of 0.50, 0.16, 0.023, and 0.0014, respectively.

Many practical performance functions are nonlinear combinations of several random variables, rather than the simple linear combination of two random variables shown in the generic formulation of Equation 6.1. For these cases, the FOSM-MV reliability index is calculated using equation 6.4.

$$\beta = \frac{g(\mu_{x1}, \mu_{x2}, \dots, \mu_{xn})}{\sqrt{\sum_{i=1}^n (a_i \cdot \sigma_i)^2}} \quad (\text{Eq. 6.4})$$

Where,

μ_{xi} = mean value of random variable i

σ_i = standard deviation of random variable i

$g(\mu_{x1}, \mu_{x2}, \dots, \mu_{xn})$ is the performance function evaluated at the mean values of the contributing random variables, and

$$a_i = \frac{\delta g}{\delta x_i} \quad (\text{Eq. 6.5})$$

Since the Damage Estimation Module is estimating damage in a probabilistic sense by describing the average expectation of damage for a structure with given characteristics, the probability of failure is used as a proxy for damage rate. The ratio of damage for a particular component on a particular location of a structure is deemed to be equivalent to the probability of component failure in that location. This assumption is accurate if the component damage can be represented as a continuum, or if a large population of properties are under consideration.

The first condition for this assumption is not valid, since building components consist of discrete elements. For example, there will always be some finite number of roof deck panels in each zone of a roof. The damage ratio on a single building for roof decking cannot be considered to have infinite resolution. In the case of a single property, the proportion of damage to discrete elements might be better estimated by using the binomial distribution considering the failure probability and the number of elements in

each location. However, when the number of properties under consideration is large, and the estimate sought is the average damage to a property with given characteristics, then the resolution increases and the assumption of a continuum of available damage ratios becomes less problematic.

As an example, consider roof panel damage in one corner zone of a roof. Only one piece of plywood may occupy this location due to the relative sizes of plywood sheets and of roof corner zones for typical residences. For a single property, only two outcomes are possible: damage or no damage. If the Damage Estimation Module estimates that the probability of damage to the roof decking in this location is 10 percent, then it is reasonable to conclude that a single property would not experience damage to roof decking in this roof area. However, if 100 properties are under consideration, and the Damage Estimation Module estimates that the probability of damage to the roof decking in this location is 9 percent, then it is reasonable to conclude that 9 of 100 properties experience damage to roof decking in this area, and the average damage rate for these 100 properties is 9 percent. That is, 9 of 100 properties would experience total damage, and the other 91 would experience no damage.

This example demonstrates a fundamental characteristic of the Damage Estimation Module: the most likely result and the average result are not the same. The Damage Estimation Module produces the average result, and because of this characteristic, the assumption that probability of failure can be considered as a proxy for damage rate is acceptable. The total damage ratio for a component over the entire building is the sum of the areas, weighted by their individual failure probabilities.

For illustration, consider the following simple hypothetical scenario. One portion of a building roof covers 10 percent of the roof area, and the probability of failure for this area of roof is 50 percent. If the probabilities of failure in all the other portions of the roof are zero, then the total damage ratio for the roof is five percent.

The following sections will describe the development of the performance functions and the selection of random variable nominal values, mean values, biases, and standard deviations (or coefficients of variation) for use in the damage module. Example calculations are in Appendix A illustrating the methodology.

6.2 Wind Load Development

The wind loads used in the damage module are based on the provisions of ASCE 7-10, *Minimum Design Loads for Buildings and Other Structures* (ASCE, 2010). The formulations for wind loading vary depending on the building surface and location being loaded, as well as the function of the system being loaded (i.e. Main Wind Force Resisting System versus Components and Cladding). Common to all of the wind load calculations is the determination of the velocity pressure, q_z (ASCE 7-10 Equations 27.3-1 and 30.3-1).

$$q_z = 0.00256 \cdot K_z \cdot K_{zt} \cdot K_d \cdot V^2 \text{ (pounds per square foot)} \quad (\text{Eq. 6.6})$$

Where,

K_z is the velocity pressure exposure coefficient,

$$K_z = \begin{cases} 2.01 \cdot \left(\frac{15}{z_g}\right)^{\left(\frac{2}{\alpha}\right)} & z < 15 \text{ feet} \\ 2.01 \cdot \left(\frac{z}{z_g}\right)^{\left(\frac{2}{\alpha}\right)}, z_g \geq z \geq 15 \text{ feet} & \end{cases} ; \quad (\text{Eq. 6.7})$$

z = height above ground, feet;

z_g is the gradient wind height in feet associated with various exposure categories, B, C, and D, (ASCE 7-10 Table 26.9-1);

α is the power law shape factor for the boundary layer wind profile associated with various exposure categories, B, C, and D (ASCE 7-10 Table 26.9-1);

K_{zt} is the topographic factor, and is universally considered to be 1.0 for this project since the coastal locations of interest will not produce topographic effects (ASCE 7-10 Section 26.8);

K_d is the directionality factor, and is considered to be 1.0 since wind direction is explicitly treated in the analysis here (ASCE 7-10 Section 26.6).

V is the 3-second gust wind speed in miles per hour, at 33 feet above ground in open terrain, and this value is delivered to the damage module from the hazard module.

Since the directionality factor and the topographic factor are not used in the damage module, the two random variables that remain in the equation for the velocity pressure are the velocity pressure exposure factor and the wind speed. The statistical

parameters used in the damage module for the exposure factor are summarized in Table 6-1. It should be noted that the exposure factor is calculated according to Equation 6.7 considering that the variables z , α , and z_g are all deterministic, and the effects of bias and uncertainty in the exposure factor are applied to the resulting value of K_z . Bias is defined as the ratio of the mean value to the nominal value where the nominal value is that value given in ASCE 7-10 (Eq. 6.7).

TABLE 6-1. EXPOSURE FACTOR STATISTICS

Exposure	α	z_g	Nominal	λ (Bias)	σ
B	7.0	1200	Eq. 6.7	1.016	0.12
C	9.5	900		0.933	0.12
D	11.5	700			

Reference: Ellingwood and Tekie, 1999

The uncertainty (coefficient of variation) in the estimate of the wind speed will be determined operationally by evaluating the accuracy of the wind field modeling performed in the hazard module, and cannot be stated *a priori*. For the purposes of illustrating the functionality of the damage module, the coefficient of variation for the wind speed has been assumed to be 0.18.

The velocity pressure is used in combination with internal and external pressure coefficients to determine the total wind pressure on a building surface. For component and cladding elements, the wind pressure is defined by ASCE 7-10 Equation 30.4-1, which is shown below as Equation 6.8.

$$p = q_z [(GC_p) - (GC_{pi})] \text{ (pounds per square foot)} \quad (\text{Eq. 6.8})$$

Where,

GC_p is an external pressure coefficient defined for specific roof and wall zones, and

GC_{pi} is an internal pressure coefficient that reflects the integrity of the building envelope and the resulting enclosure classification of the building.

For main wind force resisting system elements, the wind pressure is defined by ASCE 7-10 Equation 27.4-1, which is shown below as Equation 6.9.

$$p = q \cdot (G \cdot C_p) - q_i \cdot (GC_{pi}) \text{ (pounds per square foot)} \quad (\text{Eq. 6.9})$$

Where,

q is the velocity pressure evaluated at either the mean roof height or the wall height of a location of interest,

q_i is the velocity pressure evaluated at the level of the highest opening that can affect the internal pressurization of the structure,

G is the gust effect factor, which is defined in ASCE 7-10 Section 26.9,

C_p is an external pressure coefficient defined for specific roof and wall zones, and

GC_{pi} is an internal pressure coefficient that reflects the integrity of the building envelope and the resulting enclosure classification of the building.

The Damage Estimation Module evaluates the velocity pressure at the mean roof height in all cases. This approach is a conservative simplification that will not have a large effect on the damage estimates for one and two-story residential structures. The internal and external pressure coefficients and the gust effect factor are all treated as random variables in the damage module. The following sections will describe the selection of appropriate values and the associated statistics for the factors and coefficients included in Equations 6.8 and 6.9.

6.2.1 Internal Pressure

The total wind load on a building component is composed of contributions from both internal and external surfaces. Unless the building envelope is compromised, (e.g. by failures of roof or wall sheathing or by broken windows), the ASCE 7-10 wind load provisions consider the structure to be “enclosed.” Enclosed buildings experience limited magnitudes of internal pressure. If the building envelope is breached to a sufficient extent, or if significant openings exist in the original structure, the structure is classified as being “partially enclosed.” This condition allows the development of much higher internal pressures. Internal pressures can either act in the same direction as external pressures (promoting damage) or act in the opposite direction as external pressures, thus limiting wind damage.

The Damage Estimation Module conservatively considers internal pressure to act in the same direction as the external wind pressure, regardless of the position of dominant openings and the direction of the wind. The internal pressure is related to the velocity, q_z , through the application of an internal pressure coefficient, GC_{pi} . The statistical parameters used in the damage module for the internal pressure coefficient are summarized in Table 6-2. The damage module considers a building to be partially enclosed, and thus subject to higher internal pressures, if, in the previous time step, the probability of failure of an enclosing element at any location is greater than or equal to 0.50.

TABLE 6-2. INTERNAL PRESSURE COEFFICIENT STATISTICS

Enclosure Classification	Nominal	λ (Bias)	μ	σ	COV
Enclosed	0.18	0.833	0.150	0.05	0.333
Part. Encl.	0.55	0.833	0.458	0.05	0.109

Reference: Ellingwood and Tekie, 1999

6.2.2 Roof Component and Cladding External Pressures

The development of external pressure on local roof surfaces depends on the shape of the roof (i.e. hip or gable), the slope of the roof, and the relative dimensions of the building. Furthermore, the pressure applicable to a particular component depends on the effective wind area tributary to it. Components that gather wind pressure from larger areas are subject to less severe pressures since the occurrence of intense, local pressures has less correlation over larger areas. Tables 30.4-2A through 30.4-2C in ASCE 7-10 provide nominal values of gust pressure coefficients, GC_p , for a variety of roof shapes and slopes. The pressure coefficients are applicable to three different roof zones: (1) field areas that are away from edges or corners, (2) perimeter zones along the edges of roofs, and (3) corners.

For design, the ASCE 7-10 roof pressure areas are established regardless of wind direction, since wind direction is not known in advance of a high wind event. However, the damage module considers a time history of wind direction for a known event, and therefore a time-varying classification of roof pressure zones is warranted. A roof corner

may be classified as Zone 3 (corner) for some wind directions and classified as Zone 1 (field) for other directions.

Figures 6-2 and 6-3 show the assignment of 24 individual roof pressure areas for hip and gable roofs, respectively. These figures also show eight wind direction sectors. The assignment of the appropriate ASCE 7-10 roof pressure zone to each of the 24 areas shown in Figure 6-2 and Figure 6-3 depends on the wind angle of attack (AOA) at each time step of the hazard time history.

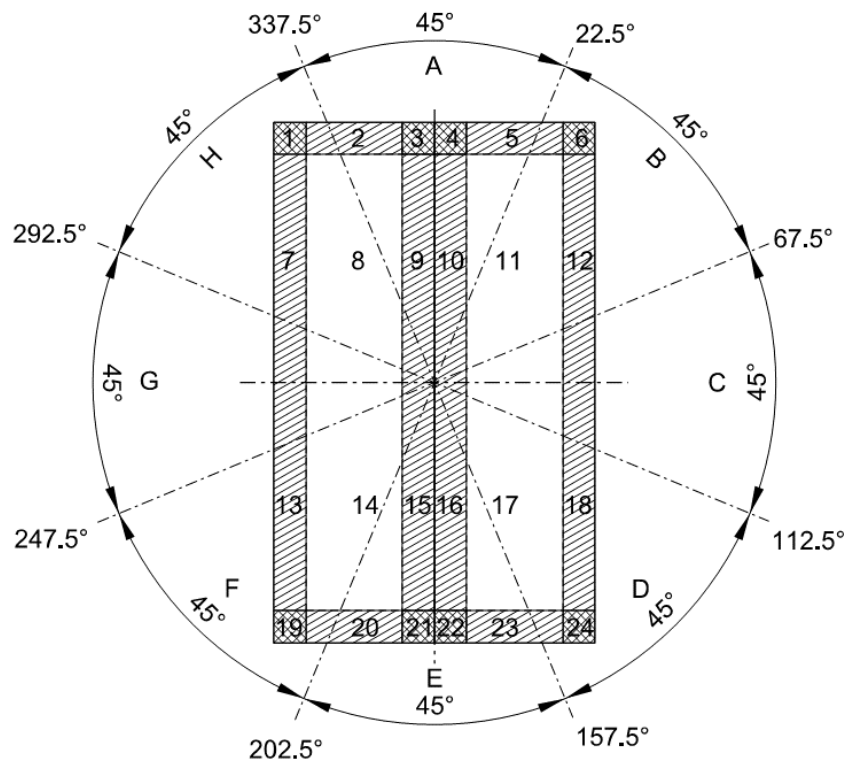


Figure 6-2: Roof Component and Cladding Areas and Wind Sectors for a Gable Roof

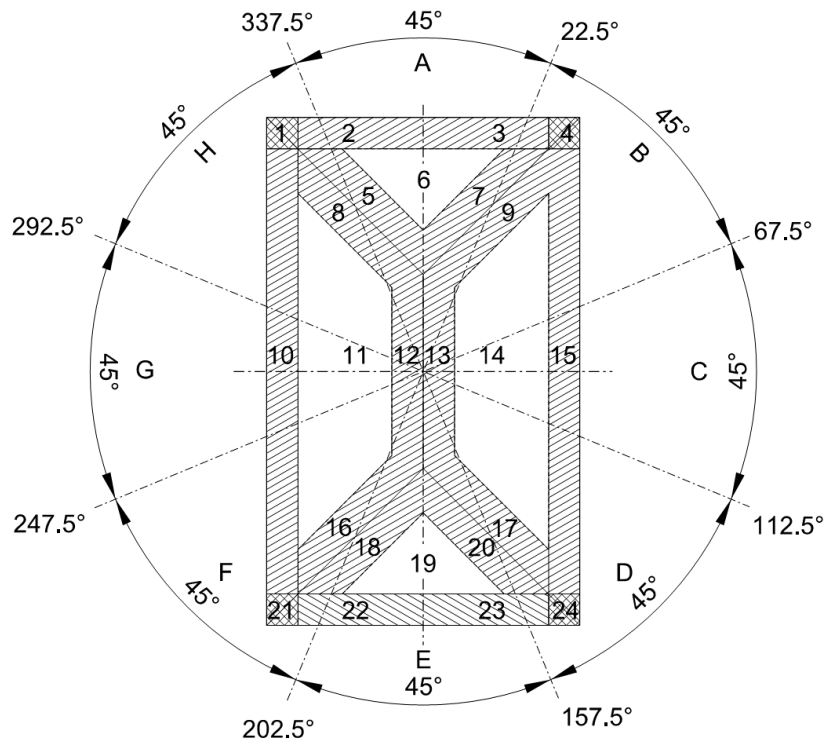


Figure 6-3: Roof Component and Cladding Areas and Wind Sectors for a Hip Roof

Table 6-3 and Table 6-4 show the roof pressure zone assignments versus AOA for gable and hip roofs, respectively. Table 6-5 lists the statistics for the random variable, GC_p , used in the calculation of the FOSM-MV reliability index. Only roof uplift pressures are used in the analysis since these are the loads that overwhelmingly contribute to roof covering and roof decking damage during windstorms.

TABLE 6-3. GABLE ROOF COMPONENT AND CLADDING PRESSURE ZONE ASSIGNMENTS AS A FUNCTION OF WIND ANGLE OF ATTACK

Sector	AOA (deg.)	Roof Area											
		1	2	3	4	5	6	7	8	9	10	11	12
A	0-22.5	2	2	2	2	2	2	1	1	1	1	1	1
B	22.5-67.5	2	2	3*	2	2	3	1	1	2	1	1	2
C	67.5-112.5	1	1	2	1	1	2	1	1	2	1	1	2
D	112.5-157.5	1	1	2	1	1	2	1	1	2	1	1	2
E	157.5-202.5	1	1	1	1	1	1	1	1	1	1	1	1
F	202.5-247.5	2	1	1	2	1	1	2	1	1	2	1	1
G	247.5-292.5	2	1	1	2	1	1	2	1	1	2	1	1
H	292.5-337.5	3	2	2	3*	2	2	2	1	1	2	1	1
A	337.5-360	2	2	2	2	2	2	1	1	1	1	1	1

Sector	AOA (deg.)	Roof Area											
		13	14	15	16	17	18	19	20	21	22	23	24
A	0-22.5	1	1	1	1	1	1	1	1	1	1	1	1
B	22.5-67.5	1	1	2	1	1	2	1	1	2	1	1	2
C	67.5-112.5	1	1	2	1	1	2	1	1	2	1	1	2
D	112.5-157.5	1	1	2	1	1	2	2	2	3*	2	2	3
E	157.5-202.5	1	1	1	1	1	1	2	2	2	2	2	2
F	202.5-247.5	2	1	1	2	1	1	3	2	2	3*	2	2
G	247.5-292.5	2	1	1	2	1	1	2	1	1	2	1	1
H	292.5-337.5	2	1	1	2	1	1	2	1	1	2	1	1
A	337.5-360	1	1	1	1	1	1	1	1	1	1	1	1

* Classified as pressure zone 2 if roof slope, $\theta \leq 7^\circ$

TABLE 6-4. HIP ROOF COMPONENT AND CLADDING PRESSURE ZONE ASSIGNMENTS AS A FUNCTION OF WIND ANGLE OF ATTACK

Sector	AOA (deg.)	Roof Area											
		1	2	3	4	5	6	7	8	9	10	11	12
A	0-22.5	2	2	2	2	1	1	1	2	2	1	1	1
B	22.5-67.5	2	2	2	3*	1	1	2	2	1	1	1	2
C	67.5-112.5	1	1	1	2	1	1	2	2	1	1	1	2
D	112.5-157.5	1	1	1	2	1	1	2	1	1	1	1	2
E	157.5-202.5	1	1	1	1	1	1	1	1	1	1	1	1
F	202.5-247.5	2	1	1	1	2	1	1	1	1	2	1	1
G	247.5-292.5	2	1	1	1	2	1	1	1	2	2	1	1
H	292.5-337.5	3*	2	2	2	2	1	1	1	2	2	1	1
A	337.5-360	2	2	2	2	1	1	1	1	2	1	1	1

Sector	AOA (deg.)	Roof Area											
		13	14	15	16	17	18	19	20	21	22	23	24
A	0-22.5	1	1	1	1	1	1	1	1	1	1	1	1
B	22.5-67.5	1	1	2	1	1	1	1	2	1	1	1	2
C	67.5-112.5	1	1	2	2	1	1	1	2	1	1	1	2
D	112.5-157.5	1	1	2	2	1	1	1	2	2	2	2	3*
E	157.5-202.5	1	1	1	2	2	1	1	1	2	2	2	2
F	202.5-247.5	2	1	1	1	2	2	1	1	3*	2	2	2
G	247.5-292.5	2	1	1	1	2	2	1	1	2	1	1	1
H	292.5-337.5	2	1	1	1	1	2	1	1	2	1	1	1
A	337.5-360	1	1	1	1	1	1	1	1	1	1	1	1

* Classified as pressure zone 2 if roof slope, $\theta \leq 25^\circ$

TABLE 6-5. ROOF COMPONENT AND CLADDING EXTERNAL PRESSURE COEFFICIENT STATISTICS.

Element	Slope (deg.)	Zone	Nominal GC_p	λ (Bias)	μ	σ	COV
Roof Cover ($A_e < 10$ sq. ft.)	≤ 7	1	-1.0	0.868	-0.868	0.08	0.092
		2	-1.8	0.947	-1.705	0.19	0.111
		3	-2.8	0.947	-2.652	0.19	0.072
	$7 < \theta \leq 27$	1	-0.9	0.868	-0.781	0.08	0.102
		2	-1.7	0.947	-1.610	0.19	0.118
		3	-2.6	0.947	-2.462	0.19	0.077
	$27 < \theta \leq 45$	1	-1.0	0.868	-0.868	0.08	0.092
		2	-1.2	0.947	-1.136	0.19	0.167
		3	-1.2	0.947	-1.136	0.19	0.167
Roof Deck ($A_e \approx 32$ sq. ft.)	≤ 7	1	-0.95	0.868	-0.825	0.08	0.097
		2	-1.5	0.947	-1.421	0.19	0.134
		3	-1.9	0.947	-1.799	0.19	0.106
	$7 < \theta \leq 27$	1	-0.85	0.868	-0.738	0.08	0.108
		2	-1.5	0.947	-1.421	0.19	0.134
		3	-2.3	0.947	-2.178	0.19	0.087
	$27 < \theta \leq 45$	1	-0.9	0.868	-0.781	0.08	0.102
		2	-1.1	0.947	-1.042	0.19	0.182
		3	-1.1	0.947	-1.042	0.19	0.182

References: ASCE (2010) and Ellingwood and Tekie (1999)

6.2.3 Wall Component and Cladding External Pressures

Development of external pressure on local wall surfaces depends on the relative dimensions of the building and the effective wind area tributary to the element under consideration. Components that gather wind pressure from larger areas are subject to less severe pressures since the occurrence of intense, local pressures has less correlation over larger areas. Table 30.4-1 in ASCE 7-10 provides nominal values of gust pressure coefficients, GC_p , for external wall surfaces. The pressure coefficients are applicable to two different roof zones: (Zone 4) field areas that are away from edges or corners, and (Zone 5) edge areas.

For design, the ASCE 7-10 wall pressure areas are established regardless of wind direction, since wind direction is not known in advance of a high wind event. However, the damage module considers a time history of wind direction for a known event, and

therefore a time-varying classification of wall pressure zones is warranted. A wall edge may be classified as Zone 5 (edge) for some wind directions and classified as Zone 4 (field) or as receiving positive pressure for other wind directions. Figure 6-4 shows the assignment of 12 individual wall pressure areas. These figures also show eight wind direction sectors.

The assignment of the appropriate ASCE 7-10 wall pressure zone to each of the 12 areas shown in Figure 6-4 depends on the wind angle of attack (AOA) at each time step of the hazard time history. Table 6-6 shows the wall pressure zone assignments versus AOA. Table 6-7 lists the statistics for the random variable, GC_p , used in the calculation of the FOSM-MV reliability index for elements located on walls (coverings, sheathing, windows, doors, and garage doors). The nominal values in Table 6-7 for the various effective wind areas are calculated based on the underlying logarithmic function for the graphical representation of the pressure coefficient values given in ASCE 7.

The damage module assumes that there are three small windows, nine large windows, two tall windows and one picture window, and these windows are evenly distributed around the perimeter of the structure. The damage module also assumes that there is one large door and one small door, with their respective areas evenly distributed over the building perimeter.

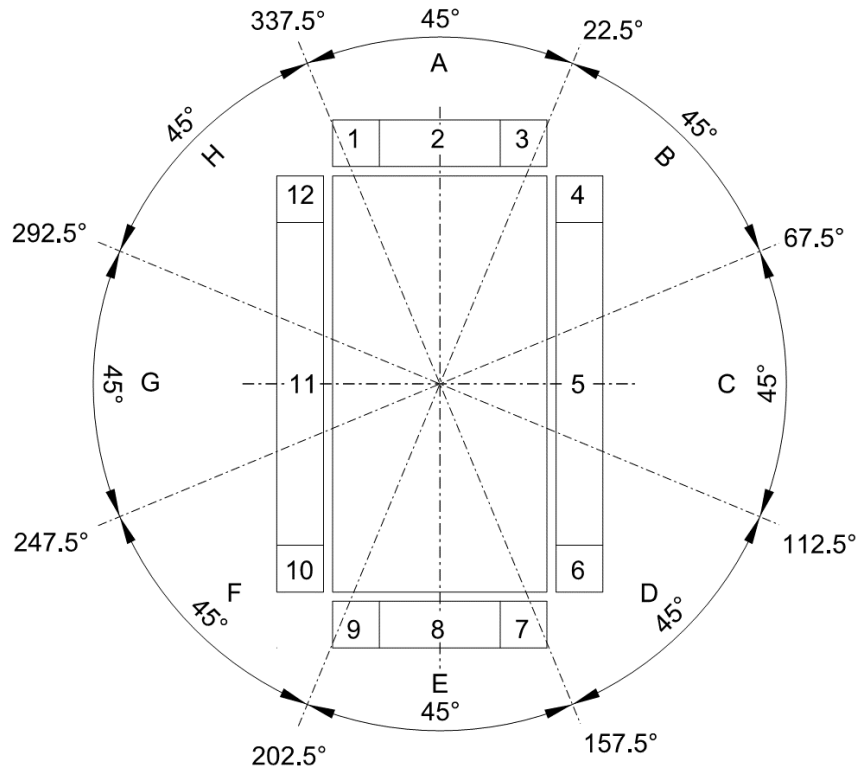


Figure 6-4: Wall Component and Cladding Areas and Wind Sectors

TABLE 6-6. WALL COMPONENT AND CLADDING PRESSURE ZONE ASSIGNMENTS AS A FUNCTION OF WIND ANGLE OF ATTACK (AOA)

Sector	AOA (deg.)	Wall Area											
		1	2	3	4	5	6	7	8	9	10	11	12
A	0-22.5	POS	POS	POS	5	4	5	5	4	5	5	4	5
B	22.5-67.5	POS	POS	POS	POS	POS	POS	5	4	5	5	4	5
C	67.5-112.5	5	4	5	POS	POS	POS	5	4	5	5	4	5
D	112.5-157.5	5	4	5	POS	POS	POS	POS	POS	POS	5	4	5
E	157.5-202.5	5	4	5	5	4	5	POS	POS	POS	5	4	5
F	202.5-247.5	5	4	5	5	4	5	POS	POS	POS	POS	POS	POS
G	247.5-292.5	5	4	5	5	4	5	5	4	5	POS	POS	POS
H	292.5-337.5	POS	POS	POS	5	4	5	5	4	5	POS	POS	POS
A	337.5-360	POS	POS	POS	5	4	5	5	4	5	5	4	5

TABLE 6-7. WALL COMPONENT AND CLADDING EXTERNAL PRESSURE COEFFICIENT STATISTICS

Element	A_e (sq. ft.)	Zone	Nominal GC_p	λ (Bias)	μ	σ	COV
Wall Cover	Minimum =	POS	1.000	0.95	0.950	0.13	0.137
	10	4	-1.100	0.9	-0.990	0.10	-0.101
		5	-1.400	0.95	-1.330	0.13	-0.098
Wall Panel	4' x 8' =	POS	0.911	0.95	0.865	0.13	0.150
	32	4	-1.011	0.9	-0.910	0.1	-0.110
		5	-1.222	0.95	-1.161	0.13	-0.112
Small Window	3.5' x 3.5' =	POS	0.984	0.95	0.935	0.13	0.139
	12.25	4	-1.084	0.9	-0.976	0.10	-0.102
		5	-1.369	0.95	-1.300	0.13	-0.100
Large Window	3.5' x 5' =	POS	0.957	0.95	0.909	0.13	0.143
	17.5	4	-1.057	0.9	-0.951	0.10	-0.105
		5	-1.314	0.95	-1.248	0.13	-0.104
Tall Window	3.5' x 6.5' =	POS	0.937	0.95	0.890	0.13	0.146
	22.75	4	-1.037	0.9	-0.933	0.10	-0.107
		5	-1.274	0.95	-1.210	0.13	-0.107
Picture Window	6.5' x 6.5' =	POS	0.889	0.95	0.845	0.13	0.154
	42.25	4	-0.989	0.9	-0.891	0.10	-0.112
		5	-1.179	0.95	-1.120	0.13	-0.116
Small Door	3' x 6.67' =	POS	0.947	0.95	0.899	0.13	0.145
	20	4	-1.047	0.9	-0.942	0.10	-0.106
		5	-1.294	0.95	-1.229	0.13	-0.106
Large Door	6' x 6.67' =	POS	0.894	0.95	0.849	0.13	0.153
	40	4	-0.994	0.9	-0.894	0.10	-0.112
		5	-1.187	0.95	-1.128	0.13	-0.115
Single Garage Door	9' x 6.67' =	POS	0.863	0.95	0.819	0.13	0.159
	60	4	-0.963	0.9	-0.866	0.10	-0.115
Double Garage Door	18' x 6.67' =	POS	0.809	0.95	0.769	0.13	0.169
	120	4	-0.909	0.9	-0.818	0.10	-0.122
Wall Studs	8' x 1.33' =	POS	0.995	0.95	0.945	0.13	0.137
	10.64	4	-1.095	0.9	-0.986	0.10	-0.101
		5	-1.390	0.95	-1.321	0.13	-0.098

References: ASCE (2010), Ellingwood and Tekie (1999), and FPHLM (2005)

6.2.4 Roof Main Wind Force Resisting System (MWFRS) External Pressures

Development of external pressure on roof surfaces tributary to roof framing depends on the relative dimensions of the building, the slope of the roof, and the direction of the wind. Figure 27.4-1 in ASCE 7-10 provides nominal values of pressure coefficients, C_p , for external roof surfaces. The pressure coefficients are tabulated for windward and leeward roof surfaces (when the wind is directed perpendicular to the roof ridge) and for portions of the roof surface along the length of the building when the wind is directed parallel to the roof ridge. The tabulated values for C_p vary with the roof slope, θ , and the height to length ratio of the building.

For design, the ASCE 7-10 MWFRS roof pressures must consider the worst condition for all wind directions, since wind direction is not known in advance of a high wind event. However, the Damage Estimation Module considers a time history of wind direction for a known event, and therefore a time-varying classification of roof surfaces is required. A roof surface may be classified as a windward surface for some wind directions and a leeward surface for other wind directions. Figures 6-5 and 6-6 show the four wind direction sectors for gable and hip roofs, respectively. The assignment of the appropriate ASCE 7-10 roof surface classification to each of the areas shown in Figure 6-5 and Figure 6-6 depends on the wind angle of attack (AOA) at each time step of the hazard time history.

Table 6-8 and Table 6-9 show the roof surface assignment versus AOA for gable and hip roof areas, respectively. Figure 6-7 and Figure 6-8 show the nominal values of the external roof pressure coefficients for windward and leeward roofs, respectively, when the wind is directed perpendicular to the ridge. Table 6-10 lists the nominal values of the external roof pressure coefficients when the wind is directed parallel to the ridge (or the roof has a slope less than 10 degrees). The damage module interpolates to find pressure coefficient values that fall between those that are plotted or tabulated. Table 6-11 lists the statistics for the random variable, C_p , used in the calculation of the FOSM-MV reliability index for roof framing elements.

The Damage Estimation Module considers roof framing elements to be part of the MWFRS since the uplift forces tributary to the entire roof truss or rafter is being compared to the uplift capacity of a roof-to-wall connector. This approach is consistent

with the commentary to ASCE 7-10 which states, “The engineer needs to use appropriate loadings for design of components, which may require certain components to be designed for more than one type of loading, for example, long-span roof trusses should be designed for loads associated with MWFRS, and individual members of trusses should also be designed for component and cladding loads.”

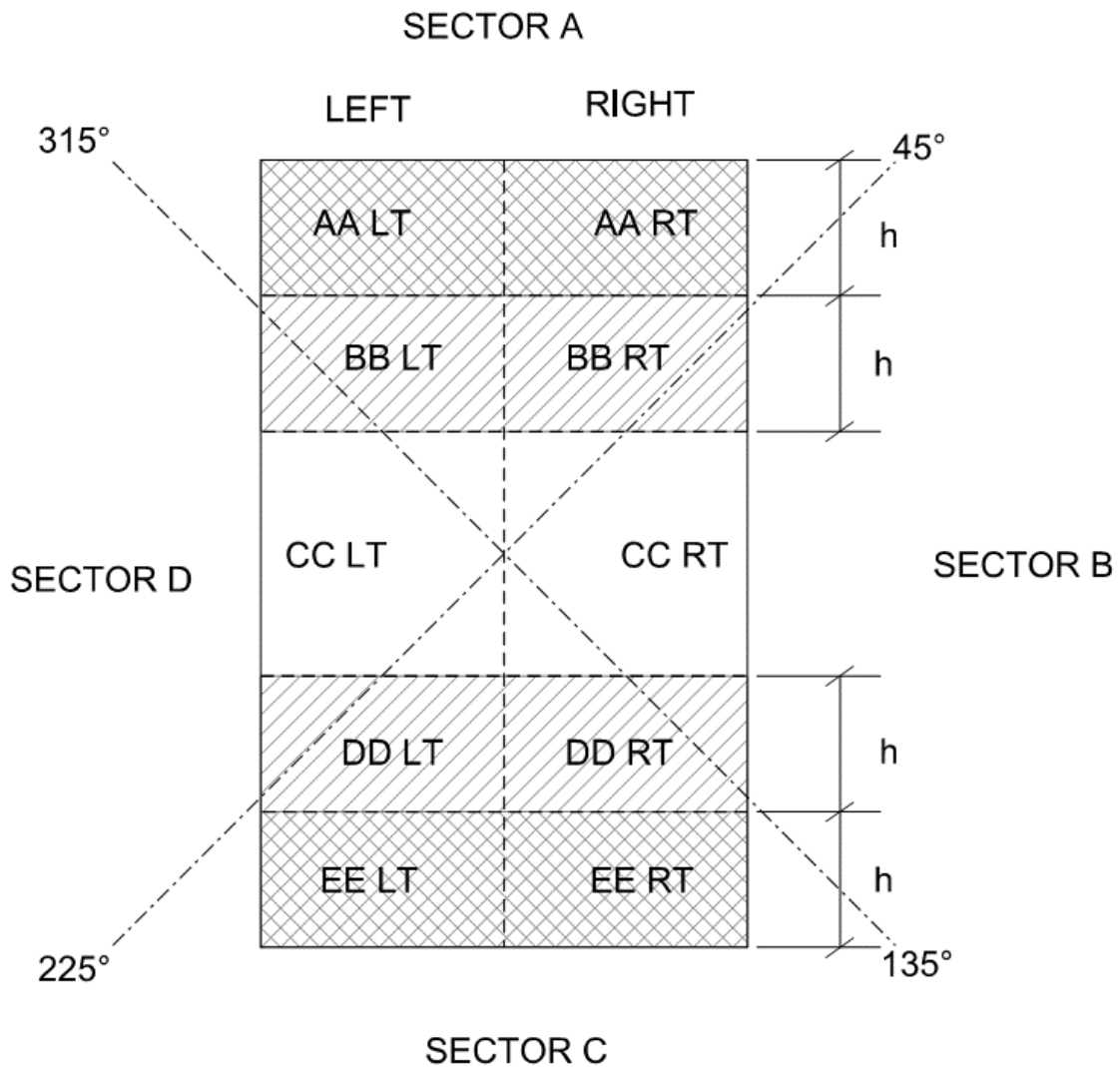


Figure 6-5: Gable Roof Wind Direction Sectors, A through D for MWFRS Loads.
 The left and right sides of the roof ridge are identified. Distances along the roof parallel to the ridge correspond to the mean roof height, h .

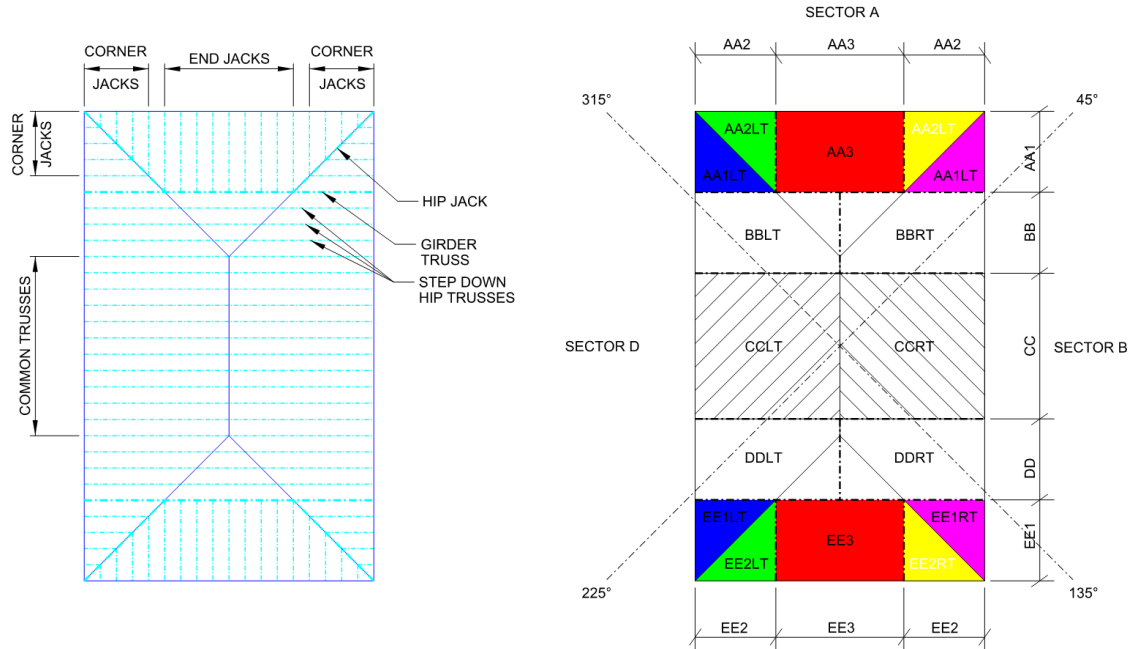


Figure 6-6: Hip Roof Wind Direction Sectors, A through D, for MWRFS Loads.

The north, south, east, and west sides of the roof are identified. Distances from windward edges AA1, BB, DD, and EE1 correspond to the mean roof height, h .

TABLE 6-8. GABLE ROOF MWFRS SURFACE CLASSIFICATIONS FOR FRAME AREAS WITH RESPECT TO WIND ANGLE OF ATTACK (AOA)

Sector	AOA (deg.)	Roof Frame Areas									
		AA LT	BB LT	CC LT	DD LT	EE LT	AA RT	BB RT	CC RT	DD RT	EE RT
A	0-45	1	2	3	3	3	1	2	3	3	3
B	45-135	5	5	5	5	5	4	4	4	4	4
C	135-225	3	3	3	2	1	3	3	3	2	1
D	225-315	4	4	4	4	4	5	5	5	5	5
A	315-360	1	2	3	3	3	1	2	3	3	3

Zone Legend:

- 1 Windward edge from 0 to h when wind is approaching parallel to ridge or perpendicular to ridge for roof slope less than 10 degrees.
- 2 Windward zone from h to 2h when wind is approaching parallel to ridge or perpendicular to ridge for roof slope less than 10 degrees.
- 3 Remaining zones when wind is approaching parallel to ridge or perpendicular to ridge for roof slope less than 10 degrees.
- 4 Windward roof when wind is perpendicular to ridge for roof slope greater than or equal to 10 degrees.
- 5 Leeward roof when wind is perpendicular to ridge for roof slope greater than or equal to 10 degrees.

TABLE 6-9. HIP ROOF MWFRS SURFACE CLASSIFICATIONS FOR FRAME AREAS WITH RESPECT TO WIND ANGLE OF ATTACK (AOA)

Sector	AOA (deg.)	Hip Roof Frame Areas															
		AA1LT	AA2LT	BBLT	CCLT	DDL	EE1LT	EE2LT	AA1RT	AA2RT	BBRT	CCRT	DDRT	EE1RT	EE2RT	AA3	EE3
A	0-45	1	4	2	3	3	3	5	1	4	2	3	3	3	5	4	4
B	45-135	5	3	5	5	5	5	3	4	1	4	4	4	4	1	3	3
C	135-225	3	5	3	3	2	1	4	3	5	3	3	2	1	4	5	5
D	225-315	4	1	4	4	4	4	1	5	3	5	5	5	5	3	3	3
A	315-360	1	4	2	3	3	3	5	1	4	2	3	3	3	5	4	4

Zone Legend:

- 1 Windward edge from 0 to h when wind is approaching parallel to ridge or perpendicular to ridge for roof slope less than 10 degrees.
- 2 Windward zone from h to 2h when wind is approaching parallel to ridge or perpendicular to ridge for roof slope less than 10 degrees.
- 3 Remaining zones when wind is approaching parallel to ridge or perpendicular to ridge for roof slope less than 10 degrees.
- 4 Windward roof when wind is perpendicular to ridge for roof slope greater than or equal to 10 degrees.
- 5 Leeward roof when wind is perpendicular to ridge for roof slope greater than or equal to 10 degrees.

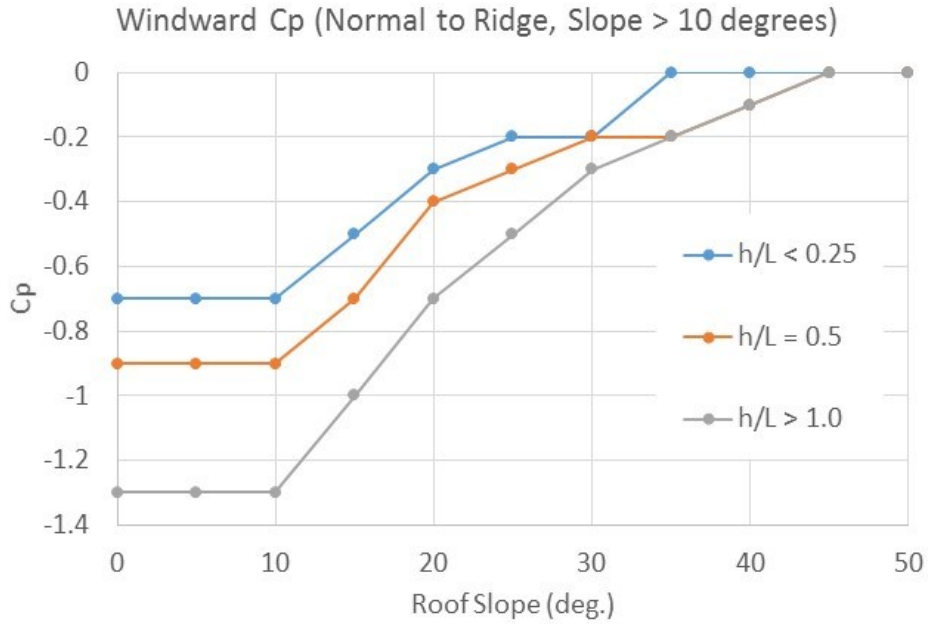


Figure 6-7a: Nominal MWFRS Windward Roof Pressure Coefficients, Uplift Case, Wind Perpendicular to Ridge (ASCE, 2010)

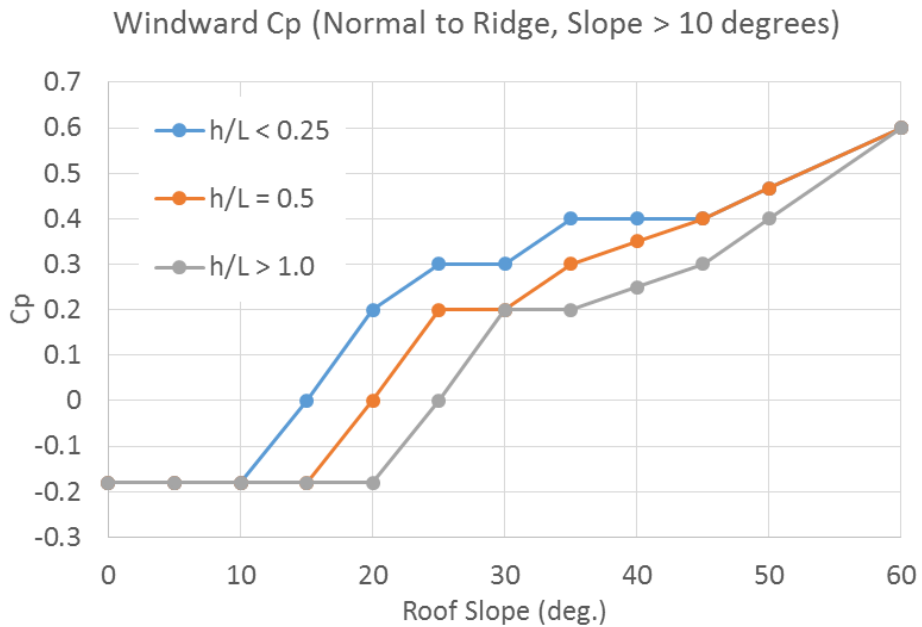


Figure 6-7b: Nominal MWFRS Windward Roof Pressure Coefficients, Gravity Case, Wind Perpendicular to Ridge (ASCE, 2010)

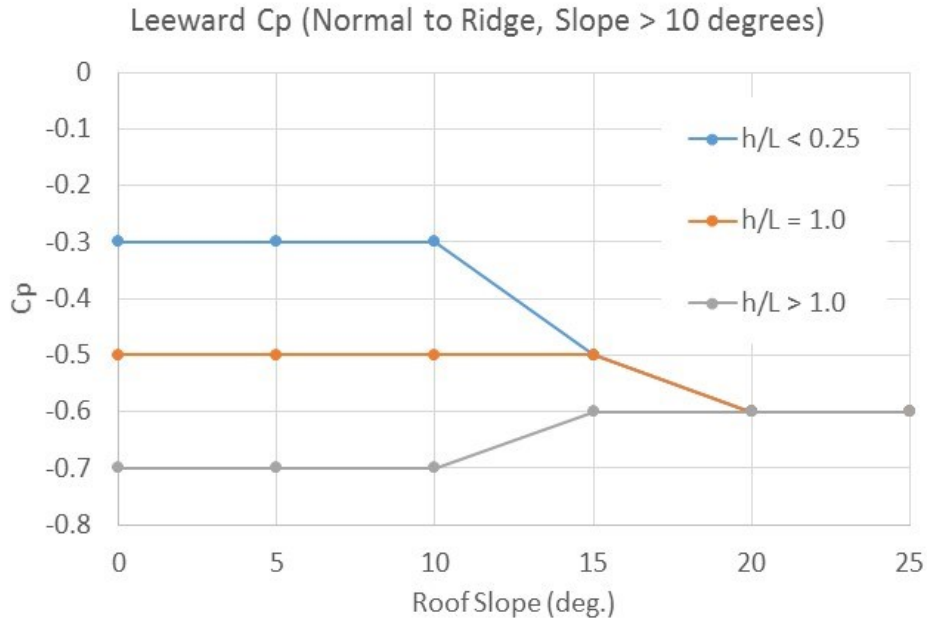


Figure 6-8a: Nominal MWFRS Leeward Roof Pressure Coefficients, Uplift Case, Wind Parallel to Ridge (ASCE, 2010)

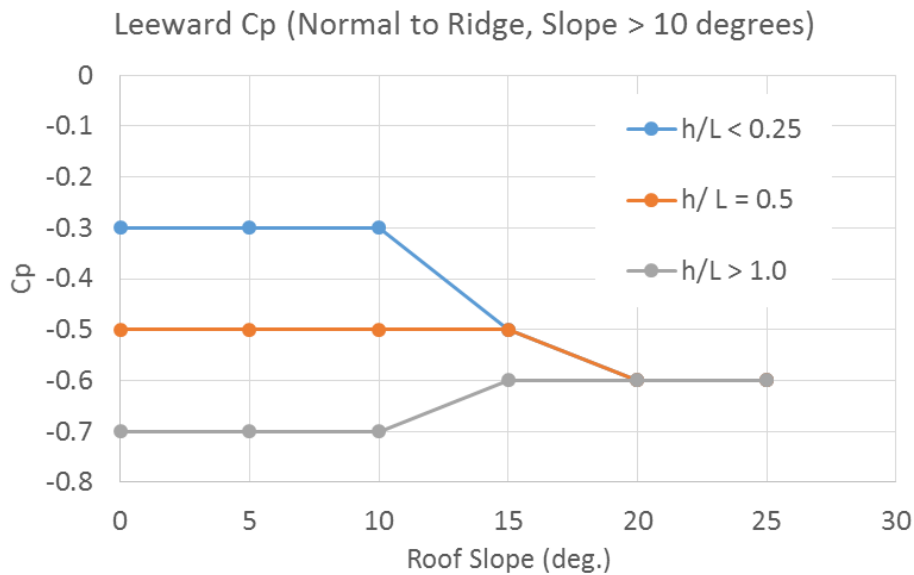


Figure 6-8b: Nominal MWFRS Leeward Roof Pressure Coefficients, Gravity Case, Wind Parallel to Ridge (ASCE, 2010)

TABLE 6-10. NOMINAL MWFRS ROOF PRESSURE COEFFICIENTS FOR SLOPE LESS THAN 10 DEGREES OR WIND PARALLEL TO RIDGE

Zone	h/L	
	< 0.5	> 1.0
1 (0 to h)	-0.9	-1.3
2 (h to 2h)	-0.5	-0.7
3 (>2h)	-0.3	-0.7

Ref. ASCE (2010)

TABLE 6-11. ROOF MWFRS EXTERNAL PRESSURE COEFFICIENT STATISTICS

Zone	λ	σ
1	0.885	0.15
2	0.885	0.15
3	0.871	0.05
4	0.986	0.14
5	0.85	0.05

Ref. Ellingwood and Tekie (1999)

6.2.5 Wall Main Wind Force Resisting System (MWFRS) External Pressures

MWFRS wind pressures acting on both roof and wall surfaces must be resisted by shear walls. Development of wall pressures depends on the relative dimensions of the building, and the direction of the wind with respect to the wall of interest. Figure 27.4-1 in ASCE 7-10 provides nominal values of pressure coefficients, C_p , for external wall surfaces. The pressure coefficients are tabulated for windward, leeward, and side wall surfaces.

The nominal value for the windward wall pressure coefficient is a constant 0.8, regardless of building geometry. The nominal values of the leeward wall pressure coefficient vary with respect to the length/width aspect ratio of the building (L/B), where the length, L , is the plan dimension of the building parallel to the wind direction, and the width, B , is the plan dimension of the building perpendicular to the wind direction. The variation of the nominal value of the leeward wall pressure coefficient with respect to plan aspect ratio is shown in Figure 6-9. Side wall pressures are neglected since their effects cancel when considering loads to the lateral force resisting system.

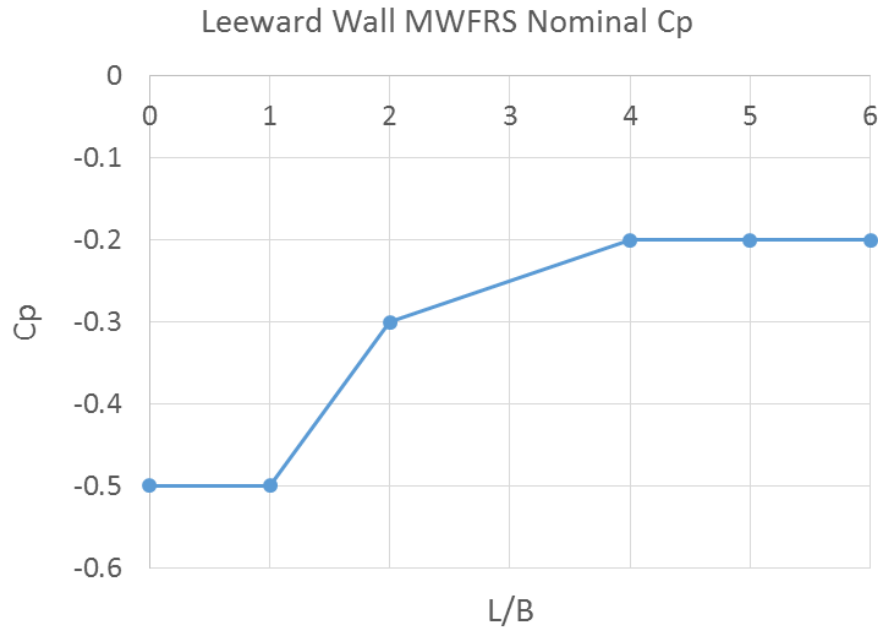


Figure 6-9: Variation of Leeward Wall MWFRS C_p with Building Plan Aspect Ratio, L/B (ASCE 7-10)

The Damage Estimation Module considers a time history of wind direction for a known event, and therefore a time-varying classification of wall surfaces is required. A wall surface may be classified as a windward surface for some wind directions and a leeward surface for other wind directions. The assignment of the appropriate ASCE 7-10 wall surface classification to each wall depends on the wind angle of attack (AOA) at each time step of the hazard time history.

Figure 6-10 identifies each of four walls and shows their locations with respect to four wind direction sectors. Table 6-12 shows the wall surface assignment versus AOA. Table 6-13 lists the statistics for the random variable, C_p , used for windward and leeward walls in the calculation of the FOSM-MV reliability index for shear walls. Half of the windward and leeward wall areas that are tributary to the tops of the shear walls via the ceiling diaphragm are considered to gather loads when evaluating the shear walls.

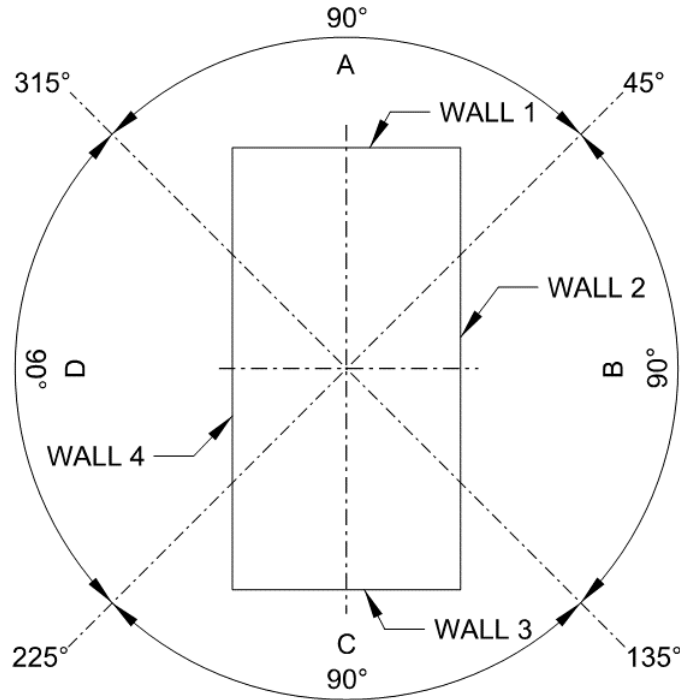


Figure 6-10: MWFRS Wall Numbers, 1 – 4, with respect to Four Wind Direction Sectors, A – D

TABLE 6-12. MWFRS WALL CLASSIFICATIONS AS WINDWARD (WW), SIDE (SW), OR LEEWARD (LW) WITH RESPECT TO WIND DIRECTION SECTOR

Sector	AOA (deg.)	Wall 1	Wall 2	Wall 3	Wall 4
A	0-45	WW	SW	LW	SW
B	45-135	SW	WW	SW	LW
C	135-225	LW	SW	WW	SW
D	225-315	SW	LW	SW	WW
A	315-360	WW	SW	LW	SW

TABLE 6-13. WALL MWFRS EXTERNAL PRESSURE COEFFICIENT (C_p) STATISTICS

Wall	Nominal	λ	σ
WW	0.8	0.875	0.1
LW	Fig. 27.4-1	0.94	0.07

Ref. Ellingwood and Tekie (1999) and ASCE (2010)

6.2.6 Gust Effect Factor

The gust effect factor, G , is used to relate a mean pressure or response to a peak pressure or response for design. The gust effect factor combines the effects of two phenomena: (1) the relative size of the structure compared to that of a typical gust of wind, and (2) the tendency of the structure to be excited dynamically in the along-wind direction. The value of the gust effect factor depends on the turbulence characteristics of the approaching wind flow, the size of the structure, and the natural frequency of the structure. For small, relatively rigid structures such as the coastal residences considered by the damage module, ASCE 7-10 allows designers to use a value of 0.85 for this factor.

Ellingwood and Tekie (1999) report the following statistics for the gust effect factor (Table 6-14), which have been incorporated into the FOSM-MV reliability index computed in the damage module. It should be noted that the paper by Ellingwood and Tekie refers to an earlier version of ASCE 7. The nominal value for the gust effect factor in Exposure B is 0.85 in the current version. However, the mean value in Table 6-14 for Exposure B is used in the damage module since it reflects the combined opinion of 20 expert respondents that participated in the authors' research and described in their paper.

TABLE 6-14. GUST EFFECT FACTOR, G , STATISTICS

Exposure	Nominal	λ	μ	σ
B	0.8	0.9625	0.77	0.09
C	0.85	0.9647	0.82	0.08
D	0.85	0.9765	0.83	0.07

Ref. Ellingwood and Tekie (1999)

6.3 Performance Functions

This section of the report describes performance functions that are applicable to each component considered in the Damage Estimation Module. The performance functions have been established for wood-frame construction only. The majority of coastal residences considered by the Damage Estimation Module will consist of wood-frame construction. Future improvements to the Damage Estimation Module may include the addition of masonry wall structures. Limiting the consideration to wood-frame

construction would result in conservative estimates of wind-induced structural collapse, since the other likely construction type, concrete masonry unit walls, would generally be more resistant to collapse.

For the majority of wind damage modes (those that affect cladding and roof components and framing), the distinctions between wall construction type will be less important since window, door, and roof construction will be similar, regardless of the wall structure type. Furthermore, sometimes distinctions are made in the insurance industry between construction types that are designated “frame,” “brick,” “stucco,” etc. These distinctions often refer to the external wall covering, and probably do not consider the underlying structure of the wall. These distinctions are relevant to fire resistance rather than wind resistance. For example, it is the experience of the Panel members that structures classified as “brick” often have a brick veneer over a wood frame.

The general form of the performance function was given in Equation 6-1. The functions presented here will include all of the variables, both deterministic and random, that are considered in the calculation of the FOSM-MV reliability index. The expressions for resistance in the performance functions include two reduction factors. One of these factors considers general conditions that affect the initial construction quality of a structure. The other factor considers variations in quality for specific components, due to both common installation defects and deterioration over time, as applicable. The values of these reduction factors were developed from an elicitation of opinions outside of the Expert Panel. This elicitation effort is described in Section 6.5.

6.3.1 Cladding Element Performance Functions

Several cladding elements considered in the damage module have the same performance function form. The functions compare the component and cladding (C&C) wind pressure to the capacity of the cladding element, which is expressed directly in units of pressure. Equation 6-10 shows this functional form, which has been applied to roof covering, roof panels, wall covering, wall panels, windows, doors, and garage doors in the damage module.

$$g = C_1 \cdot C_2 \cdot R - 0.00256 \cdot K_z \cdot (V^2) \cdot (GC_p \pm GC_{pi}) \quad (\text{Eq. 6-10})$$

Where

C_1 = Construction variability reduction factor (no units);

C_2 = Component variability reduction factor (no units);

R = Component resistance (pounds per square foot);

and all other variables are as defined previously.

Equation 6-10 is a function of seven random variables. Therefore, seven direction cosines, a_1 through a_7 are also established according to Equation 6-5. The direction cosines are partial derivatives of the performance function with respect to each random variable and are shown explicitly in the example calculations to follow.

6.3.2 Wall Stud Bending Performance Function

The failure probability of wall studs in out-of-plane bending is used as one of the criteria in the damage module to determine whether a structure is at risk for collapse due to wind loads. Equation 6-11 shows the performance function for this limit state.

$$g = C_1 \cdot \left(144 \frac{\text{psf}}{\text{psi}} \right) \frac{8 \cdot C_r \cdot S_x \cdot F_b}{s \cdot l^2} - 0.00256 \cdot K_z \cdot (V^2) \cdot (GC_p \pm GC_{pi}) \quad (\text{Eq. 6-11})$$

Where

C_r = Repetitive use factor (no units), which is taken as deterministic with a value of 1.15 (AWC, 2014a);

S_x = Section modulus (in^3) of the composite section formed by a nominal 2" x 4" wall stud and 3/8" thick sheathing, spaced at 16" on center, which is taken as deterministic with a value of 5.727 in^3 ;

F_b = Rupture stress of wood in bending (psi);

s = stud spacing (in);

l = stud length (in);

and all other variables are as defined previously.

Equation 6-11 is a function of eight random variables. Therefore, eight direction cosines, a_1 through a_8 are also established according to Equation 6-5. The direction cosines are partial derivatives of the performance function with respect to each random variable and are shown explicitly in the example calculations to follow.

6.3.3 Wall Stud to Plate Connection Performance Function

The failure probability of the connection of wall studs to top and bottom plates is used as one of the criteria in the damage module to determine whether a structure is at risk for collapse due to wind loads. The fastening of the wall studs to the top and bottom plates is considered to consist of an end nailed connection, as prescribed by the 2015 Wood Frame Construction Manual (AWC, 2014b). No additional manufactured stud-to-plate connector was assumed to be used in this connection. Equation 6-12 shows the performance function for this limit state.

$$g = C_1 \cdot \left(144 \frac{\text{psf}}{\text{psi}} \right)^2 \frac{C_{eg} \cdot K_f \cdot N \cdot Z}{s \cdot l} - 0.00256 \cdot K_z \cdot (V^2) \cdot (GC_p \pm GC_{pi}) \quad (\text{Eq. 6-12})$$

Where

C_{eg} = End grain factor (no units), which is taken as deterministic with a value of 0.67 (AWC, 2014a);

K_f = Format conversion factor (no units), which is taken as a deterministic variable with a value of 3.32 (AWC, 2014a);

N = Number of 16d nails required, taken deterministically as 2 for 8' walls and 3 for 9' and 10' walls (AWC, 2014b)

Z = Lateral capacity for fastener in pounds (AWC, 2014a);

s = stud spacing (in);

l = stud length (in);

and all other variables are as defined previously.

Equation 6-12 is a function of eight random variables. Therefore, eight direction cosines, a_1 through a_8 are also established according to Equation 6-5. The direction cosines are partial derivatives of the performance function with respect to each random variable and are shown explicitly in the example calculations to follow.

6.3.4 Roof Frame to Wall Connection Performance Function

Roof frame damage is estimated based on the probability of uplift failure of the mechanical connection between the roof framing (rafter or truss) and the wall top plate. The fastening of the roof framing to the wall top plates is considered to consist of a connection with nominal capacity prescribed by the 2015 Wood Frame Construction

Manual (AWC, 2014b). The performance function for this limit state is shown in Equation 6-13.

$$g = C_1 \cdot C_2 \cdot R - [0.00256 \cdot K_z \cdot (V^2) \cdot (G \cdot C_p \pm GC_{pi}) - D] \cdot A_t \quad (\text{Eq. 6-13})$$

Where

R = uplift resistance of roof-to-wall connection (pounds);

D = Roof dead load, taken deterministically as 10 pounds per square foot;

A_t = roof area tributary to the uplift connection (square feet), which is based on building characteristics and is taken as a deterministic variable;

and all other variables are as defined previously.

Equation 6-13 is a function of eight random variables. Therefore, eight direction cosines, a_1 through a_8 are also established according to Equation 6-5. The direction cosines are partial derivatives of the performance function with respect to each random variable and are shown explicitly in the example calculations to follow.

6.3.5 Shear Wall Performance Function

The failure probability of wood-framed shear walls is used as one of the criteria in the damage module to determine whether a structure is at risk for collapse due to wind loads. The available length of shear walls in directions both parallel and perpendicular to the roof ridge is as prescribed by the 2015 Wood Frame Construction Manual (AWC, 2014b). Equation 6-14 shows the shear wall performance function.

$$g = C_1 \cdot C_2 \cdot (L_{sw} \cdot R_{sw} + L_{gyp} \cdot R_{gyp}) - 0.00256 \cdot K_z \cdot V^2 \cdot \text{abs}(\cos(\alpha)) \cdot G \cdot [C_{p_{ww}} \cdot A_{ww} - C_{p_{lw}} \cdot A_{lw} + (C_{p_{wr}} \cdot A_{wr} - C_{p_{lr}} \cdot A_{lr}) \cdot \sin(\theta)] \quad (\text{Eq. 6-14})$$

Where

L_{sw} = Length of wood panel shear wall available for load direction under consideration (feet);

R_{sw} = Resistance capacity of wood panel shear walls (pounds per foot);

L_{gyp} = Length of gypsum board shear wall available for load direction under consideration (feet);

R_{gyp} = Resistance capacity of gypsum board shear walls (pounds per foot);

α = Wind Angle of Attack (AOA) relative direction under consideration, deterministic (degrees);

$C_{p_{ww}}$ = Windward wall MWFRS pressure coefficient (no units);

A_{ww} = Half of area of windward wall (square feet), considered to be a deterministic variable;

$C_{p_{lw}}$ = Leeward wall MWFRS pressure coefficient (no units);

A_{lw} = Half of area of leeward wall (square feet), considered to be a deterministic variable;

$C_{p_{wr}}$ = Windward roof MWFRS pressure coefficient (no units);

A_{wr} = Area of windward roof (square feet), considered to be a deterministic variable;

$C_{p_{lr}}$ = Leeward roof MWFRS pressure coefficient (no units);

A_{lr} = Area of leeward roof (square feet), considered to be a deterministic variable;

θ = Roof slope (degrees), considered to be a deterministic variable;

and all other variables are as defined previously.

Equation 6-14 is a function of thirteen random variables. Therefore, 13 direction cosines, a_1 through a_{13} are also established according to Equation 6-5. The direction cosines are partial derivatives of the performance function with respect to each random variable and are shown explicitly in the example calculations to follow.

6.4 Determination of Component Resistance to Wind Damage

Damage to buildings or components of buildings occurs when loads, Q , exceed resistances, R ($R - Q < 0$). Significant information is in the literature regarding the resistance of various residential building components primarily based on physical testing. However, there is significant variation in the published results, thus presenting challenges in determining the reasons for the differences, and in recommending the resistance values to use in the Damage Estimation Module.

The Damage Estimation Module includes specified resistances for 11 components or assemblies. Background for the currently specified resistance of each component or assembly is briefly described in separate sections. The summary means and standard

deviations for each component and assembly are summarized at the end of this section in Table 6-17.

Establishment of component and system resistance values in the recommended methodology is inherently flexible. The underlying structure of the reliability analysis is not affected by selecting different resistance statistics as long as the performance functions remain the same. In fact, the resistance statistics are probably the best parameters to modify when calibrating the Damage Estimation Module to better match observations of damage. As such, the resistance statistics presented here, and used initially in the subsequent demonstration of the recommended methodology, should be treated as reasonable initial values that may be subject to change.

6.4.1 Roof Cover

The Damage Estimation Module has the capacity to consider a variety of roof cover types and resistances, but so far there is insufficient data to distinguish the capacities of other types of coverings from that of asphalt shingles. Asphalt shingles are the predominant roof covering material used on residential buildings, and are adequate as a default material. There are many other types of roof covering products including metal panels, clay and ceramic tile, single ply membranes, modified bitumen, and wood shakes, and these products are discussed below.

Shingle coverings are rated by wind speed and then grouped into classes. The classes are D, G, and H with wind speed ratings of 90 mph, 120 mph, and 150 mph, respectively, according to ASTM D 7158 (ASTM 2011). The wind speed ratings in this ASTM Standard are established by relating the test pressure to the ASCE 7 wind pressure equations; considering a Risk Category of II or less; the worst case roof slope for the development of roof uplift pressure; a ground surface roughness category of C or rougher; and a building height of 60 feet or less. The HAZUS Technical Manual (FEMA 2012) does not stipulate a specific resistance value for asphalt roof covering.

A recent doctoral dissertation covers shingle installation and expected resistance in some detail (Dixon, 2013). It was written to address shingle failure modes and disparities in shingle performance based on estimated wind speeds and age. The dissertation specifically describes shingle bond strip strength, and highlights the role that

variations in bond strength have on ultimate resistance. The failure mode for asphalt shingles is uplift of the shingle caused by failure of the bond strip due to the pressure difference between the top and bottom of the shingle.

The dissertation also discusses the effect age has on the bond strength. The likely reduction in bond strength is estimated to be 10 percent over 7 to 13 years, and 25 percent over 14 to 20 years. This estimated strength reduction matches well with the age reduction on shingles suggested by the results of the elicitation panel discussed in Section 6.5 (10 percent reduction in 10 years, and 22 percent reduction in 20 years). The suggested mean resistance (lbs) provided by the normal bond strip as tested during the research is 37 lbs. This value equates to approximately 150 psf on the shingle bond strip surface.

The Florida Public Hurricane Loss Model (FPHLM) uses 70 psf for predicted pressure that would separate asphalt shingles from the roof surface. The FPHLM suggests that the Coefficient of Variation (COV) is 0.4 representing a wide range of possible resistance values. This resistance value was determined by combining interpretations of capacities implied by test standards and those implied by the building code. In the absence of more definitive data, and considering that the results of the Damage Estimation Module appear to align well with damage observations, the resistance value used in the TWIA Damage Estimation Module is 70 psf with a 0.4 COV.

The Texas Department of Insurance (TDI) has many roof products that have been tested in accordance with the ICC building code protocols (which reference applicable ASTM test standards). These products have been tested for both positive and negative pressure. The default value for roof cover resistance did not use this test data since the roof cover rating of a product actually used on the roof is often not known. If a certain product that has been tested in accordance with ICC protocols is used on a building, then the actual negative test pressure could be used as the expected ultimate resistance when increased by the rated factor of safety. TDI uses a factor of safety of 2.0 on all roof coverings. A COV would need to be determined from the mean tested pressures for the specified roof covering material.

6.4.2 Roof Panel

Roof panels fail in uplift from high winds. This failure can occur because of a loss of nailing resistance due to overdriven nails, nails that do not penetrate a roof framing member, or a roof panel that pulls over the nails. The variations in the failure modes can be caused by differences in panel thickness, panel material (e.g. plywood, OSB), nail size and type used for attachment, attachment method (e.g. nail gun, hammer driven), nail spacing, and the lumber species used for roof framing.

The roof panel resistance is specified in pounds per square foot (psf). The calculated ultimate resistance for panel uplift, is 124 lbs. per nail or 248 psf if the nails are spaced 6" on center which is the required spacing for many (not all) high wind areas. The COV for the IRC nail size and spacing variations is 0.27. The calculated ultimate resistance was based on materials and nails specified by the International Residential Code (IRC, 2012) and the ultimate resistances for nail embedment developed from the National Design Specification for Wood (NDS, 2012).

Roof panel uplift pressure resistances using the American Wood Council Wood Frame Construction Manual (WFCM, 2012) Table 2.4 suggests a pressure of 113 psf in the roof corner zone adjusted for Exposure C. The corner pressure of an overhang is 140 psf when adjusted for Exposure. This resistance requirement is deterministic, and hence there is no associated COV. The nail pattern required for roof panels is 6 in. on center along the panel edges and 6 in. on center in the field of the panel (6:6).

In situ nail withdrawal tests of nails from homes tested in Florida (Prevatt, 2014) had nail withdrawal values of 37.8 lb/in to 163 lb/in for 6d and 8d nails. This equates to a range of withdrawal capacity of 72 lbs. per nail to 346 lbs. per nail or a resistance of 144 psf to 692 psf. The COV for these tests ranged from 0.4 to 0.91.

A report by HUD (HUD, 1999) on nail withdrawal tests conducted by Clemson in 1995 found single nail withdrawal capacities ranging from 169 psf (COV = 0.41) to 131 psf (COV = 0.14) depending on whether the failure mode was a single nail in withdrawal or sheathing panel failure. It was found that roof panels will frequently fail completely once a fastener is compromised, thus suggesting that the largest tributary area will likely contribute to the nail failure. In addition, code minimum resistance statistics were

developed for single nails spaced 6 in. on center and determined that the resistance should be 61 psf with COV of 0.11.

The HAZUS loss model (FEMA, 2012) uses a lognormal distribution for sheathing panel resistance attached with 8d nails and determines the resistance has a mean value of 103 psf with a COV of 0.11. Attachment with 6d nails had a mean resistance of 54.6 psf with a COV of 0.11. HAZUS refers to studies conducted by Clemson, also referred to in the HUD report on Hurricane Andrew results (HUD, 1999), and suggests roof sheathing resistance should be multiplied by a factor of 2.2 because of differences in the specific gravity of the framing lumber to which the roof sheathing was attached. The suggested increase by a 2.2 factor would increase the roof panel resistance determined by Clemson to $61 \text{ psf} \times 2.2 = 134 \text{ psf}$.

The FPHLM uses a mean of 150 psf and a COV of 0.4 for roof panel resistance. The results are based on actual load tests of average failure pressures for entire roof sheathing panels on eight homes located in South Carolina. The COV of those tests was not used by FPHLM however because of the small sample size. Instead a COV = 0.4 was selected to better reflect homes built in Florida using different lumber species and workmanship quality.

After consideration of the variation in the possible roof panel resistances, the Damage Estimation Module selected the mid-point of the resistances developed by FPHLM and the 1999 HUD report and so uses 140 psf with a 0.4 COV as the roof panel resistance.

6.4.3 Wall Cover

The mean resistance rating of wall coverings is taken from the TDI product evaluation reports (TDI, 2015) and the associated test values. It is believed that wall coverings are attached sufficiently different from roof coverings so as not to behave the same way as roof coverings in a high wind. Most wall covering products are interlocking in some way or are inherently integrated together during the course of installation to create different failure modes than roof coverings.

The mean resistance rating of wall cover from the TDI product evaluation reports (TDI, 2015) is 62.75 psf in suction pressure. The COV is 0.38. The products tested include brick panels, EIFS, fiber cement, formed metal panels, lap and panel siding, and vinyl

siding. A factor of safety of 3.0 was multiplied by the rated test pressures to account for ultimate failure pressures.

After consideration of the variation in the possible wall cover resistances, the Damage Estimation Module selected the resistance developed from TDI product evaluation reports (TDI, 2015) of 200 psf (that includes a factor of safety) with a 0.38 COV as the wall cover resistance.

6.4.4 Wall Sheathing

The failure mode for wall sheathing, installed directly onto the wall framing and under the wall cover, is expected to be similar to roof sheathing panels. One exception is the nailing pattern required by the WFCM which is 6:12. The tributary area for a fastener in the field of a roof panel when rafters are spaced 24" o.c. is 1.00 sf. The tributary area for a fastener in the field of a wall panel when studs are spaced 16" o.c. is 1.33 sf. This increase in tributary area per fastener reduces the resistance by 25 percent. Therefore, the Damage Estimation Module uses 105 psf with a 0.4 COV.

6.4.5 Windows

The Damage Estimation Module specifies the mean resistance for non-impact resistant windows as 105 psf with a COV of 0.31. The mean resistance specified for impact-resistant windows is 120 psf with a 0.40 COV. The former value follows the value used by the FPHLM (2005) for small windows, and the latter value incorporates a nominal increase in capacity due to impact resistance. Although the FPHLM makes distinctions among the capacities of windows of different sizes by calculating the stress of ¼" thick plates of glass in bending, any window installed on a structure should be capable of resisting a certain design pressure, regardless of size. Therefore, the Damage Estimation Module does not make these same types of capacity distinctions.

There is also a window category titled "other/unknown" when the window type used in a particular building is not known for certain to be either non-impact or impact resistant. The mean resistance pressure and COV values for non-impact resistant windows are used for "unknown" products.

Many windows have been tested for both non-impact and impact-resistant assemblies. Some assemblies have a pre-1994 wind pressure rating and a post-1994 rating. The pre-1994 mean pressures are +/- 74 psf with a COV of 0.50 for negative pressure and 0.41 for positive pressure. The mean pressure ratings for post-1994 windows are -121 psf and +108 psf with corresponding COVs of 0.40 and 0.31, respectively. Values taken from the TDI product evaluation reports (TDI, 2015) are multiplied by a 1.5 factor of safety to convert the pressure to an ultimate resistance.

Many window protection devices such as shutters have also been tested for impact-resistance. These shutters include roll up styles, Bahama styles, accordion styles, and wood structural panels. The test results for shutters range in mean pressure values of -48 psf to -117 psf and +40 psf to +117 psf depending on the shutter type.

The HAZUS technical manual (FEMA, 2012) delineates wind resistance of windows by age. All buildings built prior to 1994 have a mean resistance of 40 psf with a 0.20 COV. Newer buildings are not provided with an assumed wind resistance.

6.4.6 Doors

Doors have been classified as small and large. The Damage Estimation Module currently considers the mean resistance of non-impact resistant doors to be 105 psf with a COV of 0.31. The mean resistance of impact-resistant doors is 120 psf with a 0.40 COV. The rationale for selecting these values is that the design resistance of doors and windows should be similar.

There is also a door category titled "other/unknown" when the door type used in a particular building is not known for certain to be either non-impact or impact resistant. The pressure and COV values for non-impact resistant doors are used for "unknown" products.

The door sizes described by the FPHLM are simply front and back doors. The mean door pressure for front doors used in the FPHLM loss model is 100 psf with a COV of 0.20. The back door is assumed to likely be larger than the front door. It is also more likely to have unprotected glazing, and is thus assigned a mean pressure of 50 psf with a COV of 0.20.

Many door assemblies have been tested for both non-impact and impact-resistant assemblies. The impact resistant products have an ultimate resistance of approximately +/- 90psf with a COV of 0.26. The non-impact rated products have an ultimate resistance of approximately +/-72 psf with a COV of 0.26. These test values cover a wide range of door sizes, door types, and manufacturers. Values taken from the TDI product evaluation reports (TDI, 2015) are multiplied by a 1.5 factor of safety to convert the pressure to an ultimate resistance.

HAZUS (FEMA, 2012) describes doors as sliding glass doors and uses 40 psf as the resistance with a COV of 0.20. The ICC 600 (ICC, 2009) hurricane standard uses -91 psf as the design pressure for both windows and doors in a 130 mph wind speed zone which represents the design wind speed along the Texas coast (equivalent to 170 mph using the ASCE 7-10 design method).

6.4.7 Garage Door

Garage doors have not been rated by size. Roll up or sectional door types are specifically recognized but both types use the current default resistance of 52 psf with a 0.30 COV. The pressure value is taken from the FPHLM although the default COV is somewhat higher than the recommended FPHLM COV of 0.20. This higher COV used in the model represents large variations in test pressure results reflected by the many door sizes and types used on garage door openings.

Many garage door assemblies have been tested for both non-impact and impact-resistant assemblies. The impact resistant products have an ultimate resistance of approximately + 63 psf and -69 psf with COVs of 0.35 and 0.32 for the respective pressures. The non-impact rated products have an ultimate resistance of approximately +48 psf and -53 psf with a COV of 0.37. These test values cover a wide range of door sizes, door types, and manufacturers.

6.4.8 Wood Stud Bending

This failure mode accounts for excessive wood stress in bending caused by wind pressure against the wall. There is variability in the grade of lumber used for wood studs, in their length, and in their spacing, all affecting the pressure at which excessive bending stress might occur.

Two species of lumber were used as the likely wood stud material: southern yellow pine (SYP) and spruce pine fir (SPF). Three grades of these materials were used as the most likely used in residential construction: Select Structural (SS), Grade #1, and Grade #2. The design values for allowable bending stress in psi (NDS, 2015) for stud grade lumber 2" – 4" wide are listed in Table 6-15.

TABLE 6-15. F_b DESIGN VALUES

Species	Select Structural	Grade #1	Grade #2
SYP	2350	1500	1100
SPF	1300	875	775

The WFCM allows wall studs to span up to 10 ft., but requires #1 SYP (or better) to be used as the material for plate heights over 9 ft. For shorter wall heights, the stud material is assumed to be either SYP #2 or SPF #2. There are no statistics on bias factors or COV for material graded #1. Therefore the values found for bias and COV (Yang, 2013) for SS and #2 materials are averaged to arrive at values for #1 material. The average bias factor used for #1 wall stud material in bending is 1.84 and the average COV is 0.343. Similarly, the Panel did not find resistance statistics for #2 SPF in the literature. So, the bias factor and COV for #2 SYP was applied to #2 SPF which are 2.099 and 0.422, respectively.

Since #1 SYP must be used for wall heights of 10 ft., the mean ultimate bending stress for this wall height is (bias factor) x (K_f LRFD conversion factor) x (SYP #1 F_b design value), or $(1.84) \times (2.54) \times (1500) = 7010$ psi. The standard deviation is $(0.343) \times (7010) = 2404$ psi. Since wall heights below 10 ft. can use both SYP and SPF, the ultimate bending stress for #2 SYP and SPF are averaged.

The ultimate bending stress for #2 SPF is calculated using information for #2 SYP since there is a lack of test data for SPF material. The ultimate bending strength for #2 SPF is (bias factor) x (K_f LRFD conversion factor) x (#2 SPF design value) or $(2.099) \times (2.54) \times (775) = 4132$ psi. The ultimate bending strength for #2 SYP is $(2.099) \times (2.54) \times (1100) = 5865$ psi. Since both materials can be used for 8 ft. and 9 ft. tall walls, a blend of the

two materials is assumed. Thus, the ultimate strength is an average of the two material strengths which yields 4998 psi. The corresponding standard deviation is 2109 psi.

In addition to development of the ultimate wall stud bending stresses, the resistance is multiplied by 1.15, the repetitive use factor used in wood framing when members are close together and able to share load. The resistance is also assumed to not just be provided by one stud, but rather by the composite action of the sheathing on the stud. In this case, the Section Modulus of one 2" x 4" stud of 3.0625 in³ is increased to 5.727 in³ when composite action with 3/8" sheathing is included in the section.

6.4.9 Wall Stud Plate Connection

The failure mode at this connection is the wood stud separating at the bottom or top wall plate. There is variability in the number of nails used to make the connection, and in how those nails are driven (end-driven through the bottom of the plate into the end grain of the stud or toe-nailed). The resistance assumes 16d (penny) nails are used in either SYP or SPF studs with shear values for nails derived from the NDS (NDS, 2014). The resistance is increased by the number of nails used, reduced by an end grain nail factor, and adjusted for use with LRFD ultimate design principles. There is no consideration for sheathing that laps over the bottom wall plate on the outside of the wall increasing resistance.

The Damage Estimation Module uses the basic shear resistance per nail at the wall plate connection of 155 lbs. when the wall height is 10 ft. or 465 lbs. at the connection. For other wall heights, the shear resistance per nail is 138 lbs. or 414 lbs. at the connection. The COV for this connection is 0.14. The shear value varies because 10 ft. walls require wood graded #1 SYP (Southern Yellow Pine) which increases the shear resistance of the nail. The FPHLM uses 1232 lbs. for a wood wall lateral failure with a 0.25 COV. HAZUS uses 776 lbs. as the estimated failure load at the stud to bottom plate connection.

6.4.10 Roof-to-Wall Connection

Roof-to-wall connections are made with a mechanical connector. This type of connection has been required for houses built near the coast since 1994. A wide range of connectors with wide ranges of capacities can be used for this connection. The

published load rating for mechanical connectors is only about 1/3 of their ultimate failure capacity. The ultimate tested capacity is expected to exceed the published ultimate capacities 95 percent of the time, so actual failure rates are expected to be very low. The resistance used in the model is developed from the WFCM (AWC, 2014) Table 2.2A of required uplift load based on roof span and dead load for Exposure C.

The resistance used in the model assumes a roof dead load of 10 psf; an ultimate resistance of the connector that is 3 times the required uplift load; and a roof framing spacing of 24". The uplift load based on roof span is a straight line function of the span. Therefore, the calculated resistance is based on the building roof span that is provided in the subject building statistics. The straight line equation is $101.46(x) + 685.29$ where 'x' is the roof span. For a predetermined set of possible roof spans, ultimate resistance values and standard deviations for the roof-to-wall connection are shown in Table 6-16.

The FPHLM indicates the roof-to-wall connector has a tensile failure mode and the connector has a mean capacity of 3720 lbs. with a COV of 0.20. The method chosen to determine resistance for the model is in good agreement with the FPHLM method. The HAZUS model uses a mean capacity of a strap for uplift resistance of 1200 lbs. with a COV of 0.3. HAZUS referenced numerous laboratory tests conducted on the capacities of both strap connections and toe-nail connections to decide what resistance values would be used for their loss model. The tested results for straps varied from 867 lbs. to 1900 lbs. with COVs ranging from 0.10 to 0.18.

Prior to 1994, toe-nail connections were the prevalent means of attaching roof framing to walls. While the current Damage Estimation Module does not cover this condition, it could be added with a 'date of construction' trigger from the building statistics (cell B45 on the Structure Description tab). The HAZUS model uses a mean uplift resistance for a toe-nailed connection of 415 lbs. with a COV of 0.25. HAZUS referenced several laboratory tests of toe-nail connection resistance and the results varied from 208 lbs. to 676 lbs. All tests were conducted on a three-8d toe-nailed connection. The prescriptive nailing requirements of the IRC yield an implied resistance of 281 lbs. with a COV of 0.28 based on a range of nail sizes and lumber species.

TABLE 6-16. ROOF-TO-WALL ULTIMATE RESISTANCE VALUES (LBS)

Roof Span (feet)*	Mean	COV	Std. Dev.
12	1903	0.2	380.6
16	2309	0.2	461.7
20	2714	0.2	542.9
24	3120	0.2	624.1
28	3526	0.2	705.2
32	3932	0.2	786.4
36	4338	0.2	867.6

* Width perpendicular to ridge.

6.4.11 Shear Wall Capacity

The possible failure of a shear wall is considered one of the ways a building collapse could occur from wind and thus is included as a failure mode. The collapse would occur because the shear wall is deflected excessively in the plane of the wall (i.e., racking), thus allowing the structure above the shear wall to collapse.

The resistance of the shear wall is the capacity of the wall in lbs./ft. of force applied along the top of the wall. There are two components to the wall – the exterior wall sheathing attached to the wall studs and the interior gypsum board attached to the studs. Both exterior and interior components contribute to the resistance and are included in this Damage Estimation Model. The model resistance of the shear wall is 913 lbs/ft. (APA, 1993) with a 0.183 COV. This is the average result from 7 laboratory load tests using 8d nails, spaced 6” on center, using 15/32” thick rated sheathing.

The FPHLM uses a shear wall failure value in their loss model of 1085 lbs./ft. with a 0.20 COV. The WFCM has published shear wall values in Table 3.17D (WFCM, 2012). The failure load for a blocked 7/16” thick structural panel attached with 8d nails spaced 6” on center on the exterior with unblocked ½” gypsum wallboard attached on the interior with 5d cooler nails spaced 7” on center is 872 lbs./ft. The recommended COV is 0.20.

6.4.12 Summary Resistances

Table 6-17 provides a summary of the current recommended resistances to use in the Damage Estimation Module. These resistances are not modified by construction or component variability factors. Such modifications are discussed in Section 6.5 of this report.

TABLE 6-17. SUMMARY OF RESISTANCES AND COVs USED IN TWIA DAMAGE ESTIMATION MODULE

Building Element or Connection	Damage Module Resistance	COV
Roof Cover	70 psf	0.40
Roof Panel Damage	140 psf	0.40
Wall Cover Damage	200 psf	0.38
Wall Sheathing	105 psf	0.40
Windows: Non-impact Resistant	105 psf	0.31
Windows: Impact Resistant	120 psf	0.40
Doors: Non-impact Resistant	105 psf	0.31
Doors: Impact Resistant	120 psf	0.40
Garage Door	52 psf	0.30
Wood Stud Bending Failure		
10 ft. Wall Height	7010 psi	0.343
< 10 ft. Wall Height	4998 psi	0.343
Wall Stud Plate Connection		
10 ft. Wall Height	465 lbs.	0.14
< 10 ft. Wall Height	414 lbs.	0.14
Roof-to-Wall Connector	See Table 6-16	0.20
Shear Wall Capacity	913 lbs./ft.	0.183

6.5 Modifications to Resistance Values

It has been observed during many post-storm damage surveys that actual construction of a building may not fully comply with building codes; prescriptive design standards such as ICC 600 or the Wood Frame Construction Manual (WFCM); material manufacturer specifications; or best practices. Widespread belief supported by such post-storm observations is that construction practices, material availability, weather, in-progress inspections, and other similar variances from ideal installations all create inherent variability in the resistance that may be achieved. This variability in resistance can occur within building component connections and construction materials.

Little research has been conducted measuring the effects of these variables on the designed resistances to imposed loads. It therefore is difficult to quantify the impact of these variables. One exception is from HAZUS Technical Manual v2.1 (FEMA, 2012) which describes a loss estimation model used by wind engineers.

Chapter 6 of the HAZUS Technical Manual considers workmanship factors in the nailing of wood frame materials together. It suggests a resistance reduction of between 0.2 and 0.25 for each of five different nailed connections. The HAZUS manual says that “there are no data available for variability for wood structures ... and strength variability is difficult to estimate”. The manual concludes that a resistance reduction of 0.2 (resistance remaining = 0.8) is reasonable, and that reduction is subsequently applied in the HAZUS model.

To account for the variability that is known, but unspecified, the Panel decided to elicit this information from a group of construction and engineering experts who had extensive experience in damage investigations after coastal storm events. Thirty experts were asked to respond to the elicitation and 24 responded. The experts were asked to estimate expected resistance reduction due to variables in construction practices that could impact overall resistance to extreme loads caused by high winds. The experts were also asked to estimate expected resistance reduction due to variability in eight different components, including the impact of age and deterioration over 25 years on four of those eight components.

6.5.1 Construction Variability Applicable to All Building Systems

The experts considered a range of systemic construction issues, meaning those issues that could influence the overall quality of construction. The experts estimated expected resistance reductions assuming: (1) no connectivity between systemic construction variability and component variability, and (2) no cumulative effects of more than one issue occurring at the same time. Listed in Table 6-18 are six areas of construction variability that the experts provided estimates of resistance reduction.

The Expected Resistance Reduction is intended to quantify how much resistance reduction the expert believes could occur if the specific item being estimated actually occurs. To be sure, the Expected Resistance Reduction can also be widely variable. The expert's experience with or judgment about that variability is therefore also important in refining the resistance reduction for each of the variability factors. Hence, each expert was asked to define the Minimum, Most Likely, and Maximum values for the Expected Resistance Reduction for each of the six construction variables.

In addition, the expert estimated the Probability of Occurrence that the specific construction issue being estimated would actually occur. The expert considered the frequency the problem had been observed in the field; the difficulty in installing or constructing within the needed tolerances to achieve maximum resistance; the number of ways that any one product or system could be incorrectly installed; or the ability to achieve required resistance with an alternative product.

The estimated Percent Reduction in Resistance for each construction variable was subsequently calculated by multiplying the Expected Resistance Reduction by the Probability of Occurrence. The Percent Reduction in Resistance was then converted to a Percent Resistance Remaining, i.e., one minus the Percent Reduction in Resistance. The value for Percent Resistance Remaining served as a reduction factor that was then applied to the resistance values used in the Damage Estimation Module.

TABLE 6-18. CONSTRUCTION VARIABILITY

Issue	Possible Forms of Variability
1. Building constructed in less than ideal weather.	a. Rain or ice, cold, wind
2. Language barriers between workers, foremen, written instructions including plans.	a. Workers do not understand English. b. Foreman does not speak English well. c. Foreman not on job continuously. d. No written instructions in worker native language.
3. Work installed with tool or method not ideal for the situation.	a. Ax or chainsaw used instead of saw. b. Hand saw used instead of electric saw. c. Nail gun used where hammer would work better or vice versa. d. Cut nails used instead of foundation bolts.
4. Building code compliance.	a. Infrequent inspections performed during construction to insure compliance with code, plans and specs. b. Heavy construction activity in community limits time inspectors can visit job sites and inspect. c. No involvement by 3 rd party inspectors hired by owner. d. Products specified with required resistance capacity are regularly substituted. e. Products specified with required resistance are not available in the project site marketplace.
5. No design professional was involved in project.	a. Only prescriptive solutions for wind resistance are used. b. Design is completed without involvement of an architect, a structural engineer or a geotechnical engineer.
6. Quality of experienced workers.	a. Heavy construction activity will reduce pool of experienced workers. b. Small population centers will strain pool of experienced workers.

The Percent Resistance Remaining results from each of the 24 respondents to the elicitation were averaged for the Maximum, Minimum, and Most Likely conditions for each of the six construction variables. It is assumed that each construction variable will not affect the same components at the same time in the same way. Hence, the Maximum, Minimum, and Most Likely values for the combined effects of all the factors affecting the construction variability reduction factor were calculated by applying the equation $1 - \sqrt{\sum(1 - R_i)^2}$ where R_i is the average Percent Resistance Remaining for each of the six construction variables. The resulting Most Likely Percent of Resistance Remaining is 87.6 percent. The Maximum and Minimum values are 92.9 percent and 77.9 percent, respectively.

There is variability in the Most Likely Percent of Resistance Remaining as represented by the Maximum and Minimum values. These maximum and minimum values are interpreted to mean that 95 percent of the actual resistance remaining would fall between the maximum and minimum values. The distribution of values for remaining capacity is assumed to be normal. This assumption means that the difference between the maximum and minimum values spans four standard deviations, or +/- two standard deviations from the mean. This approach allows calculation of the standard deviation on the average maximum and minimum values for each factor or component. This analysis results in a Coefficient of Variation (COV) of 0.043.

6.5.2 Installation Variability Appropriate for Individual Building Components

The elicitation panel members were also asked to consider the effect on the Expected Resistance Reduction of each of the possible areas of component variability listed in Table 6-19. The first column of Table 6-19 contains a component or system known to have some variability in resistance, and for which building damage has been attributed during many wind storm events. The listed component or system includes both vertical and lateral load paths, and components or systems that begin collecting the wind load and eventually distributing the load to the ground.

The second column of Table 6-19 contains a form of variability for the component or system. For example, there are several ways a roof-to-wall connection could be installed that would negatively affect the performance of that connection. Five different connection issues are listed in the column titled "Possible Forms of Component

Variability.” As much as practical, the elicitation panel member was asked to ignore cumulative effects of more than one issue occurring at the same time, but rather what the effect of variability is of just the component and form of variability being considered. Notes for Table 6-19 provide additional explanation about some of the forms of component variability.

TABLE 6-19. INSTALLATION VARIABILITY APPROPRIATE FOR INDIVIDUAL BUILDING COMPONENTS

Component or System	Possible Forms of Component Variability
1. Roof-to-wall Connections	<ul style="list-style-type: none"> a. No connector is used. b. Incorrect connector used. c. Connector correct with inadequate nails. d. Connectors nailed such that rafters split. e. Connectors installed on wrong side of wall.
2. Asphalt Roof Coverings	<ul style="list-style-type: none"> a. Shingles installed in vertical pattern instead of diagonal pattern. b. Starter strip placement incorrect. c. No asphalt cement used to assist with initial bonding of shingles.
3. Roof Panels	<ul style="list-style-type: none"> a. Fasteners do not engage a rafter or truss. b. Fasteners are over driven. c. Incorrect panel material used (i.e. too thin). d. Incorrect nailing pattern for high wind zones.
4. Wall Cladding	<ul style="list-style-type: none"> a. Fasteners do not engage a framing member. b. Fasteners only engage one layer of horizontal board cladding or vinyl cladding is not properly interlocked. c. Incorrect nailing pattern for high wind zones.
5. Windows and Doors	<ul style="list-style-type: none"> a. Incorrect unit installed for high winds and/or debris-impact areas. b. Units not installed in accordance with manufacturer’s installation instructions. c. Fasteners do not fully engage a framing member.
6. Shear Walls	<ul style="list-style-type: none"> a. Improper nailing of wall – nails too far apart, nail size inadequate, nails miss framing. b. Inadequate number of nails to resist both shear and uplift. c. Hold downs at end of shear walls are not properly installed to framing or adequately anchored to shear wall.

TABLE 6-19. (CONTINUED)

7. Wall-to-foundation Connection	<ul style="list-style-type: none"> a. Sill plates not adequately bolted to concrete or masonry foundation – bolts too far apart, bolts not secured with nuts and washers, bolts installed too close to edge of wood sill plate. b. Wall and floor system not fastened with mechanical connectors to elevated floor beams or girders. c. Load paths do not line up over beams or girders and thus failure probability increases.
----------------------------------	--

Table 6-19 Notes

Component 2: Asphalt Roof Coverings – All coverings are assumed to be shingles. Installing shingles vertical means the installer starts at the eave and works shingles vertically toward the ridge before installing shingles horizontally parallel to the eave. This approach tends to create shingles that must be weaved on the roof increasing the number of shingles with an insufficient number of fasteners. The starter strip is supposed to be a regular shingle with the tabs cut off and the shingle turned so the bonding strips will engage the first full course. Installations that have starter strips with the tabs or not turned to engage the bonding strips are incorrect. The primary failure mode for shingles is failure in the bonding between shingles. Any installation that does not allow the bonding to be fully engaged will likely have some sort of premature failure.

Component 3: Roof Panels – Fasteners not engaging means the fastener completely or partially missed the rafter or roof truss. Incorrect panel material means the roof sheathing is not adequate for the installation. It is too thin or not adequate material for the rafter spacing. Inadequate nailing pattern means there was no consideration for the high wind zones on roofs where increased nailing would be required.

Component 4: Wall Cladding – Fasteners not engaging means the fastener completely or partially missed the wall stud. Increased wall insulation methods are moving the cladding further away from the plane of the wall studs, potentially requiring longer fasteners. Horizontal cladding boards (e.g. cedar, cementitious board materials) require two fasteners at each stud and one fastener is supposed to engage the board underneath of it. Inadequate nailing pattern means there was no consideration for the high wind zones on walls where increased nailing would be required.

Component 5: Windows and Doors – Window and door units are required to be labeled with design wind pressures and compliance with ASTM standards on impact resistance. Units without these labels should be considered to have uncertain performance during high wind events.

Component 6: Shear Walls – Shear walls may be used to resist both lateral and uplift loads. The only way to determine if this design scheme was followed are the number of nails used to attach the shear wall sheathing to the framing since there must be sufficient nails to resist both load paths separately. Hold downs are steel connectors that are attached to the bottom of the shear wall and to the framing member (beam, girder, column or pile) used to resist the overturning induced into the shear wall. The construction sequencing of the hold down installation is critical to having the hold down fully resist the lateral loads. These hold down devices are very difficult to install correctly once the framing has advanced past the hold down location.

Component 7: Wall-to-foundation Connection – Bolts for sill plate connections for slab-on-grade or crawl space foundations should be installed with a template to insure bolt spacing, bolt proximity to slab edge, and bolt threads are installed to meet code and wood standard requirements. This important load path connection will unlikely achieve maximum resistance unless properly installed.

As was the case for Construction Variability, the elicitation panel experts were asked to estimate the Minimum, Most Likely, and Maximum values for Expected Resistance Reduction for each form of component variability. The experts then estimated the Probability of Occurrence which is intended to address the probability that the specific variability actually reduced the expected resistance. This step was taken irrespective of the extent to which the expert estimates the Expected Resistance Reduction. It also must be judged independently from the importance of that issue to reduced wind damage.

The estimated Percent Reduction in Resistance is the product of the Expected Resistance Reduction times the Probability of Occurrence. Results from the elicitation panel are provided in Table 6-20. Note that age or deterioration is not included as a form of variability. Yet, it is well known from field investigation that the issue is important to damage levels. The issue of age or deterioration is considered separately for some components as noted in the following section.

TABLE 6-20. INSTALLATION COMPONENT VARIABILITY RESULTS

Component or System	Percent Resistance Remaining (Mean)	Coefficient of Variation (COV)
1. Roof to wall connections	91.1	.036
2. Asphalt Roof coverings	94.4	.011
3. Roof panels	92.6	.019
4. Wall cladding	95.9	.011
5. Windows and doors	97.3	.011
6. Shear walls	94.5	.017
7. Wall to foundation connection	98.3	.007

6.5.3 Component Variability Associated with Age and Deterioration

Age and deterioration considerations have been given to a subset of the component variability issues since age, and thus deterioration, is known to be an issue for some of

these components. The elicitation panel members considered the probability that age affects the resistance of roof coverings, wall cladding, windows and doors, and the wall to foundation connections. The change in Minimum, Most Likely, and Maximum Expected Resistance Reduction was considered for time intervals of 5, 10, 15, 20, and 25 years. The Probability of Occurrence of the age or deterioration effect was also considered. These age influences potentially further reduce the resistance of the components. The age consideration as a Mean Resistance Remaining percentage (and a COV) at each of the age intervals is summarized in Table 6-21.

TABLE 6-21. INSTALLATION COMPONENT VARIABILITY RESULTS FOR AGE INTERVALS

Component or System	Percent Resistance Remaining (Mean) and Coefficient of Variation (COV) by Age Interval				
	5 yrs.	10 yrs.	15 yrs.	20 yrs.	25 yrs.
2. Asphalt Roof Coverings	93.7 (.014)	89.6 (.028)	84.7 (.037)	77.8 (.061)	68.7 (.090)
4. Wall Cladding	95.6 (.012)	93.9 (.017)	92.6 (.022)	89.7 (.030)	86.3 (.038)
5. Windows and Doors	96.7 (.013)	95.1 (.016)	93.8 (.020)	91.3 (.025)	88.7 (.031)
7. Wall-to-Foundation Connection	97.8 (.009)	96.7 (.013)	95.7 (.016)	94.2 (.020)	92.9 (.023)

These expected losses in resistance due to initial construction variability, component installation variability, and age and deterioration are used to modify the defined resistances in the Damage Estimation Module for the component or system of interest. The resistance is modified in the probability of damage calculation as follows: (Defined Resistance) x (Construction Percent of Resistance Remaining) x (Component Percent of Resistance Remaining) x (Component Age Percent of Resistance Remaining taken at the Building Age) = Modified Resistance Capacity.

6.6 Interior Damage Predictions

Interior damages are caused by a failure someplace in the building envelope. The extent of damage to roof covering, roof sheathing, siding, or windows and doors drives the extent of the interior damage. Thus the methodology applied in the Damage Estimation Module is linked to the extent of damage to those named building envelope elements. Since the extent of damage to the envelope is also driven by terrain exposure; building height; roof slope and shape; the orientation of the primary building axis compared to wind direction; the percent of window area; and the wind speed; these factors secondarily contribute to interior damage since they contribute to the component damage.

Little is written in research journals or papers about a methodology that could be used for modeling purposes when determining interior damages, or in linking interior damage to damaged building components. Since the Damage Estimation Module is using component damage as the basis for wind-caused damage to buildings, the Panel believes that the interior damage determination should also be linked to component damage.

The most extensive public work available to the Panel that linked interior damage caused by the storm types of interest was developed in HAZUS (FEMA, 2012). The Panel believes that the HAZUS methodology provides a reasonably sound approach for determining the highly variable results associated with interior damages.

HAZUS uses damage to roof covering, roof sheathing, and broken windows and doors as the primary determinants for interior damages. The interior is considered to consist of: partitions, interior doors, wall finishes, floor finishes, ceiling finishes, and the interior surfaces of exterior walls. FEMA developed two formulas for calculating interior damage to the roof covering and roof sheathing elements.

The estimated damage for roof cover in HAZUS is:

$$L_{rc} = f_1(R_{rc})[1-f_2(A_{rc})]f_3(R_{rc})V_4 \quad (\text{Eq. 6-15})$$

Where:

$$L_{rc} = \text{Damage to roof cover (multiplication of the functions)}$$

f_1 = function 1 which represents the fractional amount of the interior affected by the loss of a fraction of the roof cover.

$$f_1(R_{rc}) = 1.11R_{rc} \quad \text{for } R_{rc} \leq 0.9 \quad \text{and}$$

$$f_1(R_{rc}) = 1.0 \quad \text{for } R_{rc} > 0.9$$

R_{rc} = fraction of failed roof cover

A_{rc} = area of failed roof cover which is R_{RC} times the area of roof surface taken from plan dimensions.

f_2 = function 2 which accounts for the fact that roof cover damage is relatively small, but when it exceeds 25% the interior is totally damaged.

$$f_2(A_{rc}) = 1 - 0.005A_{RC} \quad \text{for } A_{rc} \leq 200 \text{ ft}^2 \quad \text{and}$$

$$f_2(A_{rc}) = 0 \quad \text{for } A_{rc} > 200 \text{ ft}^2$$

f_3 = function 3 which accounts for the fact that the resulting interior damage becomes more severe as the area of interior damage gets larger.

$$f_3(R_{rc}) = 0.1 \quad \text{for } R_{rc} \leq 0.05 \quad \text{or}$$

$$f_3(R_{rc}) = 2.0R_{rc} \quad \text{for } 0.05 < R_{rc} \leq 0.5 \quad \text{or}$$

$$f_3(R_{rc}) = 1.0 \quad \text{for } R_{rc} > 0.5$$

V_1 = value of the interior of the building (strikethrough and ignored for this model since the panel is determining losses as a percent of the overall building size, not value).

The estimated damage for roof sheathing in HAZUS is:

$$L_s = (3.6R_s + 0.1)V_1 + R_s V_{rf} \quad (\text{Eq. 6-16})$$

Where:

L_s = Damage to roof sheathing

R_s = fraction of missing roof sheathing for $0 < R_s < 0.25$

V_1 = value of the interior of the building (strikethrough and ignored for this model since the panel is determining losses as a percent of the overall building size, not value)

V_{rf} = value of roof framing (strikethrough and ignored for this model since the panel is determining losses as a percent of the overall building size, not value)

This portion of the interior damage is capped when the roof sheathing loss equals or exceeds 25 percent. At that point, the interior is assumed to be 100 percent damaged. Since the Panel is determining interior damages as a percent of component damage, not value, the 2nd term ($R_s V_{rf}$) is ignored.

The estimated percent damage for broken windows and doors is:

$$L_w = W_{pa} R_w \quad (\text{Eq. 6-17})$$

Where:

L_w = Damage to window and door glazing

W_{pa} = percent of window and door area in the exterior walls

R_w = fraction of broken glazing

The HAZUS interior damage due to window and door damage is a function of how much water gets into the building and sits on the floor through the broken windows and doors, up to ¼" of water at which point the building interior is assumed to be a 100 percent loss. This method was modified by the Panel to consider the percent of the wall area covered in glazing and the percent damage to that glazing. It was determined that an extrapolation of how much water would enter the building was not accurate enough to add validity to the interior loss percentage.

To illustrate application of the proposed methodology for estimating interior damage, a list of component wind damage is shown in Table 6-22 and in Table 6-23 for a surviving structure and a slab-only structure, respectively. The interior damages are highlighted in a red box. The total interior damage is the sum of: $L_{rc} + L_s + L_w$

The dark bands in each table simply represent a break in a long continuous record of damages to illustrate a few key points in the time record. For the surviving structure, the record caps at the time of maximum winds since the structure survived and no more damage is assumed to occur than what is incurred at the time of maximum winds. For the slab-only structure, the maximum wind loss stops at the time the building is washed away which occurs on 9/13/08 at 6:30. This time is highlighted with a purple box.

TABLE 6-22. WIND DAMAGE TO COMPONENTS FOR SURVIVING STRUCTURE

Time	Roof Cover	Roof Panel	Wall Cover	Wall Panel	Windows	Doors	Garage Dr	Roof Frame	Interior
9/12/08 13:30	0.9%	0.8%	0.9%	0.0%	0.0%	0.0%	0.0%	0.0%	0.0%
9/12/08 14:00	0.9%	0.8%	0.9%	0.0%	0.0%	0.0%	0.0%	0.0%	0.0%
9/12/08 14:30	1.0%	0.8%	0.9%	0.0%	0.0%	0.0%	0.0%	0.0%	0.0%
9/12/08 15:00	1.0%	0.8%	1.0%	0.0%	0.0%	0.0%	0.0%	0.0%	0.0%
9/12/08 15:30	1.0%	0.8%	1.0%	0.0%	0.0%	0.0%	0.0%	0.0%	0.0%
9/12/08 16:00	1.0%	0.8%	1.0%	0.0%	0.0%	0.0%	0.0%	0.0%	0.0%
9/13/08 3:00	2.1%	1.1%	2.4%	0.0%	0.3%	0.1%	0.0%	0.0%	0.1%
9/13/08 5:30	2.3%	1.2%	2.6%	0.0%	0.4%	0.2%	0.0%	0.0%	0.1%
9/13/08 6:00	2.7%	1.3%	2.8%	0.0%	0.5%	0.3%	0.0%	0.0%	0.1%
9/13/08 6:30	2.9%	1.3%	2.9%	0.0%	0.6%	0.4%	0.0%	0.0%	0.2%
9/13/08 7:00	3.2%	1.4%	3.2%	0.0%	0.8%	0.5%	0.0%	0.0%	0.2%
9/13/08 7:30	3.3%	1.4%	4.5%	0.0%	1.4%	1.0%	0.0%	0.0%	0.3%
9/13/08 8:00	4.2%	1.6%	5.1%	0.0%	2.0%	1.5%	0.1%	0.0%	0.4%
9/13/08 8:30	5.6%	1.9%	6.4%	0.0%	3.3%	2.9%	0.2%	0.0%	0.8%
9/13/08 9:00	6.1%	2.0%	8.3%	0.0%	5.6%	5.4%	0.4%	0.0%	1.2%
9/13/08 9:30	9.0%	2.5%	9.3%	0.1%	7.0%	7.0%	0.8%	0.0%	2.4%
9/13/08 10:00	10.0%	2.7%	12.4%	0.2%	10.7%	11.6%	1.5%	0.0%	3.4%
9/13/08 10:30	16.4%	4.2%	18.1%	0.8%	21.1%	23.0%	9.2%	0.1%	8.6%
9/13/08 11:00	16.4%	4.2%	18.1%	0.8%	21.1%	23.0%	9.2%	0.1%	8.6%

TABLE 6-23. WIND DAMAGE TO COMPONENTS FOR SLAB-ONLY STRUCTURE

Time	Roof Cover	Roof Panel	Wall Cover	Wall Panel	Windows	Doors	Garage Dr	Roof Frame	Interior
9/12/08 13:30	0.9%	0.7%	0.9%	0.0%	0.0%	0.0%	0.0%	0.0%	0.0%
9/12/08 14:00	0.9%	0.7%	0.9%	0.0%	0.0%	0.0%	0.0%	0.0%	0.0%
9/12/08 14:30	1.0%	0.8%	1.0%	0.0%	0.0%	0.0%	0.0%	0.0%	0.0%
9/12/08 15:00	1.0%	0.8%	1.0%	0.0%	0.0%	0.0%	0.0%	0.0%	0.0%
9/12/08 15:30	1.0%	0.8%	1.0%	0.0%	0.0%	0.0%	0.0%	0.0%	0.0%
9/12/08 16:00	1.0%	0.8%	1.0%	0.0%	0.0%	0.0%	0.0%	0.0%	0.0%
9/13/08 4:00	2.6%	1.2%	2.3%	0.0%	0.2%	0.1%	0.0%	0.0%	0.1%
9/13/08 4:30	2.6%	1.2%	2.3%	0.0%	0.2%	0.1%	0.0%	0.0%	0.1%
9/13/08 5:00	2.6%	1.2%	2.4%	0.0%	0.3%	0.1%	0.0%	0.0%	0.1%
9/13/08 5:30	2.8%	1.2%	2.7%	0.0%	0.4%	0.2%	0.0%	0.0%	0.1%
9/13/08 6:00	2.9%	1.2%	2.9%	0.0%	0.5%	0.3%	0.0%	0.0%	0.1%
9/13/08 6:30	3.9%	1.4%	3.1%	0.0%	0.7%	0.4%	0.0%	0.0%	0.2%
9/13/08 7:00	4.2%	1.5%	3.3%	0.0%	0.8%	0.6%	0.0%	0.0%	0.2%
9/13/08 7:30	4.6%	1.5%	3.5%	0.0%	1.1%	0.7%	0.0%	0.0%	0.3%
9/13/08 8:00	4.9%	1.6%	4.7%	0.0%	2.3%	1.8%	0.1%	0.0%	0.5%
9/13/08 8:30	7.1%	1.9%	5.4%	0.0%	3.2%	2.7%	0.1%	0.0%	1.0%
9/13/08 9:00	9.0%	2.1%	6.3%	0.0%	5.0%	5.0%	0.4%	0.0%	1.5%
9/13/08 13:30	20.6%	4.2%	18.2%	0.8%	21.0%	23.1%	14.1%	0.0%	12.0%
9/13/08 14:00	20.6%	4.2%	18.2%	0.8%	21.0%	23.1%	14.1%	0.0%	12.0%
9/13/08 14:30	20.6%	4.2%	18.2%	0.8%	21.0%	23.1%	14.1%	0.0%	12.0%
9/13/08 15:00	20.6%	4.2%	18.2%	0.8%	21.0%	23.1%	14.1%	0.0%	12.0%
9/13/08 15:30	20.6%	4.2%	18.2%	0.8%	21.0%	23.1%	14.1%	0.0%	12.0%
9/13/08 16:00	20.6%	4.2%	18.2%	0.8%	21.0%	23.1%	14.1%	0.0%	12.0%
9/13/08 16:30	20.6%	4.2%	18.2%	0.8%	21.0%	23.1%	14.1%	0.0%	12.0%

6.7 Identification of Limitations

Provided below are key limitations associated with development of the Damage Estimation Module.

1. The use of average damage ratios that are applicable for a large number of structures are being used to estimate the damage to a single property. There is large variation in the relative performances of individual structures that cannot be captured by the recommended methodology.
2. The calculation of a FOSM-MV reliability index can be sensitive to the specific formulation of the performance function. The effect of this limitation was evaluated in a sensitivity analysis. The effect was small and is reported in Appendix C.
3. Some of the random variables used in the analysis have non-normal probability distributions (e.g. gust pressure coefficients) that are approximated as Gaussian by the FOSM-MV method. The effect of this limitation was evaluated in a sensitivity analysis. The effect was small and is reported in Appendix C.
4. Error in the estimate of the wind direction produced by the Hazard Module is not considered in the reliability analysis.
5. The Damage Estimation Module only considers buildings to be rectangular in plan.
6. The Damage Estimation Module only considers wood frame construction.
7. Damage from windborne debris is not explicitly considered, but is implied when calibrating based on observations of damage due to historical storms.
8. The application of a higher internal pressure coefficient occurs at the time step following the damage that initiates the reclassification to “partially enclosed.” This simplification eliminates the need for a recursive calculation at each time step, but it may reduce the eventual magnitude of the damage estimate.
9. The application of the internal pressure is considered to be the worst case of either positive or negative internal pressurization for each component location, regardless of the wind direction and the location of the dominant opening. This simplification will lead to slightly higher wind damage estimates.
10. The number of roof frame lines is constant regardless of building geometry. The impact of this limitation is mitigated by the fact that the damage is estimated relative to the roof area.
11. The tributary area for the roof-to-wall connections is taken as deterministic even though the full building geometry is not defined and the roof truss arrangement is an idealization for a rectangular plan.

12. The proposed methodology is limited to typical low-rise residential construction. Single family residences or duplexes are both appropriate applications for the methodology, as long as the roof structure consists of light-framed trusses or rafters (either wood or cold-formed steel). However, significant deviations from the structure types presumed by the model will render the results unreliable. The performance of properties with heavy structural steel or reinforced concrete framing will not be well-represented by the model.

Regarding the first limitation about the use of average damage ratios, consider the aerial image in Figure 6-11 showing damaged roofs. The houses shown in Figure 6-11 are located in a southern Mississippi neighborhood impacted by Hurricane Katrina in 2005. Among the 34 residential structures in this image, 21 of them sustained no roof damage (indicated with a yellow zero). The other 13 residences sustained varying degrees of roof damage (estimated percent damage shown in red). Estimated roof damage and related statistics for the 34 houses shown in Figure 6-11 is summarized in Table 6-24.

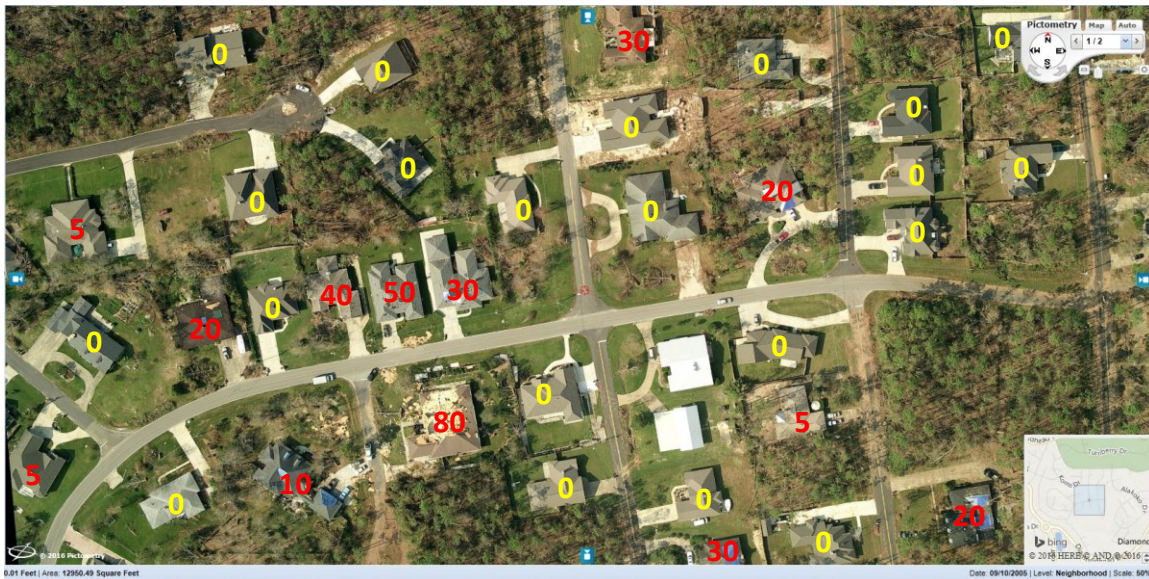


Figure 6-11. Illustration of Relative Roof Cover Damage to Residential Structures
(Source: Pictometry™)

Although the average roof damage sustained by the 34 houses is 10 percent, most of the houses sustained no roof damage (0%). Typically roof cover damage is not normally distributed. The average value is also often influenced by a few higher losses or even a single high loss. Excluding the house with 80 percent roof damage causes the average to decrease from 10 percent for 34 houses to eight percent for 33 houses. Excluding the

top three houses with the most roof damage (40%, 50%, and 80%) causes the average to decrease by half from 10 percent for 34 houses to five percent for 31 houses. As illustrated in this example, the most likely damage level and the average damage level are not the same.

TABLE 6-24. ESTIMATED ROOF COVER DAMAGE FOR ILLUSTRATIVE EXAMPLE

Estimated Roof Damage (%)	Number of Houses	Percent of All Houses
0	21	62
< 5	3	9
10	1	3
20	3	9
30	3	9
40	1	3
50	1	3
60	0	0
70	0	0
80	1	3
90	0	0
100	0	0
Total:	34	100
Average:	10%	
Median:	0%	
Houses less than or equal to Avg.	74%	
Houses greater than Avg.	26%	

The example illustrates one of the basic challenges in developing a method to estimate property damage for a slab-only structure. In the event of collapse caused by surge and waves, the range of possible wind damage states is wide. If Monte Carlo Simulation were used as the technique for estimating component wind damage probabilities rather than the FOSM-MV reliability method, then TWIA would be able to estimate the range and distribution of possible damage states. However, it would still be practically impossible to know which of the possible damage states actually occurred at a single property. Therefore, as a practical matter the Expert Panel recommends using the average result when estimating wind damage to a slab-only structure.

An important consequence of this limitation of the proposed methodology is that, all other factors being equal, and except for wind speeds of exceedingly low probability, *for a majority of slab-only cases the estimated wind damage for a given house will be greater than the damage likely to have occurred to that house.* To illustrate this point imagine that (1) all of the houses shown in Figure 6-11 were completely washed away by storm surge after the photograph was taken; and (2) the damage estimation module correctly predicted that the homes there experienced an average roof cover damage rate of 10 percent. In reality as shown in Figure 6-11 the majority of structures (24 out of 34, or 70%) actually experienced *less* roof cover damage than what was predicted by the Damage Estimation Module.

6.8 Example Calculations

Provided below is an example of calculations executed within the Damage Estimation Module to illustrate the overall approach as recommended by the Panel. Only the model inputs and resulting outputs are shown. The numerous calculation steps taken to estimate the wind damage are shown in Appendix A (Section 13).

Consider a residence with the following structural features as shown in Figure 6-12 subjected to the hazard time history shown in Figure 6-13.

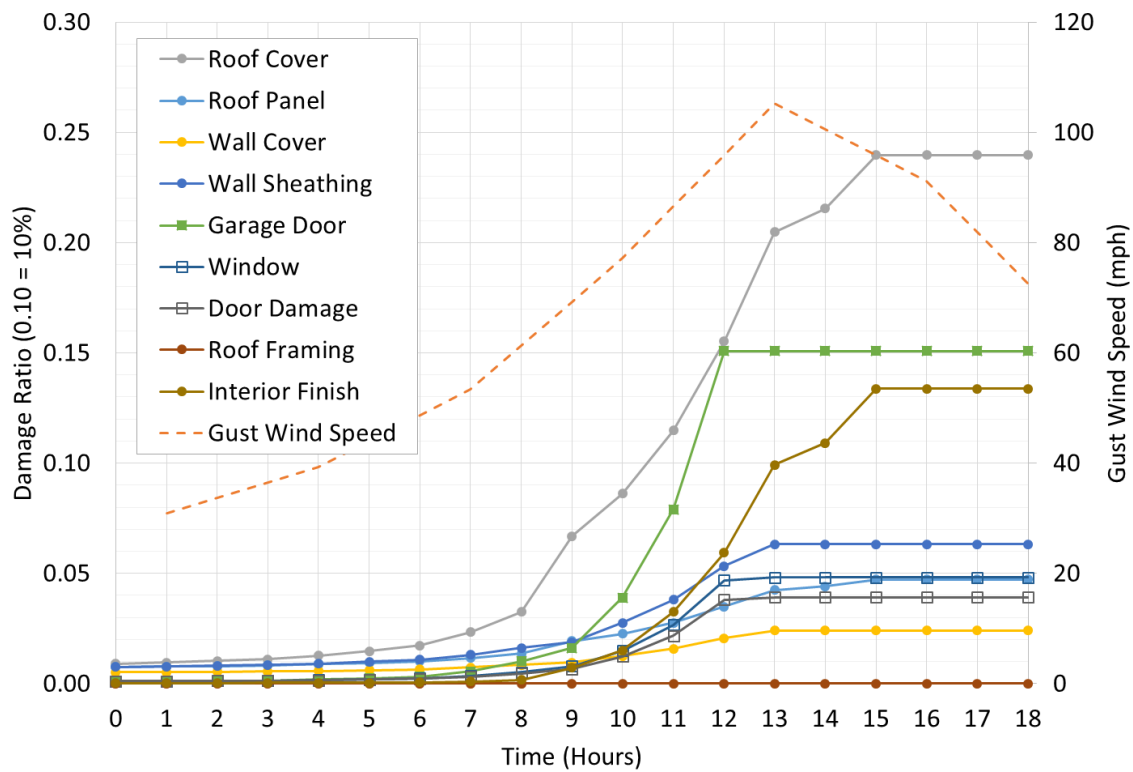
<u>Structure Input</u>		
Roof Shape	Gable	
Length	53	feet (parallel to ridge)
Width	35	feet (parallel to ridge)
Plate Height	9	feet
Eave Height	20	feet
Roof Slope	6	:12
Roof Height	24.375	feet
Number of Stories	1	Living Area
Structure Primary Axis	45	deg. (with respect to North = 0 deg.)
Terrain Exposure	D	ASCE 7 Category
Ovrhd Garage Door Type	Sectional	
Roof Cover Type	Asphalt Shingle (ASTM D7158 Class H)	
Roof Cover Age	10	years
Wall Cover Type	Vinyl Siding	
Direction of Garage Door	315	degrees
Garage Panel Door Width	Single	
Garage Attached?	Yes	
Window Type	Non-Impact Resistant	
Percent Window Area	0-25	Percent
Door Type	Non-Impact Resistant	
Opening Protection	No	
Age of Structure	20	years
<u>Calculated Values</u>		
Plan Aspect Ratio (L/B)	1.514	parallel to ridge
Plan Aspect Ratio (L/B)	0.660	perpendicular to ridge
height aspect ratio (h/L)	0.252	parallel to ridge
height aspect ratio (h/L)	0.382	perpendicular to ridge
"a" dimension	3.5	(ft) edge and corner zone dim.

Figure 6-12: Residential Structural Features

Time	Wind			Surge/Wave	
	Gust Speed	Direction	AOA	H _s (ft)	Freeboard (ft)
Hour 0	30.87	45.00	0.00	0.30	12.28
Hour 1	33.67	41.67	356.67	0.31	12.30
Hour 2	36.48	38.33	353.33	0.33	12.28
Hour 3	39.28	35.00	350.00	0.35	12.17
Hour 4	43.96	38.33	353.33	0.38	12.01
Hour 5	48.64	41.67	356.67	0.42	11.87
Hour 6	53.31	45.00	360.00	0.46	11.76
Hour 7	61.26	35.00	350.00	0.53	11.70
Hour 8	69.21	25.00	340.00	0.60	11.71
Hour 9	77.16	15.00	330.00	0.64	11.71
Hour 10	86.52	25.00	340.00	0.66	11.88
Hour 11	95.87	35.00	350.00	0.67	12.23
Hour 12	105.22	45.00	360.00	1.01	11.64
Hour 13	100.55	141.67	96.67	1.47	10.11
Hour 14	95.87	238.33	193.33	1.63	7.78
Hour 15	91.20	335.00	290.00	1.74	0.64
Hour 16	81.84	326.67	281.67	4.79	-5.31
Hour 17	72.49	318.33	273.33	5.56	-3.74
Hour 18	63.14	310.00	265.00	4.92	-1.09

Figure 6-13: Hazard Time History

The structural features should have been acquired and stored in the Property Database prior to the arrival of any storm. Once the structural features for the residence are retrieved from the Property Database, and the time history determined for the property site, the Damage Estimation Module then performs its calculations for all time steps. Afterwards the module adds up the damage to each area on the sample building for all of the considered components, yielding the time history of wind damage as shown in Figure 6-14 including the time histories of collapse probability due to each mode.



Hour	Roof Cover	Roof Panel	Wall Cover	Wall Panel	Windows	Doors	Garage Door	Roof Frame	Interior	Wind Collapse Probability	Surge & Wave Collapse Probability
0	0.9%	0.8%	0.5%	0.8%	0.1%	0.1%	0.1%	0.0%	0.0%	1.1%	0.0%
1	1.0%	0.8%	0.5%	0.8%	0.1%	0.1%	0.1%	0.0%	0.0%	1.1%	0.0%
2	1.0%	0.8%	0.5%	0.8%	0.1%	0.1%	0.1%	0.0%	0.0%	1.1%	0.0%
3	1.1%	0.8%	0.5%	0.8%	0.1%	0.1%	0.1%	0.0%	0.0%	1.2%	0.0%
4	1.3%	0.9%	0.6%	0.9%	0.2%	0.2%	0.2%	0.0%	0.0%	1.2%	0.0%
5	1.5%	0.9%	0.6%	1.0%	0.2%	0.2%	0.2%	0.0%	0.0%	1.3%	0.0%
6	1.7%	1.0%	0.7%	1.1%	0.2%	0.2%	0.2%	0.0%	0.1%	1.4%	0.0%
7	2.3%	1.2%	0.7%	1.3%	0.3%	0.3%	0.3%	0.0%	0.1%	1.6%	0.0%
8	3.3%	1.4%	0.9%	1.6%	0.5%	0.5%	0.6%	0.0%	0.2%	1.8%	0.0%
9	6.7%	1.9%	0.9%	1.9%	0.8%	0.7%	1.6%	0.0%	0.7%	2.1%	0.0%
10	8.6%	2.3%	1.2%	2.8%	1.5%	1.2%	3.9%	0.0%	1.5%	2.6%	0.0%
11	11.5%	2.8%	1.6%	3.8%	2.7%	2.2%	7.9%	0.0%	3.3%	3.3%	0.0%
12	15.5%	3.5%	2.1%	5.3%	4.7%	3.8%	15.1%	0.0%	5.9%	4.2%	0.0%
13	20.5%	4.3%	2.4%	6.3%	4.8%	3.9%	15.1%	0.0%	9.9%	3.7%	0.0%
14	21.5%	4.4%	2.4%	6.3%	4.8%	3.9%	15.1%	0.0%	10.9%	3.3%	0.0%
15	24.0%	4.7%	2.4%	6.3%	4.8%	3.9%	15.1%	0.0%	13.4%	2.9%	0.0%
16	24.0%	4.7%	2.4%	6.3%	4.8%	3.9%	15.1%	0.0%	13.4%	2.4%	37.7%
17	24.0%	4.7%	2.4%	6.3%	4.8%	3.9%	15.1%	0.0%	13.4%	1.9%	38.3%
18	24.0%	4.7%	2.4%	6.3%	4.8%	3.9%	15.1%	0.0%	13.4%	1.6%	0.3%

Figure 6-14: Estimation of Wind Damage

The interpretation of these results is as follows. The wind speed at this location increased until it reached a maximum at hour 12. At this time substantial wind damage to a number of components had occurred, and the probability of structural collapse due to wind reached its maximum value of approximately 4 percent. Presuming that the structure survived after the passage of the worst winds, some additional wind damage continued to accumulate until hour 15, since the wind speeds were still relatively high, and the wind direction was changing such that previously unaffected areas on the building were exposed to severe wind pressures.

After hour 15, the wind speeds dropped to levels that did not produce any additional damage. The peak storm surge elevation and wave heights arrived after the peak wind speeds for this storm and location. At hours 16 and 17 the combination of significant wave height and negative freeboard produced surge and wave collapse probabilities of approximately 38 percent. After this time the surge and wave levels decreased, reducing the probability of structural collapse.

The application of the proposed methodology presumes that the structure under investigation is a hurricane “slab-only” claim. It is further assumed that the structure collapsed due to either wind or surge and waves. Since the maximum probability of collapse due to surge and waves exceeded the probability of collapse due to wind by a factor of nine, it appears overwhelmingly likely that the cause of slabbing in this example was surge and waves. However, the surge collapse probability was not 100 percent; uncertainties are in the methodology; and the probability of collapse due to wind is also non-zero.

Applying the criteria described earlier in Section 6 for weighting the estimated wind damages based on the relative magnitudes of the collapse mode probabilities yields the following adjusted wind damages for roof covering and interior finishes. Wind damage to the other components would follow the same procedure.

$$D_{total_roof} = \frac{P_{surge} * D_{t_surge} + P_{wind} * D_{100\%}}{P_{surge} + P_{wind}} = \frac{(0.383) * (0.24) + (0.042) * (1.0)}{0.383 + 0.042} = 0.315$$

$$D_{total_int} = \frac{P_{surge} * D_{t_surge} + P_{wind} * D_{100\%}}{P_{surge} + P_{wind}} = \frac{(0.383) * (0.134) + (0.042) * (1.0)}{0.383 + 0.042} = 0.220$$

7 Validation of Methodology

Following development of the Hazards Module and Damage Estimation Module, the Panel began reviewing various sources of information to enable validation of the proposed methodology. For the purposes of this report the Panel considers validation as the process by which actual residential claims from tropical cyclone events are compared to results predicted by the Damage Estimation Module (see Figure 7-1). No adjustment to the model output is made per se to fit the outcomes resulting from a particular event. Table 7-1 summarizes the validation efforts described in this section.

The sources of information used by the Panel include bulk claims data from insurers, individual claim reports from private firms, open literature, and information from catastrophe loss models produced by public and private entities. The Damage Estimation Module also underwent an independent review by an ISO 9001 certified firm to verify the reliability of the Excel worksheet that was created to execute the calculations described in Section 6.



Figure 7-1: Damaged Properties following Hurricane Ike in 2008

TABLE 7-1. VALIDATION SUMMARY

Analysis	Hurricane Event	Data Source	Results	Limitations
Qualitative	Katrina (2005)	Proprietary	Assurance that proposed methodology was reasonable in terms of overall approach envisioned by the Panel.	Absence of detailed estimates of component damages.
	Katrina (2005) and Ike (2008)	TWIA	Results compared favorably with qualitative observations from post-storm damage photos.	Small data set; limited number of post-event photos of damage.
Quantitative	Charley and Ivan (2004)	Florida Citizens	In general results compared favorably with data interpreted from the claim files.	Estimated less roof frame damage than indicated from photos in the claim files.
	Rita (2005)	TWIA	Estimated damage was generally lower than the damage levels interpreted from the claim files.	Properties represented in the sample appeared to be in older developments; many of the properties were inundated, meaning the observed damage was from mixed modes.
	Ike (2008)	TWIA	With a few exceptions, the Damage Estimation Module appears to provide reasonable estimates of the magnitudes and trends of damage when compared to observations of actual damage.	Systematically overestimated overall damage for relatively low wind speeds; and overestimated damage to roof panels at all wind speeds.

7.1 Qualitative Analysis

7.1.1 Review of Select Coastal Properties

Evaluation of the methodology began with analyses of a qualitative nature. The goal was to affirm the reasonableness of the estimated hurricane damage sustained by coastal properties based on the proposed methodology. Part of this effort included obtaining damage reports from a nationwide engineering firm that had been retained by a major property insurance company following Hurricane Katrina. These reports contain information on 56 residential properties located along the north shore of Lake Pontchartrain. As illustrated in Figure 7-2 some of the structures had survived while other structures collapsed.

The 56 properties, similar in topography and configuration, were within a strip of land approximately 0.7 miles long. The firm performed an elevation survey of the 56 properties. Based on the elevation survey the properties were divided into two categories: properties with structures supported below the observed water line and structures supported above the observed water line. The reports also included descriptions of the damage sustained by each of the surviving structures.

Among the 56 properties, 38 structures were supported below the water line and were either completely missing or collapsed. The remaining 18 structures supported above the water line exhibited damage mostly to the exterior finishes and roof coverings. The reported damage was consistent with estimations produced by earlier versions of the model, given the magnitude for the storm surge and wind speeds, and the associated structural features of the buildings. This finding provided some assurance that the proposed methodology was reasonable in terms of the overall approach envisioned by the Panel.

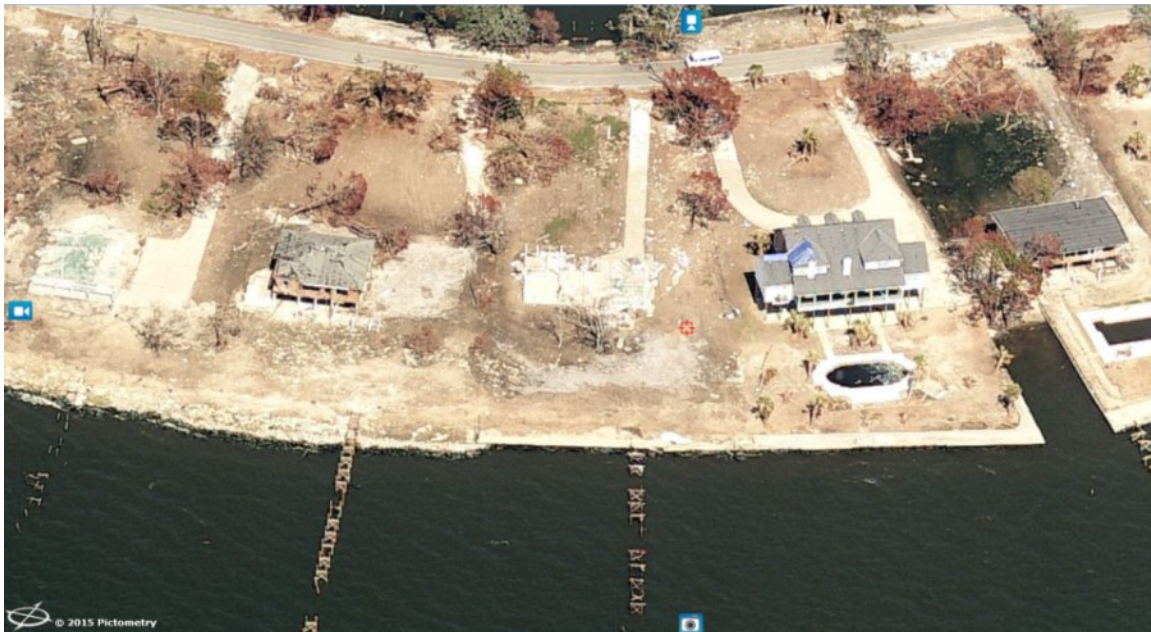


(a) Before Hurricane Katrina



(b) After Hurricane Katrina

Figure 7-2: Surviving and Slab-only Structures along Lake Pontchartrain



(c) Close-up View

Figure 7-2: (Continued)

7.1.2 Exploratory Analysis of Select Properties Subjected to Hurricanes Katrina (2005) and Ike (2008)

Efforts by the Panel to validate the performance of the Damage Estimation Module have evolved as loss data became available from various sources for different storms. One of the first exercises the Panel undertook was a comparison of the model results to the actual performance of a small number of coastal residential structures that were affected by Hurricane Katrina (FEMA 549, 2006) and Hurricane Ike (FEMA P-757, 2009). The data for these properties came from a combination of TWIA claims, post-storm field investigations by other members of the firms represented by the Panel members, and aerial imagery provided by Eagle View™.

Properties were selected in locations where some structures had toppled while other structures survived. By comparing toppled, slab-only structures to surviving structures, reliability of the collapse probability calculations from the model could be demonstrated. Furthermore, the relative levels of wind damage sustained by the surviving structures could be compared to predictions from the Damage Estimation Module.

It is important to note that wind damage estimates produced by the Damage Estimation Module are averages. So, a direct comparison of the predicted damage to that damage experienced by a small number of properties does not yield a significant quantitative result. Furthermore, the selection of properties was not random. The intent of this exercise was simply to qualitatively assess the magnitude of the damage predictions versus observations of damage among the selected properties.

Twenty-one properties located at Crystal Beach and Jamaica Beach in Galveston County, Texas; the north shore of Lake Pontchartrain in Louisiana; and Diamond Head in Mississippi were selected. Figure 7-3 shows representative properties among the 21 properties selected for analysis where one property survived while another property toppled.



(a) Crystal Beach

Figure 7-3: Representative Surviving and Slab-only Structures

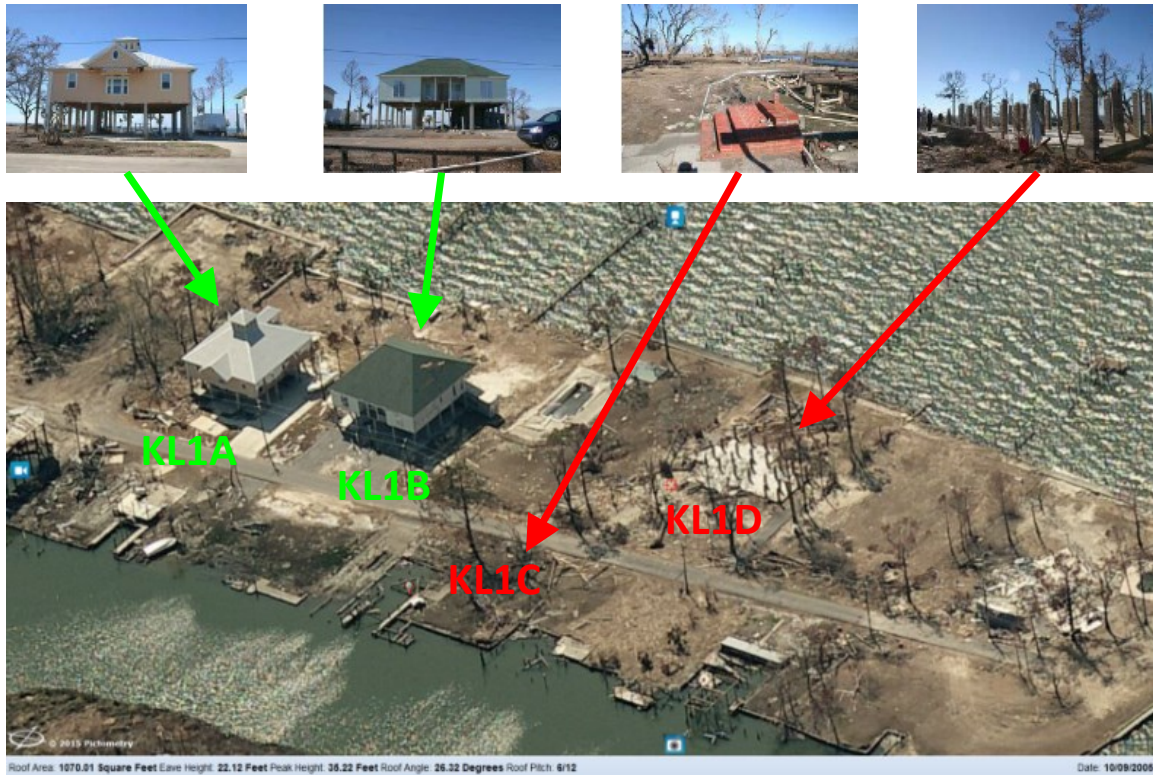


(b) Aerial View before Hurricane Ike



(c) Aerial View after Hurricane Ike

Figure 7-3: (Continued)



(d) North shore of Lake Pontchartrain after Hurricane Katrina

Figure 7-3: (Continued)

Time histories of wind speed, wind direction, storm surge elevation, and significant wave height were produced for each of the twenty-one properties considered. These time histories were used as input into the spreadsheet containing the prototype of the Damage Estimation Module. The property characteristics were determined based on insurance file data, Galveston County Appraisal District records, field observations and measurements, and interpretations of aerial photographs and claim file photographs. A summary of the some of the results from the Damage Estimation Module results is shown in Table 7.2.

For the slab-only structures, the average probability of collapse due to storm surge and waves was 74 percent. For the surviving structures, the average probability of collapse due to storm surge and waves was 24 percent. The probabilities of collapse due to wind for slab-only and surviving structures were 4.3 percent and 3.9 percent, respectively.

The damage estimation module predicted roof cover damage rates between approximately 10 percent and 40 percent for all 21 structures. Wind damage rates to other building components were of lower magnitudes. These results compared favorably with qualitative observations from post-storm damage photographs. In general, the results appear reasonable. Efforts to quantify the performance of the wind damage estimation module using larger sets of data are described in subsequent sections.

TABLE 7-2. DAMAGE ESTIMATION MODULE COLLAPSE PROBABILITY RESULTS FOR 21 SELECTED PROPERTIES

Location	Storm	Location	Slab or Surviving	Max Gust Wind Speed (mph)	Probability of Wind Collapse	Min. Free-board (ft)	Probability of Surge Collapse
ICB1	Ike	Crystal Beach, TX	Surviving	97	0.027	-0.90	0.000
ICB1a	Ike	Crystal Beach, TX	Slab	97	0.026	-3.87	0.037
ICB1b	Ike	Crystal Beach, TX	Slab	97	0.026	-5.15	0.774
ICB2a	Ike	Crystal Beach, TX	Surviving	97	0.033	-1.14	0.003
ICB2b	Ike	Crystal Beach, TX	Slab	97	0.032	-4.61	0.279
ICB3a	Ike	Crystal Beach, TX	Surviving	97	0.032	-3.65	0.052
ICB3b	Ike	Crystal Beach, TX	Partial Slab	97	0.032	-4.60	0.364
IJB4a	Ike	Jamaica Beach, TX	Surviving	85	0.024	-6.04	0.676
IJB4b	Ike	Jamaica Beach, TX	Slab	85	0.024	-8.04	0.909
KL1a	Katrina	Slidell, LA	Surviving	101	0.043	-5.31	0.383
KL1b	Katrina	Slidell, LA	Surviving	101	0.043	-4.82	0.291
KL1c	Katrina	Slidell, LA	Slab	101	0.037	-15.95	1.000
KL1d	Katrina	Slidell, LA	Slab	101	0.040	-9.69	1.000
KL1e	Katrina	Slidell, LA	Slab	101	0.041	-7.28	0.999
KL2a	Katrina	Slidell, LA	Surviving	101	0.042	-3.18	0.014
KL2b	Katrina	Slidell, LA	Surviving	101	0.042	-3.38	0.029
KL2c	Katrina	Slidell, LA	Slab	101	0.041	-5.56	0.248
KM1a	Katrina	Diamond Head, MS	Surviving	122	0.067	-8.11	0.567
KM1b	Katrina	Diamond Head, MS	Slab	122	0.061	-13.13	0.923
KM2	Katrina	Diamond Head, MS	Slab	122	0.071	-13.82	1.000
KM3	Katrina	Diamond Head, MS	Slab	122	0.070	-14.72	1.000

7.2 Quantitative Analysis

7.2.1 Hurricanes Charley and Ivan (2004)

Panel members visited Florida Citizens Insurance in Tallahassee, FL to review claims files for Hurricane Charley (FEMA 488, 2005) and Hurricane Ivan (FEMA 489, 2005) which struck Florida in 2004. A random sampling of policies that were in force during the storms and located in affected areas was acquired. Maximum gust wind speeds were assigned to each property location using the gridded H*Wind swaths that were produced by NOAA's Hurricane Research Division after the storms. Figure 7-4 shows the areas covered by the policy sampling process.

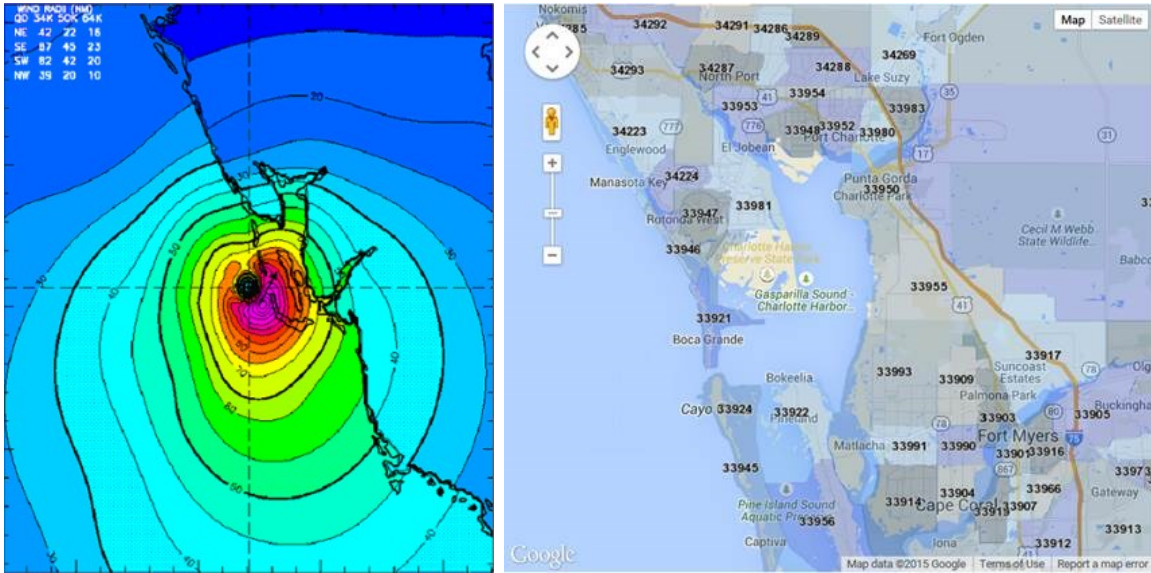
A total of 495 policies were sampled. Claim files were reviewed for the subset of those policies that filed a claim with Florida Citizens. Damage ratios for each of the components considered by the damage module were estimated for each claim. These estimates were generally subjective interpretations based on photographs and adjuster reports. It is important to note that the results of this review were maximum levels of damage for structures that did not flood. Time histories of damage cannot be extracted from insurance claim files. As such, maximum levels of component damage are the damage module quantity suitable for comparison to the historical damage.

The damage module methodology was executed 130 times, using a synthesized wind speed and direction time history. In order to cover a wide spectrum of maximum wind speeds, the amplitude of the wind speed time history was modified for each of the executions. Furthermore, the structure characteristics were varied by randomly sampling most of the variables for each execution.

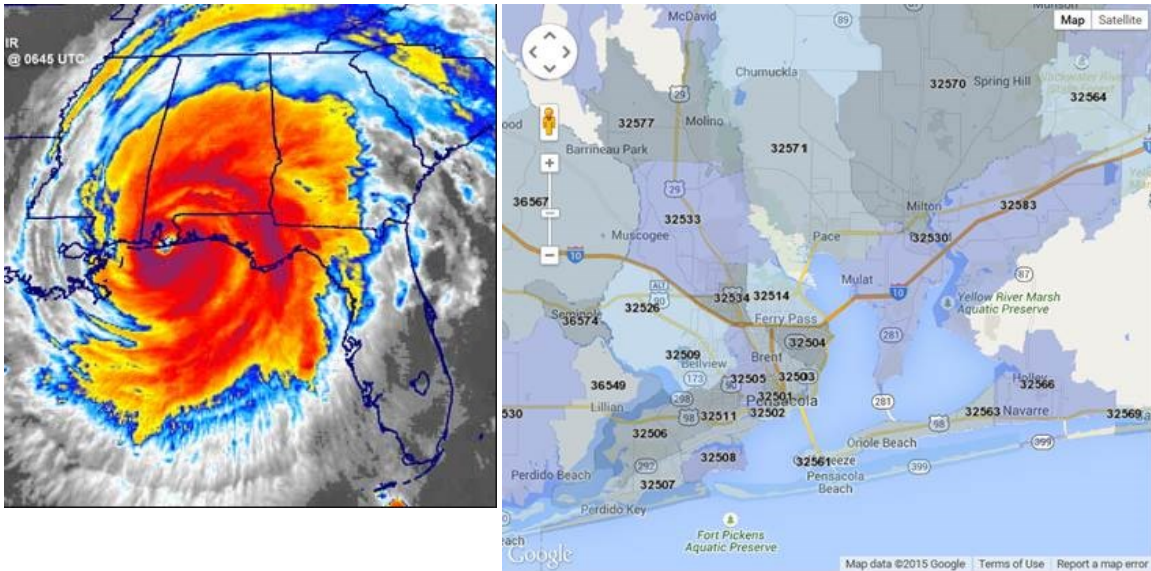
Table 7-2 through Table 7-10 compare the results from the claim file review and results from the damage module, arranged by 5 mph wind speed groups. The means and standard deviations of the component damage ratios are shown for both sets of data. The number of samples and the corresponding number of claims for each wind speed group are given for the historical storm data.

The mean values for the Charley and Ivan claims are the average damage ratio for all of the properties in the wind speed group, including properties without claims. The standard deviations were calculated similarly. For example, there were 167 properties

that contributed to the average damage to properties experiencing wind speeds of 85-90 mph, even though only 32 actually filed a claim. The contribution to the average of the 135 properties that did not file a claim was a zero.



(a) Hurricane Charley (2004)



(b) Hurricane Ivan (2004)

Figure 7-4: Florida Citizens Policy Sampling

It should be noted that the variability of the claim data and the variability of the model results are not reflecting the same processes. The standard deviation of the model results only reflects the variety of input, since the damage module will yield identical results for the same input. In reality, two structures with nominally the same construction characteristics, location, and storm experience may vary widely in the level of damage they each sustain. The variability of modeled results for roof cover damage and interior finish damage are shown in Figure 7-5 below.

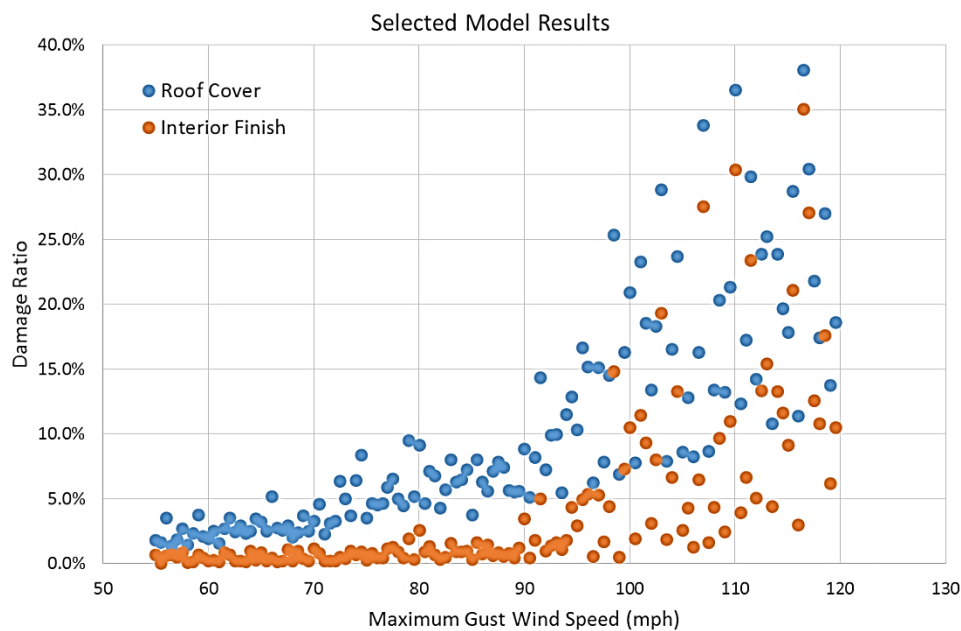


Figure 7-5: Variability of Modeled Wind Damage Results over a Variety of Wind Speeds. This figure illustrates the influence that model inputs (other than wind speed) have on estimates of wind damage.

In general, the damage module results compare favorably with the data interpreted from the claim files. One exception is that the damage module predicts less roof frame damage than appeared in the claim files for Hurricanes Charley and Ivan. As the effort to compare the Damage Estimation Module results to data from historical storms continues, adjustments to the model can be made, if necessary, to better reflect observed damage.

TABLE 7-3. CLAIMS FILE REVIEW RESULTS: ROOF COVER

Roof Cover						
WS Group	Florida Citizens (Charley & Ivan 2004)				Model (N = 130)	
	N	N Damaged	AVG D (%)	STDEV D (%)	AVG D	STDEV D
55-60	N/A	N/A	N/A	N/A	2.3%	0.8%
60-65	N/A	N/A	N/A	N/A	2.6%	0.6%
65-70	N/A	N/A	N/A	N/A	3.0%	0.9%
70-75	4	0	0.0	0.0	4.7%	1.9%
75-80	17	2	3.5	10.0	5.4%	1.7%
80-85	3	1	6.7	11.5	6.6%	1.5%
85-90	167	32	5.4	13.4	6.3%	1.3%
90-95	64	12	5.3	12.8	9.4%	3.0%
95-100	91	31	13.7	25.4	13.5%	5.8%
100-105	61	22	18.6	29.4	17.9%	6.8%
105-110	18	5	6.7	12.8	15.7%	7.9%
110-115	23	11	19.6	26.9	21.4%	8.1%
115-120	44	8	7.7	19.3	22.5%	8.3%
120-125	3	0	0.0	0.0	N/A	N/A
TOTAL	495	124				

TABLE 7-4. CLAIMS FILE REVIEW RESULTS: ROOF PANEL

Roof Panel						
WS Group	Florida Citizens (Charley & Ivan 2004)				Model (N = 130)	
	N	N Damaged	AVG D (%)	STDEV D (%)	AVG D	STDEV D
55-60	N/A	N/A	N/A	N/A	1.1%	0.1%
60-65	N/A	N/A	N/A	N/A	1.2%	0.1%
65-70	N/A	N/A	N/A	N/A	1.2%	0.1%
70-75	4	0	0.0	0.0	1.5%	0.2%
75-80	17	0	0.0	0.0	1.7%	0.3%
80-85	3	0	0.0	0.0	1.8%	0.2%
85-90	167	1	0.1	0.8	1.9%	0.2%
90-95	64	1	0.3	2.5	2.4%	0.5%
95-100	91	5	1.6	10.8	2.7%	0.6%
100-105	61	10	3.0	8.2	3.3%	0.8%
105-110	18	0	0.0	0.0	3.3%	1.2%
110-115	23	2	1.3	4.6	3.9%	1.3%
115-120	44	1	0.5	3.0	4.5%	1.1%
120-125	3	0	0.0	0.0	N/A	N/A
TOTAL	495	20				

TABLE 7-5. CLAIMS FILE REVIEW RESULTS: WALL COVER

Wall Cover						
WS Group	Florida Citizens (Charley & Ivan 2004)				Model (N = 130)	
	N	N Damaged	AVG D (%)	STDEV D (%)	AVG D	STDEV D
55-60	N/A	N/A	N/A	N/A	0.7%	0.0%
60-65	N/A	N/A	N/A	N/A	0.8%	0.1%
65-70	N/A	N/A	N/A	N/A	0.8%	0.1%
70-75	4	0	0.0	0.0	0.9%	0.1%
75-80	17	0	0.0	0.0	1.0%	0.1%
80-85	3	0	0.0	0.0	1.1%	0.2%
85-90	167	15	1.2	4.2	1.2%	0.2%
90-95	64	10	1.6	3.7	1.5%	0.4%
95-100	91	27	3.7	6.6	1.6%	0.3%
100-105	61	14	3.6	7.5	2.0%	0.5%
105-110	18	4	2.2	4.3	2.0%	0.5%
110-115	23	7	5.2	9.0	2.4%	0.6%
115-120	44	8	2.7	7.3	2.7%	0.7%
120-125	3	0	0.0	0.0	N/A	N/A
TOTAL	495	85				

TABLE 7-6. CLAIMS FILE REVIEW RESULTS: WALL SHEATHING

Wall Sheathing						
WS Group	Florida Citizens (Charley & Ivan 2004)				Model (N = 130)	
	N	N Damaged	AVG D (%)	STDEV D (%)	AVG D	STDEV D
55-60	N/A	N/A	N/A	N/A	0.0%	0.0%
60-65	N/A	N/A	N/A	N/A	0.0%	0.0%
65-70	N/A	N/A	N/A	N/A	0.0%	0.0%
70-75	4	0	0.0	0.0	0.0%	0.0%
75-80	17	0	0.0	0.0	0.0%	0.0%
80-85	3	0	0.0	0.0	0.0%	0.0%
85-90	167	0	0.0	0.0	0.0%	0.0%
90-95	64	0	0.0	0.0	0.0%	0.0%
95-100	91	1	0.1	1.0	0.0%	0.0%
100-105	61	1	0.3	2.6	0.0%	0.0%
105-110	18	0	0.0	0.0	0.0%	0.0%
110-115	23	0	0.0	0.0	0.0%	0.1%
115-120	44	1	0.2	1.5	0.1%	0.2%
120-125	3	0	0.0	0.0	N/A	N/A
TOTAL	495	3				

TABLE 7-7. CLAIMS FILE REVIEW RESULTS: WINDOWS

Windows						
WS Group	Florida Citizens (Charley & Ivan 2004)				Model (N = 130)	
	N	N Damaged	AVG D (%)	STDEV D (%)	AVG D	STDEV D
55-60	N/A	N/A	N/A	N/A	1.0%	0.4%
60-65	N/A	N/A	N/A	N/A	1.3%	0.4%
65-70	N/A	N/A	N/A	N/A	1.3%	0.4%
70-75	4	0	0.0	0.0	1.4%	0.7%
75-80	17	0	0.0	0.0	1.6%	0.5%
80-85	3	0	0.0	0.0	2.0%	0.8%
85-90	167	13	1.2	4.6	2.1%	1.1%
90-95	64	6	1.5	5.0	3.2%	1.3%
95-100	91	17	4.6	10.8	2.4%	1.4%
100-105	61	14	5.4	12.1	4.8%	1.4%
105-110	18	2	1.1	3.2	4.5%	1.8%
110-115	23	3	1.3	3.4	5.8%	1.7%
115-120	44	6	3.4	11.6	7.0%	2.5%
120-125	3	0	0.0	0.0	N/A	N/A
TOTAL	495	61				

TABLE 7-8. CLAIMS FILE REVIEW RESULTS: DOORS

Doors						
WS Group	Florida Citizens (Charley & Ivan 2004)				Model (N = 130)	
	N	N Damaged	AVG D (%)	STDEV D (%)	AVG D	STDEV D
55-60	N/A	N/A	N/A	N/A	0.8%	0.5%
60-65	N/A	N/A	N/A	N/A	1.1%	0.5%
65-70	N/A	N/A	N/A	N/A	1.1%	0.6%
70-75	4	0	0.0	0.0	0.8%	0.7%
75-80	17	1	1.2	4.9	1.2%	0.5%
80-85	3	0	0.0	0.0	1.6%	0.8%
85-90	167	10	2.6	10.7	2.1%	0.9%
90-95	64	2	1.0	6.4	2.9%	1.0%
95-100	91	9	4.6	14.9	2.3%	1.1%
100-105	61	6	4.6	14.3	3.9%	1.4%
105-110	18	1	2.8	11.8	3.7%	1.2%
110-115	23	3	6.5	17.2	4.9%	1.8%
115-120	44	3	3.4	12.7	6.3%	2.1%
120-125	3	0	0.0	0.0	N/A	N/A
TOTAL	495	35				

TABLE 7-9. CLAIMS FILE REVIEW RESULTS: GARAGE DOORS

Garage Doors						
WS Group	Florida Citizens (Charley & Ivan 2004)				Model (N = 130)	
	N	N Damaged	AVG D (%)	STDEV D (%)	AVG D	STDEV D
55-60	N/A	N/A	N/A	N/A	0.2%	0.2%
60-65	N/A	N/A	N/A	N/A	0.2%	0.2%
65-70	N/A	N/A	N/A	N/A	0.3%	0.3%
70-75	4	0	0.0	0.0	0.3%	0.4%
75-80	17	0	0.0	0.0	0.4%	0.5%
80-85	3	0	0.0	0.0	0.5%	0.6%
85-90	167	2	0.6	7.7	1.2%	1.0%
90-95	64	2	3.1	17.5	1.4%	2.0%
95-100	91	2	2.2	14.7	2.2%	2.6%
100-105	61	4	6.6	25.0	3.2%	4.0%
105-110	18	1	5.6	23.6	4.6%	5.1%
110-115	23	2	8.7	28.8	6.7%	7.8%
115-120	44	2	4.5	21.1	6.4%	10.5%
120-125	3	0	0.0	0.0	N/A	N/A
TOTAL	495	15				

TABLE 7-10. CLAIMS FILE REVIEW RESULTS: ROOF FRAMING

Roof Framing						
WS Group	Florida Citizens (Charley & Ivan 2004)				Model (N = 130)	
	N	N Damaged	AVG D (%)	STDEV D (%)	AVG D	STDEV D
55-60	N/A	N/A	N/A	N/A	0.0%	0.0%
60-65	N/A	N/A	N/A	N/A	0.0%	0.0%
65-70	N/A	N/A	N/A	N/A	0.0%	0.0%
70-75	4	0	0.0	0.0	0.0%	0.0%
75-80	17	0	0.0	0.0	0.0%	0.0%
80-85	3	0	0.0	0.0	0.0%	0.0%
85-90	167	0	0.0	0.0	0.0%	0.0%
90-95	64	0	0.0	0.0	0.0%	0.0%
95-100	91	1	0.1	1.0	0.0%	0.0%
100-105	61	3	0.7	3.1	0.0%	0.0%
105-110	18	0	0.0	0.0	0.0%	0.0%
110-115	23	1	0.4	2.1	0.0%	0.0%
115-120	44	1	0.2	1.5	0.0%	0.0%
120-125	3	0	0.0	0.0	N/A	N/A
TOTAL	495	6				

TABLE 7-11. CLAIMS FILE REVIEW RESULTS: INTERIOR FINISHES

Interior Finishes						
WS Group	Florida Citizens (Charley & Ivan 2004)				Model (N = 130)	
	N	N Damaged	AVG D (%)	STDEV D (%)	AVG D	STDEV D
55-60	N/A	N/A	N/A	N/A	0.5%	0.3%
60-65	N/A	N/A	N/A	N/A	0.4%	0.3%
65-70	N/A	N/A	N/A	N/A	0.5%	0.4%
70-75	4	0	0.0	0.0	0.6%	0.3%
75-80	17	1	2.5	6.1	0.8%	0.5%
80-85	3	0	0.0	0.0	1.1%	0.6%
85-90	167	24	4.6	12.2	0.9%	0.4%
90-95	64	9	5.1	14.2	2.2%	1.5%
95-100	91	24	10.4	20.1	4.8%	4.2%
100-105	61	21	16.8	27.3	8.6%	5.5%
105-110	18	5	6.9	11.5	7.1%	7.9%
110-115	23	7	13.0	21.1	12.8%	8.7%
115-120	44	9	9.1	20.2	15.3%	10.0%
120-125	3	0	0.0	0.0	N/A	N/A
TOTAL	495	100				

7.2.2 Hurricanes Rita (2005)

At the request of the Panel, TWIA provided data related to damage and losses due to Hurricane Rita in 2005. At the time of Hurricane Rita 3,273 TWIA policies were in effect in Jefferson County, Texas, and were classified as shown in Table 7-11.

TABLE 7-12. SELECT TWIA POLICIES

City *	Risks	Designated Area
Beaumont	963	Inland 2
Cheek	1	Inland 2
China	6	Inland 2
Fannett	8	Inland 2
Groves	414	Inland 1
Hamshire	17	Inland 1
Labelle	7	Inland 1
Nederland	318	Inland 1
Nome	5	Inland 2
Port Acres	4	Inland 1
Port Arthur	1,252	Inland 1 / Seaward
Port Neches	236	Inland 1
SABINE	2	Seaward
Sabine Pass	33	Seaward
Winnie	7	Inland 1
Total	3,273	

From these 3,273 policies, TWIA randomly selected 200 policies for detailed review by the Panel. Maximum gust wind speeds were assigned to each property location in the sample using the gridded H*Wind swaths that were produced by the Hurricane Research Division of NOAA after the storm.

In contrast to Florida Citizens, TWIA opened a claim on every property in the area affected by Hurricane Rita. Wind damage ratios for each of the components considered by the damage module were estimated for each claim, with the exception of out-of-plane wall damage and shear wall damage. While it was the intention to limit this portion of the validation effort to damage solely caused by wind, it became clear during the review that some properties had been inundated. For this reason damage modes associated with structural collapse (out-of-plane wall failures and shear wall failures) were omitted in the

analysis. It is possible that other damage modes, such as garage door damage and damage to interior finishes, were also affected by storm surge and waves.

The estimates of wind damage were generally subjective interpretations based on photographs and adjuster reports. Since time histories of damage cannot be extracted from insurance claim files, maximum levels of component damage are the damage module result suitable for comparison to the historical damage. The estimation of wind damage was further complicated by the presence of roof tarps on many of the properties. It was not possible to view the entire roofs in these cases, and interpretations of roof cover and roof panel damage may be in error. Based on what was visible in the file photographs and aerial photographs of the surrounding areas, the maximum roof cover damage ratio was limited to 50%, even though adjusters may have recommended payments for complete roof replacements.

For the comparison of the model results with the Florida Citizens claims, the damage module methodology was executed 130 times, using a synthesized wind speed and direction time history. To cover a wide spectrum of maximum wind speeds, the amplitude of the wind speed time history was modified for each of the executions. Furthermore, the structure characteristics were varied by randomly sampling most of the variables for each execution. The same model runs were used for comparisons with Hurricane Rita damage. Since the spectrum of wind speeds in Jefferson County was narrow, only 90 of the 130 model runs were of a corresponding range of wind speeds.

Table 7-12 through Table 7-20 compare the results from the claim file review and results from the damage module, arranged by 5 mph wind speed groups. The means and standard deviations of the component damage ratios are shown for both sets of data. The number of samples and the corresponding number of properties experiencing some damage for each wind speed group are given for the historical storm data.

The mean values for the Rita claims are the average damage ratio for all of the properties in the wind speed group, including properties without claims. The standard deviations were calculated similarly. For example, there were 20 properties that contributed to the average damage to properties experiencing wind speeds of 85-90 mph, even though only two properties actually showed damage. The contribution to the average of the 18 properties that did not experience damage was zero.

It should be noted that the variability of the claim data and the variability of the model results are not reflecting the same processes. The standard deviation of the model results only reflects the variety of input, since the damage module will yield identical results for the same input. In reality, two structures with nominally the same construction characteristics, location, and storm experience may vary widely in the level of damage they each sustain.

In general, the damage module results are lower than the damage levels interpreted from the Rita claim files. The ranges of observed damage are quite large, and the average values predicted by the model are typically within one standard deviation of the average observed damage level. Some differences between the validation efforts using the Florida Citizens data and the TWIA data are: (1) Panel personnel involved; (2) TWIA opened claim files on all properties as a rule, and (3) some of the TWIA properties had been affected by flooding to some degree.

Furthermore, it was the general impression on the part of the Panel members reviewing the Rita claim data that the properties represented in the sample were in older developments. Component ages, especially roof cover age, are known to be strong drivers of damage. Since structure and component ages were not isolated in this portion of the validation effort, it is not possible to determine whether age-related deterioration contributed to differences between the modeled and observed damages. As the effort to compare results from the Damage Estimation Module to data from historical storms continues, adjustments to the model can occur, if necessary, to better reflect observed damage.

TABLE 7-13. RITA CLAIMS FILE REVIEW RESULTS: ROOF COVER

Roof Cover						
WS Group	TWIA (Rita 2005)				Model	
	N	N Damaged	AVG D (%)	STDEV D (%)	AVG D	STDEV D
55-60	N/A	N/A	N/A	N/A	2.3%	0.8%
60-65	N/A	N/A	N/A	N/A	2.6%	0.6%
65-70	44	39	24.8	18.3	3.0%	0.9%
70-75	88	73	26.3	19.8	4.7%	1.9%
75-80	45	39	25.5	18.1	5.4%	1.7%
80-85	20	2	31.5	18.8	6.6%	1.5%
85-90	3	0	0	0	6.3%	1.3%
90-95	N/A	N/A	N/A	N/A	9.4%	3.0%
95-100	N/A	N/A	N/A	N/A	13.5%	5.8%
TOTAL	200	153				

TABLE 7-14. RITA CLAIMS FILE REVIEW RESULTS: ROOF PANEL

Roof Panel						
WS Group	TWIA (Rita 2005)				Model	
	N	N Damaged	AVG D (%)	STDEV D (%)	AVG D	STDEV D
55-60	N/A	N/A	N/A	N/A	1.1%	0.1%
60-65	N/A	N/A	N/A	N/A	1.2%	0.1%
65-70	44	8	2.2	5.1	1.2%	0.1%
70-75	88	11	1.9	6.5	1.5%	0.2%
75-80	45	9	3.0	6.9	1.7%	0.3%
80-85	20	5	5.8	12.3	1.8%	0.2%
85-90	3	1	3.3	5.8	1.9%	0.2%
90-95	N/A	N/A	N/A	N/A	2.4%	0.5%
95-100	N/A	N/A	N/A	N/A	2.7%	0.6%
TOTAL	200	34				

TABLE 7-15. RITA CLAIMS FILE REVIEW RESULTS: WALL COVER

Wall Cover						
WS Group	TWIA (Rita 2005)				Model	
	N	N Damaged	AVG D (%)	STDEV D (%)	AVG D	STDEV D
55-60	N/A	N/A	N/A	N/A	0.7%	0.0%
60-65	N/A	N/A	N/A	N/A	0.8%	0.1%
65-70	44	15	7.8	15.2	0.8%	0.1%
70-75	88	33	5.9	9.5	0.9%	0.1%
75-80	45	17	6.7	10.9	1.0%	0.1%
80-85	20	5	5.5	10.2	1.1%	0.2%
85-90	3	1	3.3	5.8	1.2%	0.2%
90-95	N/A	N/A	N/A	N/A	1.5%	0.4%
95-100	N/A	N/A	N/A	N/A	1.6%	0.3%
TOTAL	200	71				

TABLE 7-16. RITA CLAIMS FILE REVIEW RESULTS: WALL SHEATHING

Wall Sheathing						
WS Group	TWIA (Rita 2005)				Model	
	N	N Damaged	AVG D (%)	STDEV D (%)	AVG D	STDEV D
55-60	N/A	N/A	N/A	N/A	0.0%	0.0%
60-65	N/A	N/A	N/A	N/A	0.0%	0.0%
65-70	44	4	1.0	4.3	0.0%	0.0%
70-75	88	2	0.3	1.8	0.0%	0.0%
75-80	45	1	0.2	1.5	0.0%	0.0%
80-85	20	2	1.0	3.1	0.0%	0.0%
85-90	3	0	0.0	0.0	0.0%	0.0%
90-95	N/A	N/A	N/A	N/A	0.0%	0.0%
95-100	N/A	N/A	N/A	N/A	0.0%	0.0%
TOTAL	200	9				

TABLE 7-17. RITA CLAIMS FILE REVIEW RESULTS: WINDOWS

Windows						
WS Group	TWIA (Rita 2005)				Model	
	N	N Damaged	AVG D (%)	STDEV D (%)	AVG D	STDEV D
55-60	N/A	N/A	N/A	N/A	1.0%	0.4%
60-65	N/A	N/A	N/A	N/A	1.3%	0.4%
65-70	44	11	5.0	12.1	1.3%	0.4%
70-75	88	16	4.5	12.6	1.4%	0.7%
75-80	45	14	4.8	7.8	1.6%	0.5%
80-85	20	8	9.5	14.2	2.0%	0.8%
85-90	3	0	0.0	0.0	2.1%	1.1%
90-95	N/A	N/A	N/A	N/A	3.2%	1.3%
95-100	N/A	N/A	N/A	N/A	2.4%	1.4%
TOTAL	200	49				

TABLE 7-18. RITA CLAIMS FILE REVIEW RESULTS: DOORS

Doors						
WS Group	TWIA (Rita 2005)				Model	
	N	N Damaged	AVG D (%)	STDEV D (%)	AVG D	STDEV D
55-60	N/A	N/A	N/A	N/A	0.8%	0.5%
60-65	N/A	N/A	N/A	N/A	1.1%	0.5%
65-70	44	3	3.4	12.7	1.1%	0.6%
70-75	88	5	3.4	14.8	0.8%	0.7%
75-80	45	2	2.2	10.4	1.2%	0.5%
80-85	20	2	5.0	15.4	1.6%	0.8%
85-90	3	1	16.7	28.9	2.1%	0.9%
90-95	N/A	N/A	N/A	N/A	2.9%	1.0%
95-100	N/A	N/A	N/A	N/A	2.3%	1.1%
TOTAL	200	13				

TABLE 7-19. RITA CLAIMS FILE REVIEW RESULTS: GARAGE DOORS

Garage Doors						
WS Group	TWIA (Rita 2005)				Model	
	N	N Damaged	AVG D (%)	STDEV D (%)	AVG D	STDEV D
55-60	N/A	N/A	N/A	N/A	0.2%	0.2%
60-65	N/A	N/A	N/A	N/A	0.2%	0.2%
65-70	44	6	13.6	34.7	0.3%	0.3%
70-75	88	14	15.9	36.8	0.3%	0.4%
75-80	45	6	11.1	29.9	0.4%	0.5%
80-85	20	1	5.0	22.4	0.5%	0.6%
85-90	3	0	0.0	0.0	1.2%	1.0%
90-95	N/A	N/A	N/A	N/A	1.4%	2.0%
95-100	N/A	N/A	N/A	N/A	2.2%	2.6%
TOTAL	200	27				

TABLE 7-20. RITA CLAIMS FILE REVIEW RESULTS: ROOF FRAMING

Roof Framing						
WS Group	TWIA (Rita 2005)				Model	
	N	N Damaged	AVG D (%)	STDEV D (%)	AVG D	STDEV D
55-60	N/A	N/A	N/A	N/A	0.0%	0.0%
60-65	N/A	N/A	N/A	N/A	0.0%	0.0%
65-70	44	5	1.1	3.2	0.0%	0.0%
70-75	88	6	0.7	2.5	0.0%	0.0%
75-80	45	4	1.2	4.4	0.0%	0.0%
80-85	20	0	0.0	0.0	0.0%	0.0%
85-90	3	1	3.3	5.8	0.0%	0.0%
90-95	N/A	N/A	N/A	N/A	0.0%	0.0%
95-100	N/A	N/A	N/A	N/A	0.0%	0.0%
TOTAL	200	16				

TABLE 7-21. RITA CLAIMS FILE REVIEW RESULTS: INTERIOR FINISHES

Interior Finishes						
WS Group	TWIA (Rita 2005)				Model	
	N	N Damaged	AVG D (%)	STDEV D (%)	AVG D	STDEV D
55-60	N/A	N/A	N/A	N/A	0.5%	0.3%
60-65	N/A	N/A	N/A	N/A	0.4%	0.3%
65-70	44	19	14.2	19.7	0.5%	0.4%
70-75	88	43	18.8	24.0	0.6%	0.3%
75-80	45	30	25.6	24.1	0.8%	0.5%
80-85	20	16	30.0	23.8	1.1%	0.6%
85-90	3	2	16.7	14.4	0.9%	0.4%
90-95	N/A	N/A	N/A	N/A	2.2%	1.5%
95-100	N/A	N/A	N/A	N/A	4.8%	4.2%
TOTAL	200	110				

7.2.3 Hurricanes Ike (2008)

Panel members requested to review TWIA claim files for Hurricane Ike which struck Texas in 2008 (FEMA P-757, 2009). TWIA subsequently delivered to the Panel a random sampling of 500 claims, of which 471 contained useful data. The Panel assigned maximum gust wind speeds to each property location using the gridded H*Wind swaths that were produced after the storm by the Hurricane Research Division of NOAA. Figure 7-6 shows the areas covered by the claim sampling process.

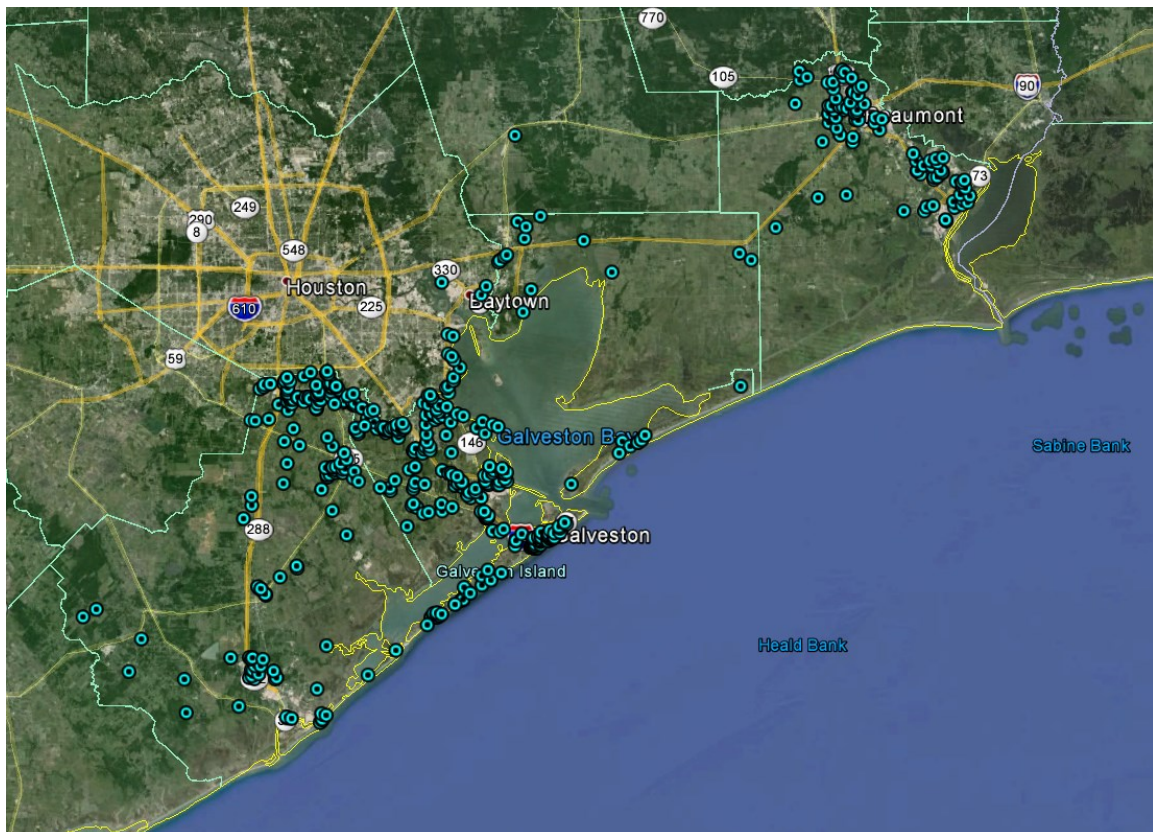


Figure 7-6: Locations of Randomly Sampled TWIA Hurricane Ike Property Claims

Since the random sampling of properties affected by Hurricane Ike only contained claims, it was crucial to determine the rate at which TWIA policy holders filed claims. These rates were determined on the basis of wind speed through a second random

sampling of 900 TWIA policies, regardless of whether or not the policy holder filed a claim. From this data, a least squares method was used to develop a relationship between the maximum gust wind speed and the rate at which policy holders filed claims. Figure 7-7 shows the sampled claim rates and the modeled function versus wind speed.

The modeled claim rate function was used to adjust the observed damage rates. For example, if roof cover damage ratios in the claims data were observed to be 20 percent for maximum gust wind speeds of 90 mph, then the adjusted damage ratio would be $0.20 \times 0.48 = 0.096$ (or 9.6%) when the “non-claim” properties are considered. The damage ratios observed in the Hurricane Ike claim data are summarized in Table 7-21 below. The damage ratios have been corrected using the modeled claim rate shown in Figure 7-7.

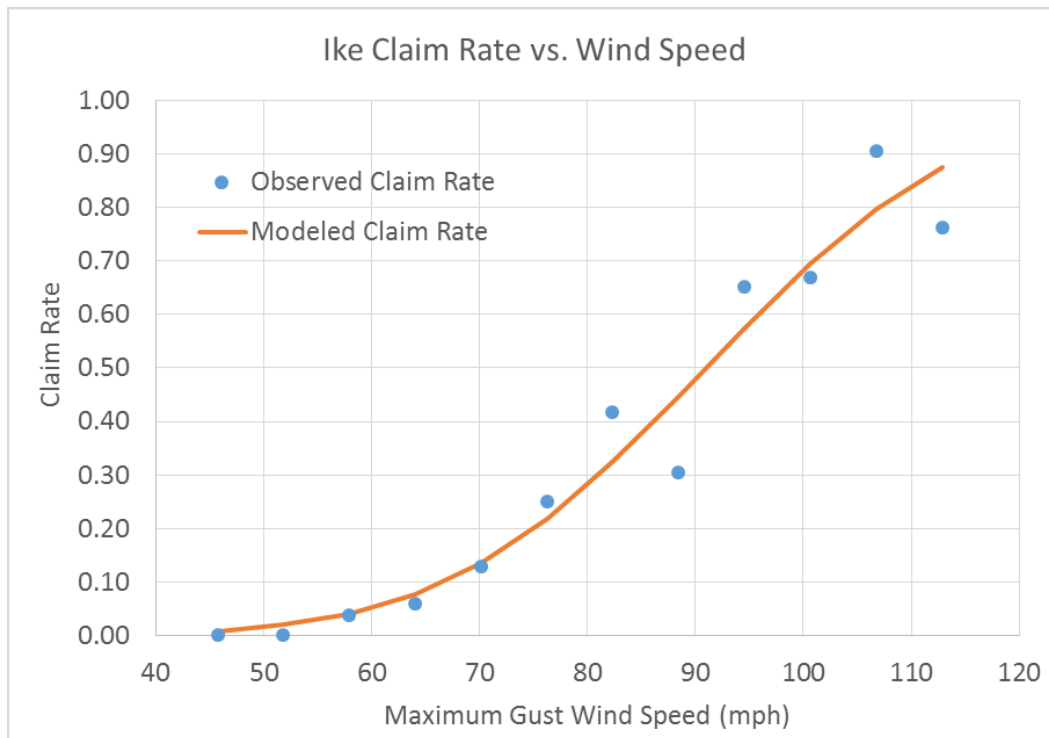


Figure 7-7: Rate of TWIA Property Insurance Claims versus Wind Speed for Hurricane Ike

TABLE 7-22. OBSERVED DAMAGE RATIOS FROM TWIA HURRICANE IKE CLAIMS

WS Group	Roof Cover	Roof Panel	Roof Framing	Wall Cover	Wall Panel	Windows	Doors	Garage Doors	Interior Finish	Number of Claims
60-65	0.0%	0.0%	0.0%	1.6%	0.0%	0.0%	0.0%	0.0%	0.0%	1
65-70	0.2%	0.0%	0.0%	0.2%	0.0%	0.0%	0.0%	0.0%	1.8%	3
70-75	2.6%	0.0%	0.0%	0.0%	0.0%	1.7%	0.0%	0.0%	2.2%	2
75-80	2.7%	0.0%	0.0%	0.0%	0.0%	0.0%	0.0%	0.0%	0.0%	1
80-85	1.6%	0.1%	0.1%	0.3%	0.0%	0.2%	0.0%	1.1%	1.7%	15
85-90	8.5%	1.3%	1.1%	0.8%	0.0%	0.8%	0.0%	0.0%	3.2%	10
90-95	6.1%	0.4%	0.3%	1.2%	0.0%	0.9%	0.5%	0.9%	9.0%	93
95-100	6.6%	0.4%	0.2%	1.5%	0.2%	0.8%	1.1%	2.1%	8.3%	239
100-105	13.3%	0.7%	0.2%	2.7%	0.2%	2.6%	3.0%	8.3%	5.0%	90
105-110	14.8%	0.0%	0.0%	4.0%	0.0%	0.0%	6.7%	26.9%	1.7%	12
110-115	19.5%	3.3%	2.2%	6.5%	0.0%	0.0%	0.0%	0.0%	10.9%	4
115-120	9.0%	0.0%	0.0%	0.0%	0.0%	0.0%	0.0%	0.0%	0.0%	1

Quantitative analysis of observed damage from Hurricanes Charley (2004), Ivan (2004), Rita (2005), and Ike (2008) have been presented in this section. Figure 7-8 through Figure 7-15 summarize the results of the analysis and show comparisons of the observed damage ratios to those predicted by the damage estimation module.

The damage module methodology was executed 130 times, using a synthesized wind speed and direction time history. To cover a wide spectrum of maximum wind speeds, the amplitude of the wind speed time history was modified for each of the executions. Furthermore, the structure characteristics were varied by randomly sampling most of the variables for each execution.

It should be noted that the variability of the claim data and the variability of the model results are not reflecting the same processes. The variance of the model results only reflects the variety of input, since the damage module will yield identical results for the same input. In reality, two structures with nominally the same construction characteristics, location, and storm experience may vary widely in the level of damage they each sustain.

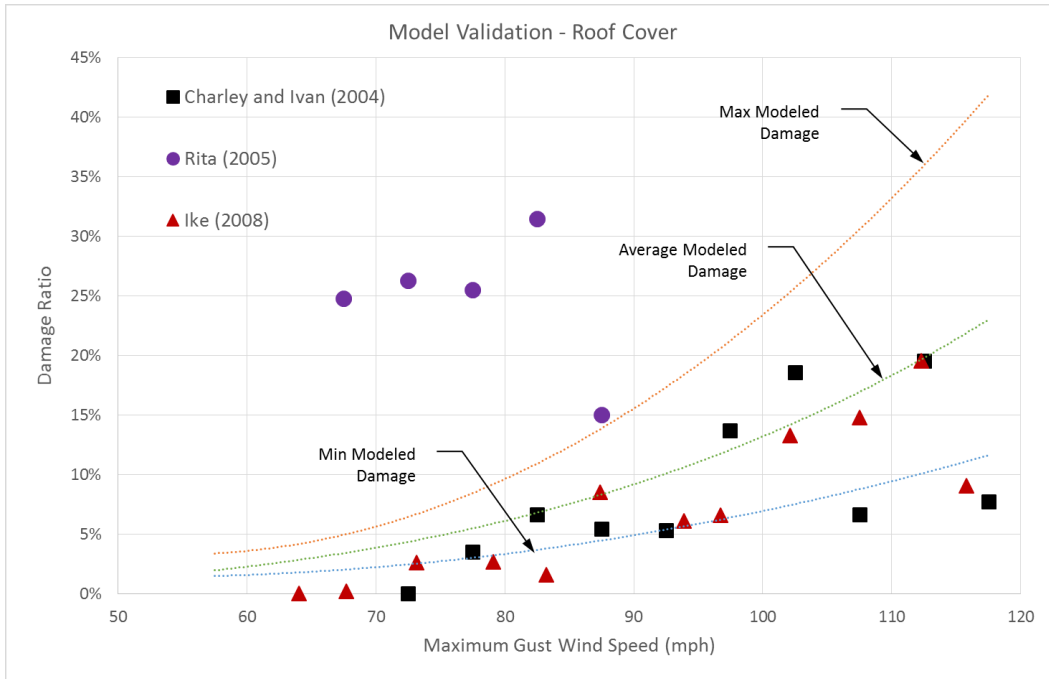


Figure 7-8: Observed versus Predicted Roof Cover Damage

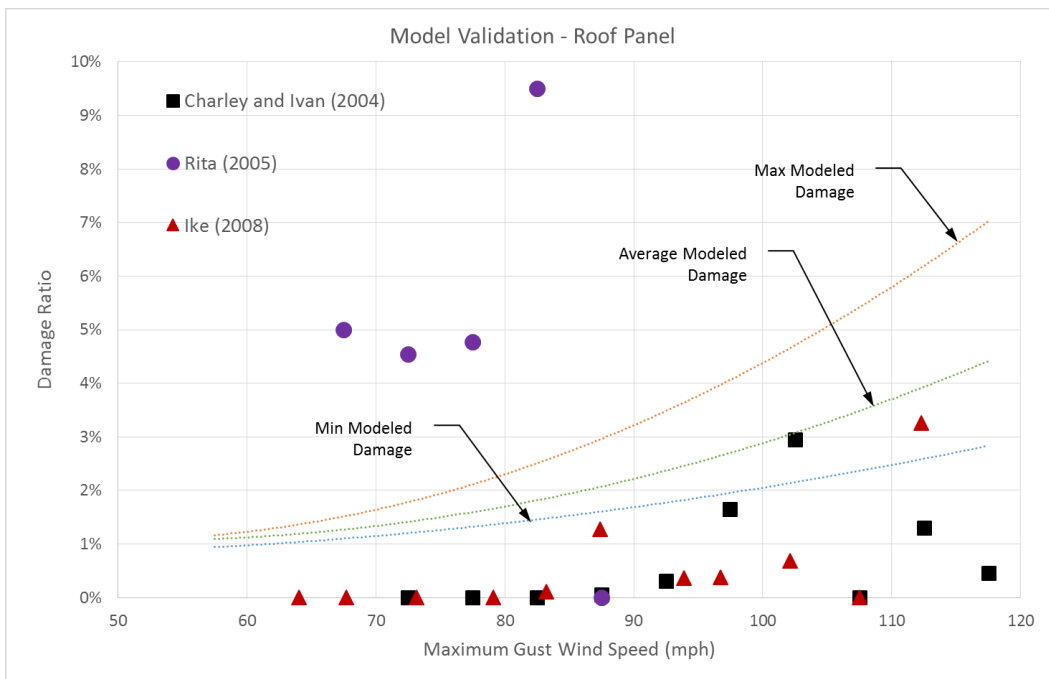


Figure 7-9: Observed versus Predicted Roof Panel Damage

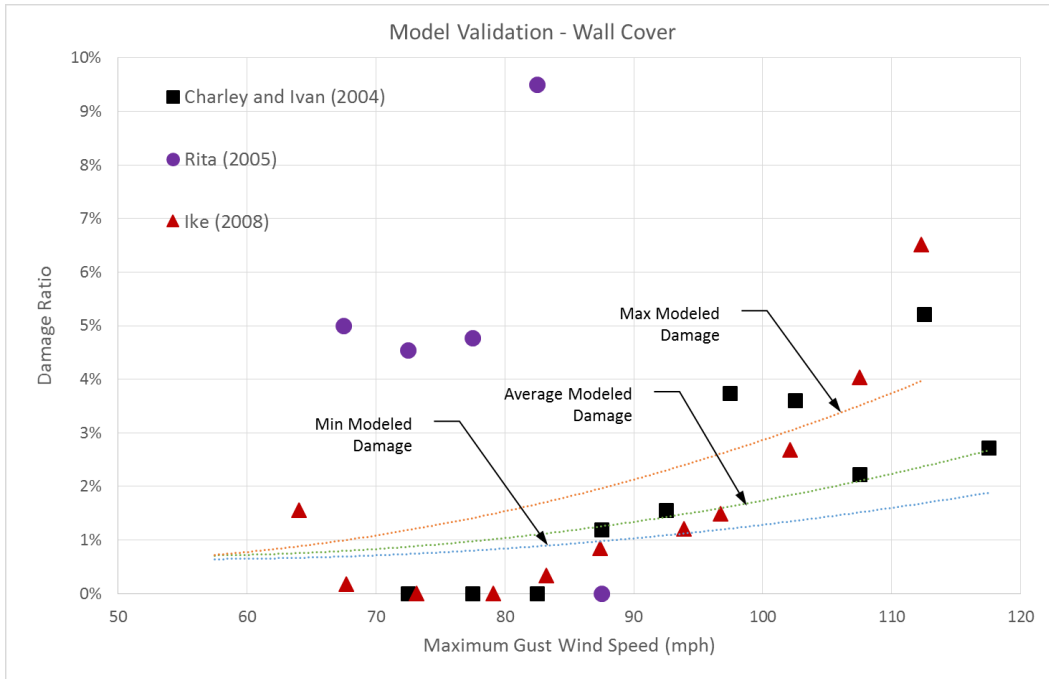


Figure 7-10: Observed versus Predicted Wall Cover Damage

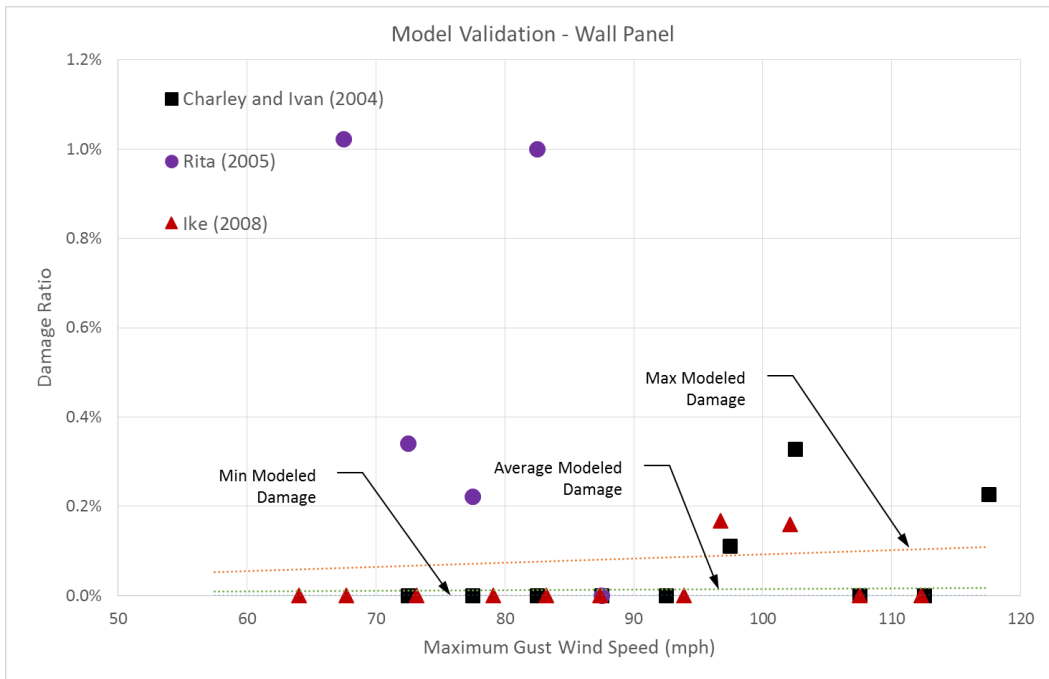


Figure 7-11: Observed versus Predicted Wall Panel Damage

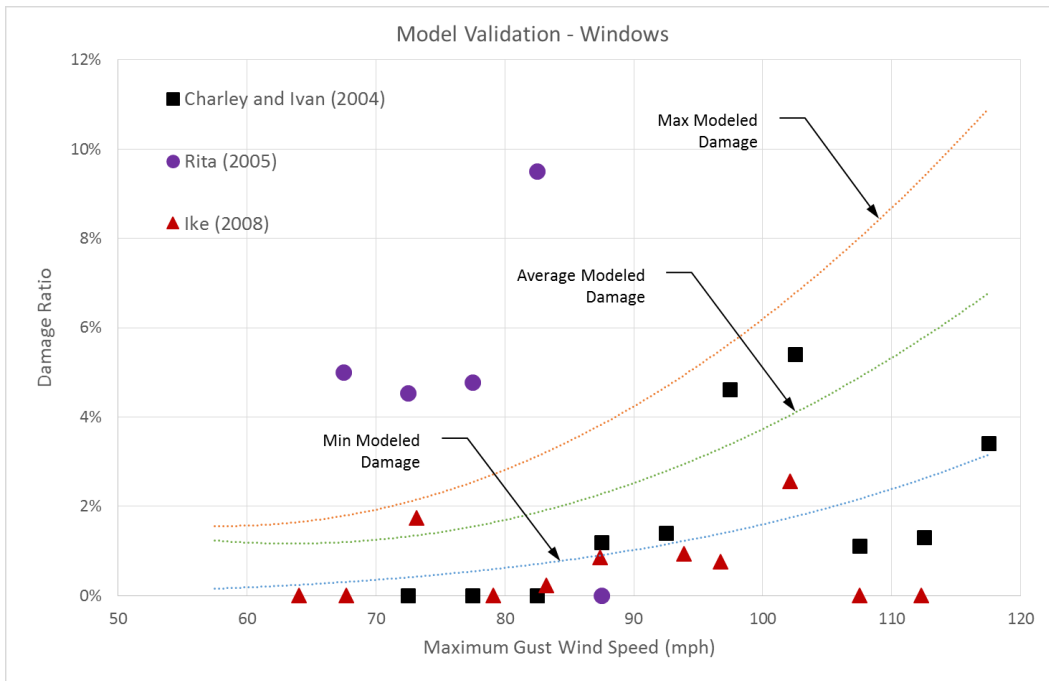


Figure 7-12: Observed versus Predicted Window Damage

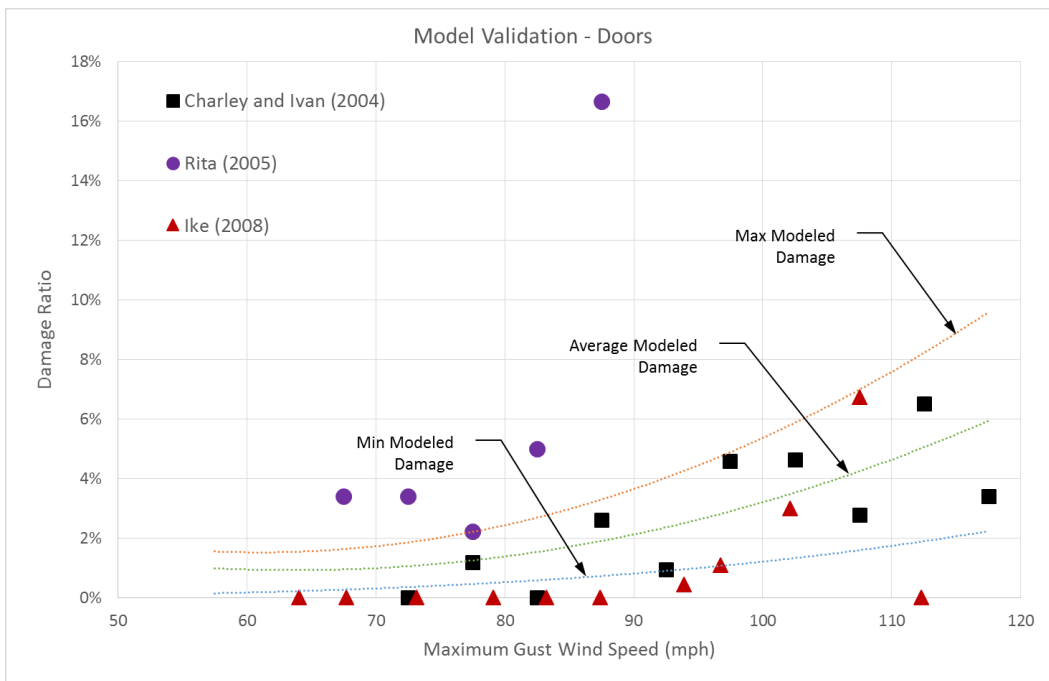


Figure 7-13: Observed versus Predicted Door Damage

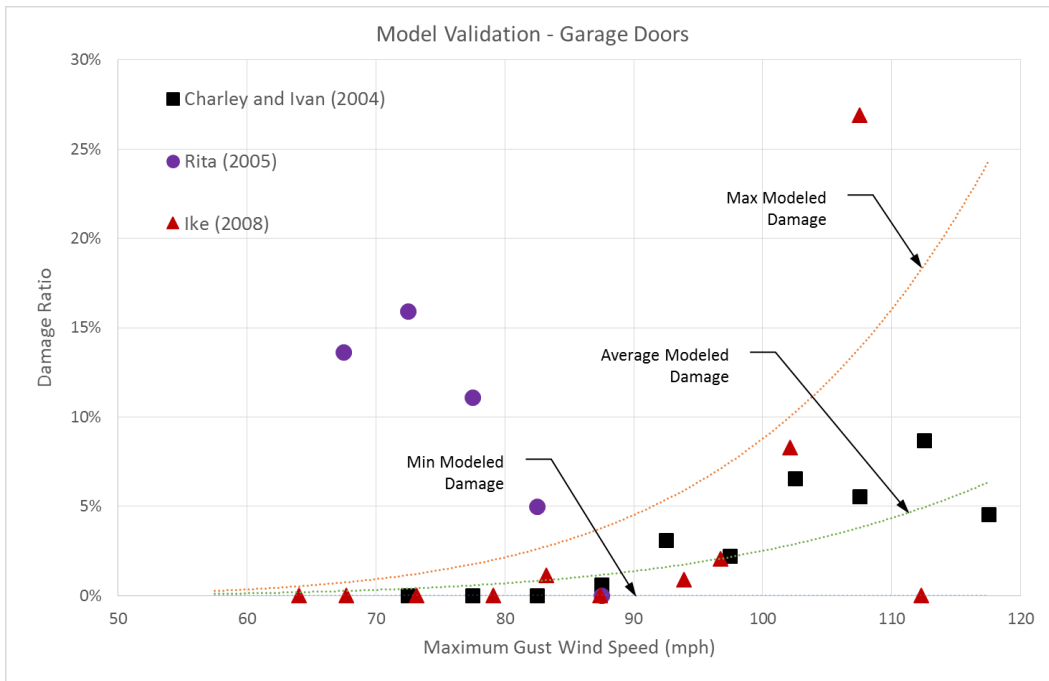


Figure 7-14: Observed versus Predicted Garage Door Damage

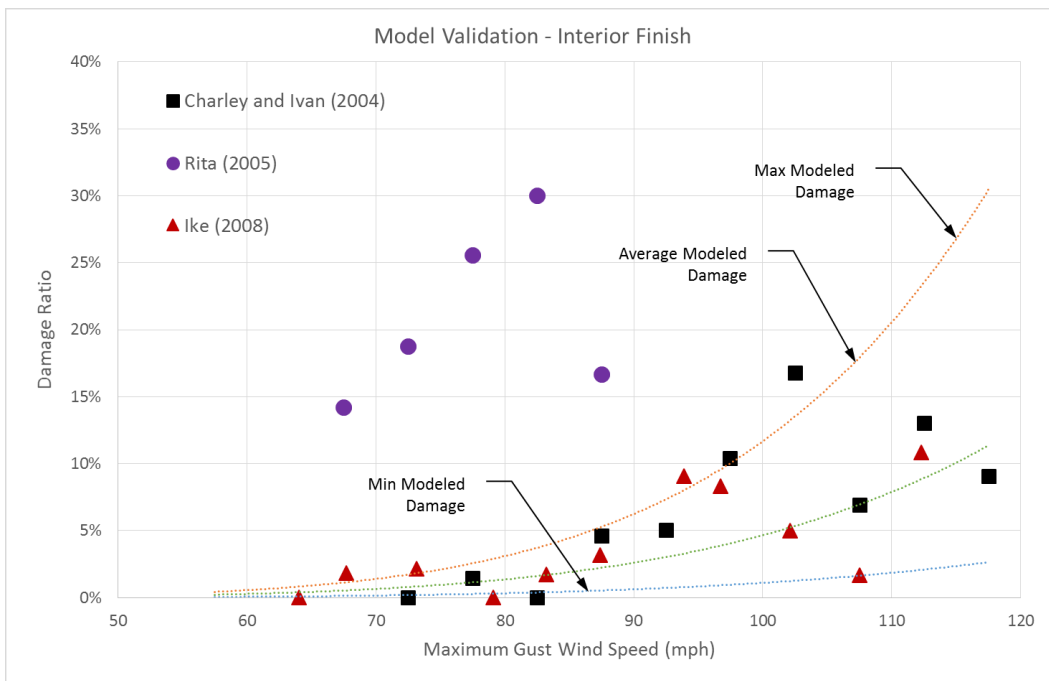


Figure 7-15: Observed versus Predicted Interior Finish Damage

In general, the Damage Estimation Module appears to provide reasonable estimates of the magnitudes and trends of damage when compared to observations of damage from actual storms, with the following exceptions:

- The damage observed for Hurricane Rita from the TWIA claim files deviates significantly from both the predictions of the Damage Estimation Module and the damage observed for the other three storms. Furthermore, there is no clear relationship between the magnitude of Rita damage and wind speed, which is counterintuitive and contrary to the observations from other storms. Possible explanations for these deviations have been proposed in Section 7.2.2 of this report.
- It appears that the Damage Estimation Module systematically overestimates damage for relatively low wind speeds. An exception to this trend is damage to interior finishes. It is understood that interior finishes can be damaged by building envelope leaks and wind driven rain, but the Damage Estimation Module is not currently capable of considering this effect. Interior damage is currently only triggered by actual damage to other building components.
- The Damage Estimation Module appears to systematically overestimate damage to roof panels at all of the wind speeds considered so far in the validation effort.
- The Damage Estimation Module appears to underestimate the rate at which wall panel damage increases with wind speed.

It may be possible to address some of these deviations from observed damage by calibrating the statistics for the random variables influencing the performance functions. If the Panel is able to achieve better agreement with the damage observations implied by the claim samples acquired so far, then a second validation effort would be warranted to compare the performance of a calibrated Damage Estimation Module to damage observations from new claim file samples.

8 Economic Loss Module

The Damage Estimation Module provides estimates of residential damage at the building or component level, and timing due to wind, surge, and waves. When estimating building economic loss, the proposed methodology is to rely on TWIA adjusters to determine the repair or replacement costs. The basis for the associated scope of work is the damage estimates produced by the Damage Estimation Module for the affected building components.

For example, if the model estimates that 10 percent of a roof covering was damaged by wind, then the adjuster would determine the appropriate scope of work and associated cost to repair or replace the roof covering. It is the current position of the Panel that TWIA adjusters will likely have better local knowledge of the monetary values for specific property components, and therefore should not rely on the model *per se* to calculate such valuations. Figure 8-1 illustrates the components of the Economic Loss Module.

Building features will presumably reside within the database of information maintained by TWIA for each residential policy. These features should ostensibly enable the adjuster to reasonably estimate component repair or replacement costs for each residence. Absent such information, the model will assume a base case for each building component. However, prior to estimating economic losses, the adjuster can obtain updated information on the building components; re-enter them into the database; use the model to obtain an updated estimate of building damage at the component level; and then estimate building component losses as outlined in Figure 3-1.

Estimating contents losses based on the building damage obtained from the damage prediction module is difficult. (Contents losses are separate from interior losses associated with damage to items like interior doors, wall finishes, floor finishes, ceiling finishes, and the interior surfaces of exterior walls.) Contents loss estimates are dependent on multiple independent factors, and therefore are highly variable. The science for estimating contents losses is not well established. To be sure, empirical relationships have been developed by private catastrophe loss modeling companies and

government agencies (e.g. FEMA), although these relationships likely replicate the approaches already taken by the insurance industry to estimate such losses.

As with building damage, it is the current opinion of the Panel that TWIA likely has better knowledge of contents values for specific properties, and therefore should not rely on the model to estimate contents valuations and associated losses. The Panel is willing to review the approaches taken by TWIA to estimate contents losses based on the Panel's knowledge and experience.

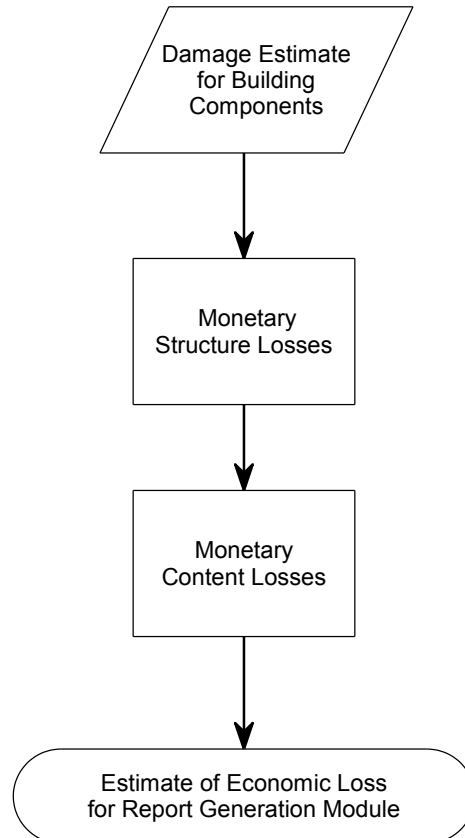


Figure 8-1: Economic Loss Module Flowchart

9 Report Generation Module

The Report Generation Module requires information from pre-storm and post-storm site-specific information; wind and storm surge hazard information and building vulnerability; and damage information to produce an automated report that represents the results of the damage determination model as illustrated in Figure 9-1.

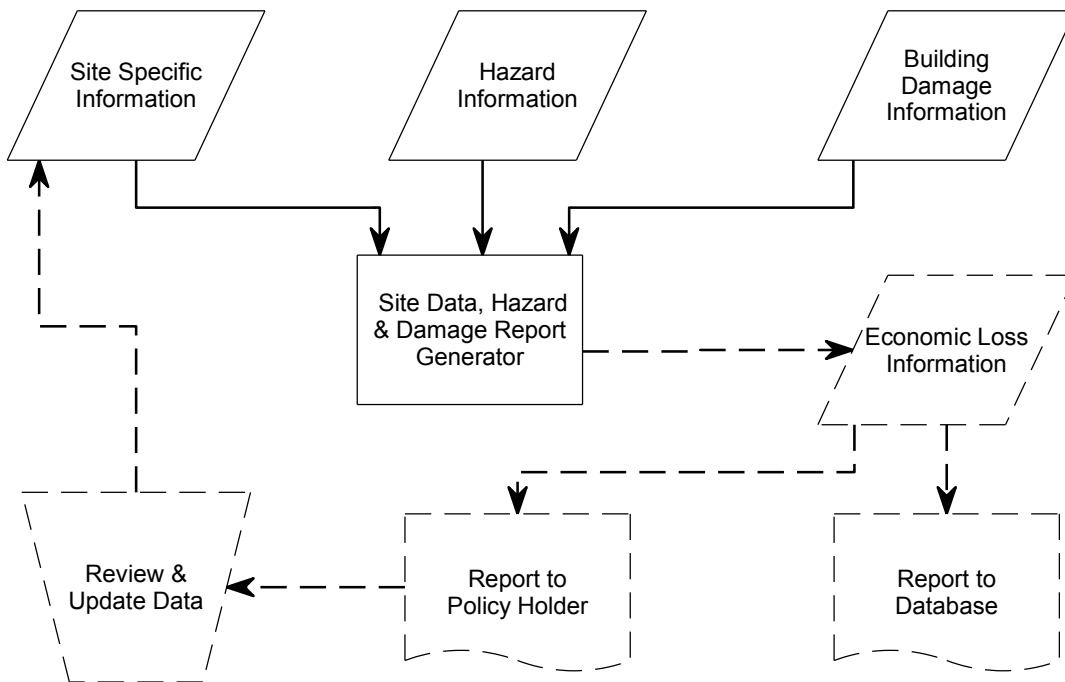


Figure 9-1: Report Generation Module Flowchart
 (TWIA responsible for components marked with dashed lines)

The report output could be delivered in ways that are needed by TWIA insurance adjusters or other designated users. The Panel recommends that results from the Report Generation Module be delivered to two parties.

- One complete report for TWIA to provide an archived result of the entire damage and loss reporting activity for each property investigated, including providing copies of versions of the report that might be developed from input corrections provided from owner corrections.
- A copy of this complete report for the building owner so the owner could verify or correct the building, damage, or hazard magnitude information used as inputs to the model; any corrections to the inputs could then be used to modify the calculated damage results.

10 Summary

The proposed methodology was developed for use only with residential slab cases because of the high frequency of occurrence relative to commercial construction and the difficulty with conventional claims adjustment for such cases. For other cases where partial buildings remain, the recommended damage determination method is to send an adjuster or engineer to the site for purposes of determining building damage by hazard type.

The Hazard Module provides information about the highest wind speeds and the greatest storm surge depths along with time histories of the event, including the times when the peaks were experienced. The wind hazard and storm surge models within the Hazard Module are required to produce results that are consistent with results obtained from actual engineering surveys or analysis. The storm surge model is driven by the same wind model used for wind hazard development.

The Damage Estimation Module calculates the probability of failure of various building components and structural systems during the progress of the storm. The component failure probabilities are weighted by the affected areas to estimate damage rates. The storm surge vulnerability is represented as a probability of total collapse based on the hazard, site, and building properties. More accurate damage estimates can be developed when model results are refined with observational results.

The model results provide percent damage estimates for the building components. TWIA or its insurance adjustment professionals are able to use the percent damage to determine financial losses and insurance policy payouts. All of the property-specific information stored in the database will be communicated via the Report Generation Module, including any modifications to either the data inputs or the economic loss results. The proposed methodology also readily allows incorporation of new research on hazard characterization, damage investigations, or vulnerabilities of building components as they become available.

11 Recommendations

11.1 Proposed Methodology

Provided below is a summary of the recommendations pertaining to the proposed methodology as discussed in the prior sections of this report. This summary reflects recommendations that the Panel considers essential for proper implementation of the methodology. It also includes recommendations that, although not necessarily essential, would nonetheless provide beneficial improvements to model performance when estimating winds damages sustained by the structure during the course of an event.

11.1.1 Essential

- TWIA shall enter into ongoing agreements to model waves and surge in high resolution during any significant events that impact the Texas coast, with details as given in Section 5.2.
- TWIA shall enter into ongoing agreements to perform physical measurements of waves, surge, and high water marks during any significant events that impact the Texas coast, with details as given in Section 5.3.
- TWIA shall develop the capability to model probability of collapse from waves and surge (for the damage estimation module) during an event as detailed in Section 5.4.
- Use an observational model for constructing a wind field to drive the storm surge model with details as given in Section 4.2.
- Compute a time history of wind damage to building components and structural systems at various structure locations using structural reliability theory with details as given in Section 6. The analysis shall consider building and site characteristics that are known to affect wind loading and structural performance.
- Employ both a probabilistic based approach and an observational approach to optimize estimations of wind damage to the structure.

- The wind field used for damage modeling shall be the same wind field model used to drive the storm surge model, and shall be a best-available reanalysis wind field that incorporates measurements made during the storm (observational model). The drag coefficient shall feature a high wind cutoff that is defensible from observations or the scientific literature.

11.1.2 *Beneficial*

- Consider incorporating more sophisticated (and potentially more accurate) methods for conducting the reliability analysis used for computing the time histories of wind damage. Candidate methods include Monte Carlo Simulation or the Rackwitz-Fiessler method (see Appendix C). These methods are less computationally efficient than the FOSM-MV method, and the Panel recommends that the possible improvement in accuracy be weighed against the larger programming cost.
- Consider including representations of the wind exposure category for eight direction sectors in the Damage Estimation Module. Terrain exposure is one of the most important factors affecting wind damage, and the methodology currently proposed and demonstrated assumes that the worst exposure category affecting a property is applicable to all wind directions.

If the Texas Insurance Commissioner decides to adopt the recommended methodology of the Panel for slab-only claims as part of the TWIA claims adjustment process, then preparations should be made for determining these losses for the upcoming hurricane season and beyond. The preparations should include making arrangements to collect storm-related pre- and post-event data, and to store this information in a database. The arrangements could include contracts or memoranda of understanding with other government agencies, universities, or private companies. The contracted services should be procured through qualifications-based solicitations.

11.2 Pre-storm Actions

Recommendation No. 1: TWIA should acquire *pre-storm* high resolution aerial and on-ground photographs of potentially affected properties to define building characteristics and terrain. TWIA should populate a database of building characteristics as defined by

the Panel (see Section 5) for structures that could be exposed to wind and surge hazards. These two activities are significant efforts, and therefore will be on the critical path to properly implement the proposed methodology.

Recommendation No. 2: TWIA should make arrangements for high resolution (50m overland) wave and surge modeling for the purposes of risk evaluation, pre-storm planning, and post-storm loss adjustment. Contracts should be in place prior to the start of hurricane season.

Recommendation No. 3: Plans and capabilities should be developed to obtain good quality wave, surge, and wind field data that will be useful to TWIA. This data would consist of measurements of hazard conditions during a storm using rapidly deployable and robust instrumentation and the collection of high water marks after a storm. This task should be performed in concert with federal agencies and other organizations.

11.3 Post-storm Actions

Recommendation No. 4: Plans should be set up to acquire and process high resolution airborne photography and Lidar measurements as soon *post-storm* as possible. These photos and measurements should then be incorporated into computational hydrodynamic models to ensure the greatest possible accuracy. The post-storm photos are also used in the observational branch of the Damage Estimation Module.

11.4 Ongoing Model Validation

Recommendation No. 5: Continually validate the model to determine if any elements of the current Hazard Module or Damage Estimation Module should be adjusted based on either actual claims data or other model methodologies as such information becomes available.

Recommendation No. 6: Initiate a performance review of the model, when used, after every coastal storm event in Texas. This effort would provide an opportunity to continually improve on model inputs and methodology based on the storm effects and associated claims data collected along the Texas coastline following an event.

12 References

1. APA (1993), "Wood Structural Panel Shear Walls," American Plywood Association, Technical Services Division, Report 154.
2. ASCE/SEI Standard 7-10, Minimum Design Loads for Buildings and Other Structures, American Society of Civil Engineers, Reston, VA.
3. ASTM D7158 / D7158M-11 (2011), Standard Test Method for Wind Resistance of Asphalt Shingles (Uplift Force/Uplift Resistance Method), ASTM International, West Conshohocken, PA.
4. AWC (2014), National Design Specification for Wood Construction, 2015 Edition, ANSI/AWC NDS-2015, American Wood Council, Leesburg, VA.
5. Dixon, Craig R. (2013), dissertation paper, "The Wind Resistance of Asphalt Roofing Shingles," University of Florida.
6. Ellingwood, B. and Tekie, P. B. (1999), "Wind load statistics for probability-based structural design." *J. Struct. Eng.*, ASCE, 125(4), 453-463.
7. FEMA 488 (2005), Hurricane Charley in Florida, Mitigation Assessment Team Report.
8. FEMA 489 (2005), Hurricane Ivan in Florida, Mitigation Assessment Team Report.
9. FEMA 549 (2006), Hurricane Katrina in the Gulf Coast, Mitigation Assessment Team Report.
10. FEMA P-757 (2009), Hurricane Ike in Texas and Louisiana, Mitigation Assessment Team Report.
11. FEMA (2012), Multi-hazard Loss Estimation Methodology, HAZUS MH Technical Manual v2.1, Washington, DC.
12. Florida Public Hurricane Loss Methodology (2005), Volume II, "Predicting the Vulnerability of Typical Residential Buildings to Hurricane Damage."
13. Freund, R. J. and Wilson, W. J. (2003), Statistical Methods, Second Edition, Academic Press, Elsevier Science.
14. Holland, G. J. (1980), "An Analytic Model of the Wind and Pressure Profiles in Hurricanes," *Monthly Weather Review*, 108, 1212-1218.
15. Holland, G. J. (2008), "A revised Hurricane Pressure-Wind Model," *Monthly Weather Review*, 136, 3432-3445.

16. Hope, M., Westerink, J.J., Kennedy, A.B., Kerr, P., Dietrich, J.C., Dawson, C., Bender, C.J., Smith, J., Jensen, R., Zijlema, M., Holthuijsen, L., Luettich, R., Powell, M., Cardone, V., Cox, A.T., Pourtaheri, H., Roberts, H., Atkinson, J., Tanaka, S., Westerink, J., and Westerink, L. (2013). "Hindcast and Validation of Hurricane Ike (2008) Waves, Forerunner, and Storm Surge," *J. Geophys. Res.-Oceans*, 118, 4424-4460, doi:10.1002/jgrc.20314.
17. HUD (1999), "Reliability of Conventional Residential Construction: An Assessment of Roof Component Performance in Hurricane Andrew and Typical Wind Regions of the United States", NAHB Research Center.
18. ICC (2008), Standard for Residential Construction in High Wind Regions, International Code Council, American National Standard ICC 600-2008, Washington, DC.
19. International Code Council (2012), International Residential Code.
20. Nowak, Andrzej S. and Collins, Kevin R. (2000), Reliability of Structures, McGraw-Hill.
21. Peraza, David B., Coulbourne, William L., and Griffith, Morgan (2014), Engineering Investigations of Hurricane Damage – Wind versus Water, American Society of Civil Engineers, Reston, VA.
22. Prevatt, David P., et al (2014), "In Situ Nail Withdrawal Strengths in Wood Roof Structures", *Journal of Structural Engineering*.
23. TDI (2015), Product Evaluation Index, Texas Department of Insurance, Austin, TX, <http://www.tdi.texas.gov/wind/prod/>
24. Tomiczek, T.1, Kennedy, A.B., and Rogers, S.P. (2014), "Collapse limit state fragilities of wood-framed residences from storm surge and waves during Hurricane Ike", *J. Waterway, Port, Coastal and Ocean Eng.-ASCE*, 140(1), 43-55, doi: 10.1061/(ASCE)WW.1943-5460.0000212.
25. Yang, Mengyu (2013), "Flexural Strength Reliability of Visually Graded Southern Pine Dimensional Lumber," Clemson University Master's Thesis.
26. Willoughby, H. E., Darling, R. W. R., and Rahn, M. E. (2006), "Parametric Representation of the Primary Hurricane Vortex. Part II: A New Family of Sectionally Continuous Profiles," *Monthly Weather Review*, 134, 1102-1120.

13 Appendices

A – Example Calculations

B – Expert Panel CVs

C – Sensitivity Analysis of Failure Probability Calculation Techniques

A – Example Calculations

Example Calculations

This document provides example calculations to illustrate the methodology recommended for the wind damage module.

Consider a structure with the following characteristics:

Structure Input

Roof Shape	Gable	
Length	53	feet (parallel to ridge)
Width	35	feet (parallel to ridge)
Plate Height	9	feet
Eave Height	20	feet
Roof Slope	6	:12
Roof Height	24.375	feet
Number of Stories	1	Living Area
Structure Primary Axis	45	deg. (with respect to North = 0 deg.)
Terrain Exposure	D	ASCE 7 Category
Ovrhd Garage Door Type	Sectional	
Roof Cover Type	Asphalt Shingle (ASTM D7158 Class H)	
Roof Cover Age	10	years
Wall Cover Type	Vinyl Siding	
Direction of Garage Door	315	degrees
Garage Panel Door Width	Single	
Garage Attached?	Yes	
Window Type	Non-Impact Resistant	
Percent Window Area	0-25	Percent
Door Type	Non-Impact Resistant	
Opening Protection	No	
Age of Structure	20	years

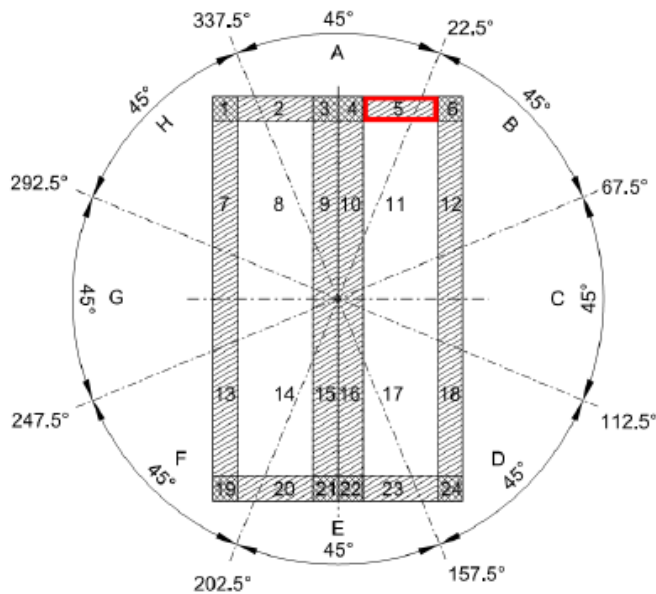
Calculated Values

Plan Aspect Ratio (L/B)	1.514	parallel to ridge
Plan Aspect Ratio (L/B)	0.660	perpendicular to ridge
height aspect ratio (h/L)	0.252	parallel to ridge
height aspect ratio (h/L)	0.382	perpendicular to ridge
"a" dimension	3.5	(ft) edge and corner zone dim.

Consider that the structure experiences the following wind speed time history:

Time	Gust Speed (mph)	Direction (WRT North)	AOA (WRT Axis)
hour 0	30.87	45.0	0.0
hour 1	33.67	41.7	356.7
hour 2	36.48	38.3	353.3
hour 3	39.28	35.0	350.0
hour 4	43.96	38.3	353.3
hour 5	48.64	41.7	356.7
hour 6	53.31	45.0	360.0
hour 7	61.26	35.0	350.0
hour 8	69.21	25.0	340.0
hour 9	77.16	15.0	330.0
hour 10	86.52	25.0	340.0
hour 11	95.87	35.0	350.0
hour 12	105.22	45.0	360.0
hour 13	100.55	141.7	96.7
hour 14	95.87	238.3	193.3
hour 15	91.20	335.0	290.0
hour 16	81.84	326.7	281.7
hour 17	72.49	318.3	273.3
hour 18	63.14	310.0	265.0

The following calculations will estimate the degree of damage to ROOF COVERING in area 5 that occurs at hour 12. Roof area 5 is identified on the figure below:



Roof Covering performance function:

$$g(C_1, C_2, R_{rc}, K_z, V, GC_p, GC_{pi}) := C_1 \cdot C_2 \cdot R_{rc} - 0.00256 \cdot K_z \cdot V^2 \cdot (GC_p + GC_{pi})$$

Roof Covering performance function direction cosines:

$$a_1(C_1, C_2, R_{rc}, K_z, V, GC_p, GC_{pi}) := \frac{d}{dC_1} g(C_1, C_2, R_{rc}, K_z, V, GC_p, GC_{pi}) \rightarrow C_2 \cdot R_{rc}$$

$$a_2(C_1, C_2, R_{rc}, K_z, V, GC_p, GC_{pi}) := \frac{d}{dC_2} g(C_1, C_2, R_{rc}, K_z, V, GC_p, GC_{pi}) \rightarrow C_1 \cdot R_{rc}$$

$$a_3(C_1, C_2, R_{rc}, K_z, V, GC_p, GC_{pi}) := \frac{d}{dR_{rc}} g(C_1, C_2, R_{rc}, K_z, V, GC_p, GC_{pi}) \rightarrow C_1 \cdot C_2$$

$$a_4(C_1, C_2, R_{rc}, K_z, V, GC_p, GC_{pi}) := \frac{d}{dK_z} g(C_1, C_2, R_{rc}, K_z, V, GC_p, GC_{pi}) \rightarrow -0.00256 \cdot V^2 \cdot (GC_p + GC_{pi})$$

$$a_5(C_1, C_2, R_{rc}, K_z, V, GC_p, GC_{pi}) := \frac{d}{dV} g(C_1, C_2, R_{rc}, K_z, V, GC_p, GC_{pi}) \rightarrow -0.00512 \cdot K_z \cdot V \cdot (GC_p + GC_{pi})$$

$$a_6(C_1, C_2, R_{rc}, K_z, V, GC_p, GC_{pi}) := \frac{d}{dGC_p} g(C_1, C_2, R_{rc}, K_z, V, GC_p, GC_{pi}) \rightarrow -0.00256 \cdot K_z \cdot V^2$$

$$a_7(C_1, C_2, R_{rc}, K_z, V, GC_p, GC_{pi}) := \frac{d}{dGC_{pi}} g(C_1, C_2, R_{rc}, K_z, V, GC_p, GC_{pi}) \rightarrow -0.00256 \cdot K_z \cdot V^2$$

Define the mean values and standard deviations of each of the seven random variables in the performance function:

$\mu_{C1} := 0.876$	$\sigma_{C1} := 0.0377$	Construction Variability Reduction Factor
$\mu_{C2} := 0.9$	$\sigma_{C2} := 0.028$	Component Reduction Factor for roof covering for a 10-year old roof cover.
$\mu_{R_{rc}} := 70$	$\sigma_{R_{rc}} := 28$	Roof covering resistance in units of pounds per square foot.
$\mu_{K_z} := 1.0463$	$\sigma_{K_z} := 0.12$	Exposure factor.
$\mu_V := 105.22$	$\sigma_V := 0.18 \cdot \mu_V = 18.94$	Gust wind speed in miles per hour.
$\mu_{GC_p} := 1.6099$	$\sigma_{GC_p} := 0.19$	For the wind angle of attack at the hour of interest, area 5 is classified as a roof perimeter.
$\mu_{GC_{pi}} := 0.15$	$\sigma_{GC_{pi}} := 0.05$	The internal pressure coefficient assumes that the building is "enclosed," but this condition would be checked based on damage at the previous time step in an actual run of the model.

Evaluate the performance function using the mean values of the random variables.

$$\mu_g := E(\mu_{C1}, \mu_{C2}, \mu_{Rrc}, \mu_{Kz}, \mu_V, \mu_{GCp}, \mu_{GCpi}) = 2.999$$

This is the average reserve capacity of the roof covering in area 5 in units of pounds per square foot.

Evaluate the values of the direction cosines, using the mean values of the random variables.

$$a_{1_rc} := a_1(\mu_{C1}, \mu_{C2}, \mu_{Rrc}, \mu_{Kz}, \mu_V, \mu_{GCp}, \mu_{GCpi}) = 63$$

$$a_{2_rc} := a_2(\mu_{C1}, \mu_{C2}, \mu_{Rrc}, \mu_{Kz}, \mu_V, \mu_{GCp}, \mu_{GCpi}) = 61.32$$

$$a_{3_rc} := a_3(\mu_{C1}, \mu_{C2}, \mu_{Rrc}, \mu_{Kz}, \mu_V, \mu_{GCp}, \mu_{GCpi}) = 0.788$$

$$a_{4_rc} := a_4(\mu_{C1}, \mu_{C2}, \mu_{Rrc}, \mu_{Kz}, \mu_V, \mu_{GCp}, \mu_{GCpi}) = -49.88$$

$$a_{5_rc} := a_5(\mu_{C1}, \mu_{C2}, \mu_{Rrc}, \mu_{Kz}, \mu_V, \mu_{GCp}, \mu_{GCpi}) = -0.992$$

$$a_{6_rc} := a_6(\mu_{C1}, \mu_{C2}, \mu_{Rrc}, \mu_{Kz}, \mu_V, \mu_{GCp}, \mu_{GCpi}) = -29.655$$

$$a_{7_rc} := a_7(\mu_{C1}, \mu_{C2}, \mu_{Rrc}, \mu_{Kz}, \mu_V, \mu_{GCp}, \mu_{GCpi}) = -29.655$$

Compute the standard deviation of the performance function at the mean values of the random variables:

$$\sigma_{rc} := \sqrt{a_{1_rc}^2 \cdot \sigma_{C1}^2 + a_{2_rc}^2 \cdot \sigma_{C2}^2 + a_{3_rc}^2 \cdot \sigma_{Rrc}^2 + a_{4_rc}^2 \cdot \sigma_{Kz}^2 + a_{5_rc}^2 \cdot \sigma_V^2 + a_{6_rc}^2 \cdot \sigma_{GCp}^2 + a_{7_rc}^2 \cdot \sigma_{GCpi}^2}$$

$$\sigma_{rc} = 30.31$$

Calculate the FOSM-MV reliability index for roof cover in area 5 at hour 12:

$$\beta := \frac{\mu_g}{\sigma_{rc}} = 0.099$$

Determine the probability of failure for roof cover in area 5 at hour 12:

$$P_f := \text{pnorm}(-\beta, 0, 1) = 0.461 \quad \text{The reliability index is used as an input in the standard normal distribution.}$$

Determine the contribution to total roof rover damage due to damage in area 5 at hour 12.

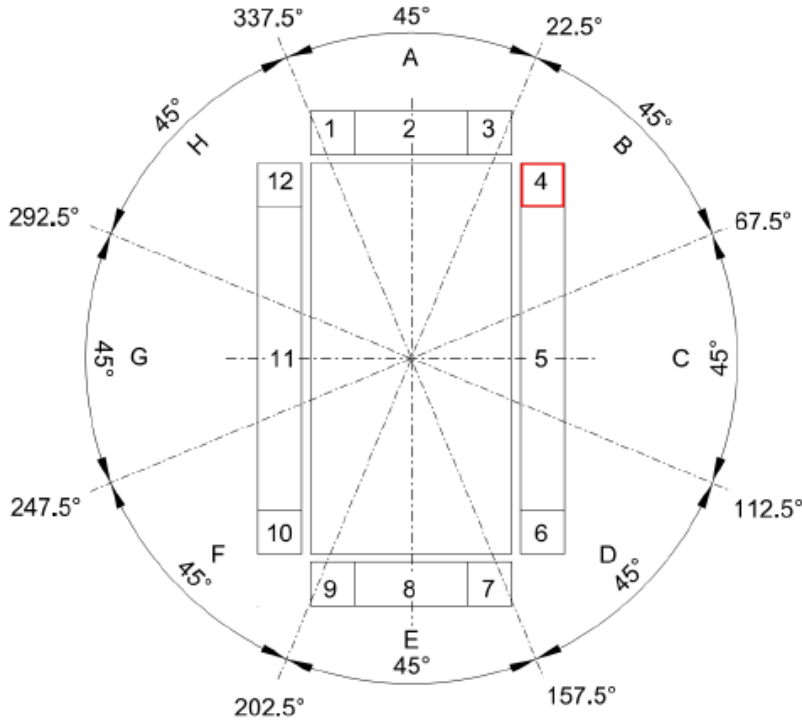
$$A_5 := \left[\frac{35\text{ft}}{2} - 2 \cdot (3.5\text{ft}) \right] \cdot (3.5\text{ft}) = 36.75 \cdot \text{ft}^2$$

$$A_T := 35\text{ft} \cdot 53\text{ft} = 1855 \cdot \text{ft}^2$$

$$\text{Damage} := P_f \cdot \left(\frac{A_5}{A_T} \right) = 0.009$$

Summary: 0.9% of the total roof area is expected to be damaged as a result of wind acting on area 5 at hour 12. These calculations are performed at each time step and for each of the 24 roof areas to determine the total expected degree of roof cover damage, as a ratio of the roof area. If the damage for an individual area at a subsequent time step is lower than that at a previous time step, the previous damage degree is reported.

The following calculations will estimate the degree of damage to Wall Studs in Bending in area 4 that occurs at hour 12. Wall area 4 is identified on the figure below:



Wall stud bending performance function:

$$g(C_1, C_r, S_x, F_b, s, l, K_z, V, GC_p, GC_{pi}) := \frac{C_1 \cdot 144 \cdot s \cdot C_r \cdot S_x \cdot F_b}{s \cdot l^2} - 0.00256 \cdot K_z \cdot V^2 \cdot (GC_p + GC_{pi})$$

Deterministic variable values:

$S_x := 5.727$

Section modulus of composite section formed by stud and 3/8" thick wood panel.

$C_r := 1.15$

Repetitive use factor (NDS 2015)

Wall stud bending performance function direction cosines:

$$\frac{\partial g}{\partial C_1}(C_1, C_r, S_x, F_b, s, l, K_z, V, GC_p, GC_{pi}) := \frac{d}{dC_1} g(C_1, C_r, S_x, F_b, s, l, K_z, V, GC_p, GC_{pi}) \rightarrow \frac{1152 \cdot C_r \cdot F_b \cdot S_x}{l^2 \cdot s}$$

$$\begin{aligned}
 \frac{\partial a_1}{\partial C_1}(C_1, C_r, S_x, F_b, s, l, K_z, V, GC_p, GC_{pi}) &:= \frac{d}{dC_1} g(C_1, C_r, S_x, F_b, s, l, K_z, V, GC_p, GC_{pi}) \rightarrow \frac{1152 \cdot C_1 \cdot C_r \cdot S_x}{l^{2.5}} \\
 \frac{\partial a_2}{\partial C_r}(C_1, C_r, S_x, F_b, s, l, K_z, V, GC_p, GC_{pi}) &:= \frac{d}{dC_r} g(C_1, C_r, S_x, F_b, s, l, K_z, V, GC_p, GC_{pi}) \rightarrow \frac{1152 \cdot C_1 \cdot C_r \cdot F_b \cdot S_x}{l^{2.5 \cdot 2}} \\
 \frac{\partial a_3}{\partial S_x}(C_1, C_r, S_x, F_b, s, l, K_z, V, GC_p, GC_{pi}) &:= \frac{d}{dS_x} g(C_1, C_r, S_x, F_b, s, l, K_z, V, GC_p, GC_{pi}) \rightarrow \frac{2304 \cdot C_1 \cdot C_r \cdot F_b \cdot S_x}{l^{3.5}} \\
 \frac{\partial a_4}{\partial F_b}(C_1, C_r, S_x, F_b, s, l, K_z, V, GC_p, GC_{pi}) &:= \frac{d}{dF_b} g(C_1, C_r, S_x, F_b, s, l, K_z, V, GC_p, GC_{pi}) \rightarrow -0.00256 \cdot V^2 \cdot (GC_p + GC_{pi}) \\
 \frac{\partial a_5}{\partial s}(C_1, C_r, S_x, F_b, s, l, K_z, V, GC_p, GC_{pi}) &:= \frac{d}{ds} g(C_1, C_r, S_x, F_b, s, l, K_z, V, GC_p, GC_{pi}) \rightarrow -0.00512 \cdot K_z \cdot V \cdot (GC_p + GC_{pi}) \\
 \frac{\partial a_6}{\partial l}(C_1, C_r, S_x, F_b, s, l, K_z, V, GC_p, GC_{pi}) &:= \frac{d}{dl} g(C_1, C_r, S_x, F_b, s, l, K_z, V, GC_p, GC_{pi}) \rightarrow -0.00256 \cdot K_z \cdot V^2 \\
 \frac{\partial a_7}{\partial K_z}(C_1, C_r, S_x, F_b, s, l, K_z, V, GC_p, GC_{pi}) &:= \frac{d}{dK_z} g(C_1, C_r, S_x, F_b, s, l, K_z, V, GC_p, GC_{pi}) \rightarrow -0.00256 \cdot K_z \cdot V^2 \\
 \frac{\partial a_8}{\partial V}(C_1, C_r, S_x, F_b, s, l, K_z, V, GC_p, GC_{pi}) &:= \frac{d}{dV} g(C_1, C_r, S_x, F_b, s, l, K_z, V, GC_p, GC_{pi}) \rightarrow -0.00256 \cdot K_z \cdot V^2
 \end{aligned}$$

Define the mean values and standard deviations of each of the eight random variables in the performance function:

$\mu_{GC_p} := 0.876$	$\sigma_{GC_p} := 0.0377$	Construction Variability Reduction Factor
$\mu_{F_b} := 4998$	$\sigma_{F_b} := 2109$	Maximum bending stress (psi) for wall 9' stud, using #2 SYP or SPF.
$\mu_s := 16$	$\sigma_s := 0.5$	Wall stud spacing (inches).
$\mu_l := 108$	$\sigma_l := 0.5$	Wall stud length (inches)
$\mu_{K_z} := 1.0463$	$\sigma_{K_z} := 0.12$	Exposure Factor
$\mu_V := 105.22$	$\sigma_V := 0.18 \cdot \mu_V = 18.94$	Gust wind speed in miles per hour.
$\mu_{GC_{pV}} := 1.3205$	$\sigma_{GC_{pV}} := 0.13$	For the wind angle of attack at the hour of interest, area 4 is classified as an edge zone.
$\mu_{GC_{piV}} := 0.15$	$\sigma_{GC_{piV}} := 0.05$	The internal pressure coefficient assumes that the building is "enclosed," but this condition would be checked based on damage at the previous time step in an actual run of the model.

Evaluate the performance function using the mean values of the random variables.

$$\mu_{g_s} := g(\mu_{C_1}, \mu_{C_r}, \mu_{S_x}, \mu_{F_b}, \mu_s, \mu_l, \mu_{K_z}, \mu_V, \mu_{GC_p}, \mu_{GC_{pi}}) = 134.389 \text{ This is the average reserve capacity of the wall studs in area 4 in units of pounds per square foot.}$$

Evaluate the values of the direction cosines, using the mean values of the random variables.

$$a_{1_sb} := a_1(\mu_{C_1}, \mu_{C_r}, \mu_{S_x}, \mu_{F_b}, \mu_s, \mu_l, \mu_{K_z}, \mu_V, \mu_{GC_p}, \mu_{GC_{pi}}) = 203.192$$

$$a_{2_sb} := a_2(\mu_{C1}, C_T, S_x, \mu_{Fb}, \mu_s, \mu_1, \mu_{Kz}, \mu_V, \mu_{GCP}, \mu_{GCPi}) = 0.036$$

$$a_{3_sb} := a_3(\mu_{C1}, C_T, S_x, \mu_{Fb}, \mu_s, \mu_1, \mu_{Kz}, \mu_V, \mu_{GCP}, \mu_{GCPi}) = -11.125$$

$$a_{4_sb} := a_4(\mu_{C1}, C_T, S_x, \mu_{Fb}, \mu_s, \mu_1, \mu_{Kz}, \mu_V, \mu_{GCP}, \mu_{GCPi}) = -3.296$$

$$a_{5_sb} := a_5(\mu_{C1}, C_T, S_x, \mu_{Fb}, \mu_s, \mu_1, \mu_{Kz}, \mu_V, \mu_{GCP}, \mu_{GCPi}) = -41.677$$

$$a_{6_sb} := a_6(\mu_{C1}, C_T, S_x, \mu_{Fb}, \mu_s, \mu_1, \mu_{Kz}, \mu_V, \mu_{GCP}, \mu_{GCPi}) = -0.829$$

$$a_{7_sb} := a_7(\mu_{C1}, C_T, S_x, \mu_{Fb}, \mu_s, \mu_1, \mu_{Kz}, \mu_V, \mu_{GCP}, \mu_{GCPi}) = -29.655$$

$$a_{8_sb} := a_8(\mu_{C1}, C_T, S_x, \mu_{Fb}, \mu_s, \mu_1, \mu_{Kz}, \mu_V, \mu_{GCP}, \mu_{GCPi}) = -29.655$$

Compute the standard deviation of the performance function at the mean values of the random variables:

$$\sigma_{sb} := \sqrt{a_{1_sb}^2 \cdot \sigma_{C1}^2 + a_{2_sb}^2 \cdot \sigma_{Fb}^2 + a_{3_sb}^2 \cdot \sigma_s^2 + a_{4_sb}^2 \cdot \sigma_1^2 + a_{5_sb}^2 \cdot \sigma_{Kz}^2 + a_{6_sb}^2 \cdot \sigma_V^2 + a_{7_sb}^2 \cdot \sigma_{GCP}^2 + a_{8_sb}^2 \cdot \sigma_{GCPi}^2}$$

$$\sigma_{sb} = 77.603$$

Calculate the FOSM-MV reliability index for stud bending in area 4 at hour 12:

$$\beta_{MV} := \frac{\mu_g}{\sigma_{sb}} = 1.732$$

Determine the probability of failure for stud bending in area 4 at hour 12:

$$P_{f,MV} := \text{pnorm}(-\beta, 0, 1) = 0.042 \quad \text{The reliability index is used as an input in the standard normal distribution.}$$

Determine the contribution to total stud bending damage due to damage in area 4 at hour 12.

$$A_4 := (9 \text{ ft}) \cdot (3.5 \text{ ft}) = 31.5 \text{ ft}^2$$

$$A_{TV} := (9 \text{ ft})(2.53 \text{ ft} + 2.35 \text{ ft}) = 1584 \text{ ft}^2$$

$$\text{Damage}_{MV} := P_f \left(\frac{A_4}{A_T} \right) = 0.001$$

Remark: The wall stud bending limit state is used as one of the tests for likelihood of structural collapse due to wind. In this case, the probability of wall stud bending failure in area 4 at hour 12 is 4.2%. The maximum probability of failure for the limit states of wall stud bending, stud-to-plate connection, and shear wall failure are used to represent the probability of collapse due to wind.

The following calculations will estimate the degree of damage to the Stud to Plate Connections in area 4 that occurs at hour 12. Wall area 4 is identified on the figure above:

Wall stud-to-plate connection performance function:

$$g(C_1, C_{eg}, K_f, Z, N, s, l, K_z, V, GC_p, GC_{pi}) := \frac{C_1 \cdot 144 \cdot 2 \cdot C_{eg} \cdot K_f \cdot N \cdot Z}{s \cdot l} - 0.00256 \cdot K_z \cdot V^2 \cdot (GC_p + GC_{pi})$$

Deterministic variable values:

- $C_{eg} := 0.67$ End Grain factor (NDS 2015).
- $K_f := 3.32$ Format conversion factor (NDS 2015)
- $N := 3$ Three 16d nails are required for a 9' tall wall

Wall stud-to-plate connection performance function direction cosines:

$$a_{11}(C_1, C_{eg}, K_f, Z, N, s, l, K_z, V, GC_p, GC_{pi}) := \frac{d}{dC_1} g(C_1, C_{eg}, K_f, Z, N, s, l, K_z, V, GC_p, GC_{pi}) \rightarrow \frac{288 \cdot C_{eg} \cdot K_f \cdot N \cdot Z}{l \cdot s}$$

$$a_{12}(C_1, C_{eg}, K_f, Z, N, s, l, K_z, V, GC_p, GC_{pi}) := \frac{d}{dZ} g(C_1, C_{eg}, K_f, Z, N, s, l, K_z, V, GC_p, GC_{pi}) \rightarrow \frac{288 \cdot C_1 \cdot C_{eg} \cdot K_f \cdot N}{l \cdot s}$$

$$a_{13}(C_1, C_{eg}, K_f, Z, N, s, l, K_z, V, GC_p, GC_{pi}) := \frac{d}{ds} g(C_1, C_{eg}, K_f, Z, N, s, l, K_z, V, GC_p, GC_{pi}) \rightarrow -\frac{288 \cdot C_1 \cdot C_{eg} \cdot K_f \cdot N \cdot Z}{l \cdot s^2}$$

$$a_{14}(C_1, C_{eg}, K_f, Z, N, s, l, K_z, V, GC_p, GC_{pi}) := \frac{d}{dl} g(C_1, C_{eg}, K_f, Z, N, s, l, K_z, V, GC_p, GC_{pi}) \rightarrow -\frac{288 \cdot C_1 \cdot C_{eg} \cdot K_f \cdot N \cdot Z}{l^2 \cdot s}$$

$$a_{15}(C_1, C_{eg}, K_f, Z, N, s, l, K_z, V, GC_p, GC_{pi}) := \frac{d}{dK_z} g(C_1, C_{eg}, K_f, Z, N, s, l, K_z, V, GC_p, GC_{pi}) \rightarrow -0.00256 \cdot V^2 \cdot (GC_p + GC_{pi})$$

$$a_{16}(C_1, C_{eg}, K_f, Z, N, s, l, K_z, V, GC_p, GC_{pi}) := \frac{d}{dV} g(C_1, C_{eg}, K_f, Z, N, s, l, K_z, V, GC_p, GC_{pi}) \rightarrow -0.00512 \cdot K_z \cdot V \cdot (GC_p + GC_{pi})$$

$$a_{17}(C_1, C_{eg}, K_f, Z, N, s, l, K_z, V, GC_p, GC_{pi}) := \frac{d}{dGC_p} g(C_1, C_{eg}, K_f, Z, N, s, l, K_z, V, GC_p, GC_{pi}) \rightarrow -0.00256 \cdot K_z \cdot V^2$$

$$a_{18}(C_1, C_{eg}, K_f, Z, N, s, l, K_z, V, GC_p, GC_{pi}) := \frac{d}{dGC_{pi}} g(C_1, C_{eg}, K_f, Z, N, s, l, K_z, V, GC_p, GC_{pi}) \rightarrow -0.00256 \cdot K_z \cdot V^2$$

Define the mean values and standard deviations of each of the eight random variables in the performance function:

- $\mu_{C_1} := 0.876$ $\sigma_{C_1} := 0.0377$ Construction Variability Reduction Factor
- $\mu_Z := 137.96$ $\sigma_Z := 19.25$ Lateral capacity of nails. SPF and SYP are both allowed for 9' walls.
- $\mu_w := 16$ $\sigma_w := 0.5$ Wall stud spacing (inches).

$\mu_{WV} := 108$	$\sigma_{WV} := 0.5$	Wall stud length (inches)
$\mu_{Kz} := 1.0463$	$\sigma_{Kz} := 0.12$	Exposure Factor
$\mu_{WV} := 105.22$	$\sigma_{WV} := 0.18 \cdot \mu_{WV} = 18.94$	Gust wind speed in miles per hour.
$\mu_{GCp} := 1.3205$	$\sigma_{GCp} := 0.13$	For the wind angle of attack at the hour of interest, area 4 is classified as an edge zone.
$\mu_{GCpi} := 0.15$	$\sigma_{GCpi} := 0.05$	The internal pressure coefficient assumes that the building is "enclosed," but this condition would be checked based on damage at the previous time step in an actual run of the model.

Evaluate the performance function using the mean values of the random variables.

$\mu_{R_s} := \xi(\mu_{C1}, C_{eg}, K_f, \mu_Z, N, \mu_s, \mu_1, \mu_{Kz}, \mu_V, \mu_{GCp}, \mu_{GCpi}) = 90.806$ This is the average reserve capacity of the wall stud-to-plate connection in area 4 in units of pounds per square foot.

Evaluate the values of the direction cosines, using the mean values of the random variables.

$a_{1_sp} := a_1(\mu_{C1}, C_{eg}, K_f, \mu_Z, N, \mu_s, \mu_1, \mu_{Kz}, \mu_V, \mu_{GCp}, \mu_{GCpi}) = 153.439$
 $a_{2_sp} := a_2(\mu_{C1}, C_{eg}, K_f, \mu_Z, N, \mu_s, \mu_1, \mu_{Kz}, \mu_V, \mu_{GCp}, \mu_{GCpi}) = 0.974$
 $a_{3_sp} := a_3(\mu_{C1}, C_{eg}, K_f, \mu_Z, N, \mu_s, \mu_1, \mu_{Kz}, \mu_V, \mu_{GCp}, \mu_{GCpi}) = -8.401$
 $a_{4_sp} := a_4(\mu_{C1}, C_{eg}, K_f, \mu_Z, N, \mu_s, \mu_1, \mu_{Kz}, \mu_V, \mu_{GCp}, \mu_{GCpi}) = -1.245$
 $a_{5_sp} := a_5(\mu_{C1}, C_{eg}, K_f, \mu_Z, N, \mu_s, \mu_1, \mu_{Kz}, \mu_V, \mu_{GCp}, \mu_{GCpi}) = -41.677$
 $a_{6_sp} := a_6(\mu_{C1}, C_{eg}, K_f, \mu_Z, N, \mu_s, \mu_1, \mu_{Kz}, \mu_V, \mu_{GCp}, \mu_{GCpi}) = -0.829$
 $a_{7_sp} := a_7(\mu_{C1}, C_{eg}, K_f, \mu_Z, N, \mu_s, \mu_1, \mu_{Kz}, \mu_V, \mu_{GCp}, \mu_{GCpi}) = -29.655$
 $a_{8_sp} := a_8(\mu_{C1}, C_{eg}, K_f, \mu_Z, N, \mu_s, \mu_1, \mu_{Kz}, \mu_V, \mu_{GCp}, \mu_{GCpi}) = -29.655$

Compute the standard deviation of the performance function at the mean values of the random variables:

$$\sigma_{sp} := \sqrt{a_{1_sp}^2 \cdot \sigma_{C1}^2 + a_{2_sp}^2 \cdot \sigma_Z^2 + a_{3_sp}^2 \cdot \sigma_s^2 + a_{4_sp}^2 \cdot \sigma_1^2 + a_{5_sp}^2 \cdot \sigma_{Kz}^2 + a_{6_sp}^2 \cdot \sigma_V^2 + a_{7_sp}^2 \cdot \sigma_{GCp}^2 + a_{8_sp}^2 \cdot \sigma_{GCpi}^2}$$

$\sigma_{sp} = 26.301$

Calculate the FOSM-MV reliability index for stud-to-plate connections in area 4 at hour 12:

$\beta_{MV} := \frac{\mu_{R_s}}{\sigma_{sp}} = 3.452$

Determine the probability of failure for stud-to-plate connections in area 4 at hour 12:

$$P_{d,v} := \text{pnorm}(-\beta, 0, 1) = 0.000278 \quad \text{The reliability index is used as an input in the standard normal distribution.}$$

Determine the contribution to total stud-to-plate damage due to damage in area 4 at hour 12.

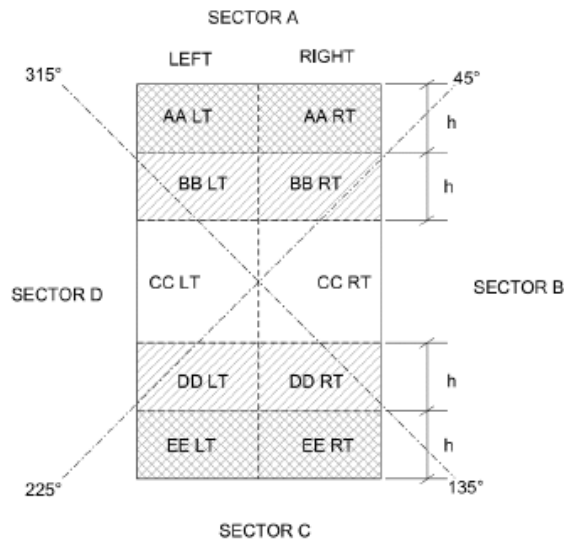
$$A_4 := (9\text{ft}) \cdot (3.5\text{ft}) = 31.5 \cdot \text{ft}^2$$

$$A_T := (9\text{ft})(2.53\text{ft} + 2.35\text{ft}) = 1584 \cdot \text{ft}^2$$

$$\text{Damage} := P_f \left(\frac{A_4}{A_T} \right) = 0$$

Remark: The stud-to-plate connection limit state is used as one of the tests for likelihood of structural collapse due to wind. In this case, the probability of wall stud-to-plate connection failure in area 4 at hour 12 is 0.028%. The maximum probability of failure for the limit states of wall stud bending, stud-to-plate connection, and shear wall failure are used to represent the probability of collapse due to wind.

The following calculations will estimate the degree of damage to ROOF FRAMING for roof area AALT that occurs at hour 12. Frame Lines 1L through 4L are identified on the figure below:



Roof Framing performance function:

$$g(C_1, C_2, R_{TW}, K_z, V, G, C_p, GC_{pi}, D, A_t) := C_1 \cdot C_2 \cdot R_{TW} - \left[0.00256 \cdot K_z \cdot V^2 \cdot (G \cdot C_p + GC_{pi}) - D \right] \cdot A_t$$

Establish the values of the deterministic variables:

$D := 10$ Roof dead load in pounds per square foot.
 $A_t := \frac{1}{2} \cdot 35 \cdot 2 = 35$ Area tributary to one wall connection, assuming that the framing spans the entire width of the home and is spaced at 2'-0".

Roof Framing performance function direction cosines:

$$\begin{aligned} \bar{a}_1(C_1, C_2, R_{rw}, K_z, V, G, C_p, GC_{pi}, D, A_t) &:= \frac{d}{dC_1} g(C_1, C_2, R_{rw}, K_z, V, G, C_p, GC_{pi}, D, A_t) \rightarrow C_2 \cdot R_{rw} \\ \bar{a}_2(C_1, C_2, R_{rw}, K_z, V, G, C_p, GC_{pi}, D, A_t) &:= \frac{d}{dC_2} g(C_1, C_2, R_{rw}, K_z, V, G, C_p, GC_{pi}, D, A_t) \rightarrow C_1 \cdot R_{rw} \\ \bar{a}_3(C_1, C_2, R_{rw}, K_z, V, G, C_p, GC_{pi}, D, A_t) &:= \frac{d}{dR_{rw}} g(C_1, C_2, R_{rw}, K_z, V, G, C_p, GC_{pi}, D, A_t) \rightarrow C_1 \cdot C_2 \\ \bar{a}_4(C_1, C_2, R_{rw}, K_z, V, G, C_p, GC_{pi}, D, A_t) &:= \frac{d}{dK_z} g(C_1, C_2, R_{rw}, K_z, V, G, C_p, GC_{pi}, D, A_t) \rightarrow -0.00256 \cdot A_t \cdot V^2 \cdot (GC_{pi} + C_p \cdot G) \\ \bar{a}_5(C_1, C_2, R_{rw}, K_z, V, G, C_p, GC_{pi}, D, A_t) &:= \frac{d}{dV} g(C_1, C_2, R_{rw}, K_z, V, G, C_p, GC_{pi}, D, A_t) \rightarrow -0.00512 \cdot A_t \cdot K_z \cdot V \cdot (GC_{pi} + C_p \cdot G) \\ \bar{a}_6(C_1, C_2, R_{rw}, K_z, V, G, C_p, GC_{pi}, D, A_t) &:= \frac{d}{dG} g(C_1, C_2, R_{rw}, K_z, V, G, C_p, GC_{pi}, D, A_t) \rightarrow -0.00256 \cdot A_t \cdot C_p \cdot K_z \cdot V^2 \\ \bar{a}_7(C_1, C_2, R_{rw}, K_z, V, G, C_p, GC_{pi}, D, A_t) &:= \frac{d}{dC_p} g(C_1, C_2, R_{rw}, K_z, V, G, C_p, GC_{pi}, D, A_t) \rightarrow -0.00256 \cdot A_t \cdot G \cdot K_z \cdot V^2 \\ \bar{a}_8(C_1, C_2, R_{rw}, K_z, V, G, C_p, GC_{pi}, D, A_t) &:= \frac{d}{dGC_{pi}} g(C_1, C_2, R_{rw}, K_z, V, G, C_p, GC_{pi}, D, A_t) \rightarrow -0.00256 \cdot A_t \cdot K_z \cdot V^2 \end{aligned}$$

Define the mean values and standard deviations of each of the seven random variables in the performance function:

$\mu_{C1} := 0.876$ $\sigma_{C1} := 0.0377$ Construction Variability Reduction Factor
 $\mu_{C2} := 0.91$ $\sigma_{C2} := 0.03276$ Component Reduction Factor for roof framing.
 $\mu_{R_{rw}} := 101.46 \cdot 35 + 685.29 = 4236.39$ Roof-to-wall connection resistance in units of pounds implied by conformance with the WFCM (AWS 2014b).
 $\sigma_{R_{rw}} := 0.2 \cdot \mu_{R_{rw}} = 847.278$
 $\mu_{K_z} := 1.0463$ $\sigma_{K_z} := 0.12$ Exposure factor.
 $\mu_{V} := 105.22$ $\sigma_{V} := 0.18 \cdot \mu_V = 18.94$ Gust wind speed in miles per hour.
 $\mu_{C_p} := 0.885 - 0.9 = 0.796$ For the wind angle of attack at the hour of interest, Frame Lines 1L-4L are on the windward edge with the wind blowing parallel to the ridge, therefore the nominal value of $GC_p = -0.9$.

$$\sigma_{Cp} := 0.15$$

$$\mu_G := 0.9765 - 0.85 = 0.83$$

Gust effect factor

$$\sigma_G := 0.07$$

$$\mu_{GCpi} := 0.15$$

$$\sigma_{GCpi} := 0.05$$

The internal pressure coefficient assumes that the building is "enclosed," but this condition would be checked based on damage at the previous time step in an actual run of the model.

Evaluate the performance function using the mean values of the random variables.

$$\mu_{Rg} := E(\mu_{C1} \cdot \mu_{C2} \cdot \mu_{Rrw} \cdot \mu_{Kz} \cdot \mu_V \cdot \mu_G \cdot \mu_{Cp} \cdot \mu_{GCpi} \cdot D, A_t) = 2885.214$$

This is the average reserve capacity of the roof connections in units of pounds.

Evaluate the values of the direction cosines, using the mean values of the random variables.

$$a_{1_rw} := a_1(\mu_{C1} \cdot \mu_{C2} \cdot \mu_{Rrw} \cdot \mu_{Kz} \cdot \mu_V \cdot \mu_G \cdot \mu_{Cp} \cdot \mu_{GCpi} \cdot D, A_t) = 3.855 \times 10^3$$

$$a_{2_rw} := a_2(\mu_{C1} \cdot \mu_{C2} \cdot \mu_{Rrw} \cdot \mu_{Kz} \cdot \mu_V \cdot \mu_G \cdot \mu_{Cp} \cdot \mu_{GCpi} \cdot D, A_t) = 3.711 \times 10^3$$

$$a_{3_rw} := a_3(\mu_{C1} \cdot \mu_{C2} \cdot \mu_{Rrw} \cdot \mu_{Kz} \cdot \mu_V \cdot \mu_G \cdot \mu_{Cp} \cdot \mu_{GCpi} \cdot D, A_t) = 0.797$$

$$a_{4_rw} := a_4(\mu_{C1} \cdot \mu_{C2} \cdot \mu_{Rrw} \cdot \mu_{Kz} \cdot \mu_V \cdot \mu_G \cdot \mu_{Cp} \cdot \mu_{GCpi} \cdot D, A_t) = -804.613$$

$$a_{5_rw} := a_5(\mu_{C1} \cdot \mu_{C2} \cdot \mu_{Rrw} \cdot \mu_{Kz} \cdot \mu_V \cdot \mu_G \cdot \mu_{Cp} \cdot \mu_{GCpi} \cdot D, A_t) = -16.002$$

$$a_{6_rw} := a_6(\mu_{C1} \cdot \mu_{C2} \cdot \mu_{Rrw} \cdot \mu_{Kz} \cdot \mu_V \cdot \mu_G \cdot \mu_{Cp} \cdot \mu_{GCpi} \cdot D, A_t) = -826.697$$

$$a_{7_rw} := a_7(\mu_{C1} \cdot \mu_{C2} \cdot \mu_{Rrw} \cdot \mu_{Kz} \cdot \mu_V \cdot \mu_G \cdot \mu_{Cp} \cdot \mu_{GCpi} \cdot D, A_t) = -861.493$$

$$a_{8_rw} := a_8(\mu_{C1} \cdot \mu_{C2} \cdot \mu_{Rrw} \cdot \mu_{Kz} \cdot \mu_V \cdot \mu_G \cdot \mu_{Cp} \cdot \mu_{GCpi} \cdot D, A_t) = -1.038 \times 10^3$$

Compute the standard deviation of the performance function at the mean values of the random variables:

$$\sigma_{rw} := \sqrt{a_{1_rw}^2 \cdot \sigma_{C1}^2 + a_{2_rw}^2 \cdot \sigma_{C2}^2 + a_{3_rw}^2 \cdot \sigma_{Rrw}^2 + a_{4_rw}^2 \cdot \sigma_{Kz}^2 + a_{5_rw}^2 \cdot \sigma_V^2 + a_{6_rw}^2 \cdot \sigma_G^2 + a_{7_rw}^2 \cdot \sigma_{Cp}^2 + a_{8_rw}^2 \cdot \sigma_{GCpi}^2}$$

$$\sigma_{rw} = 784.861$$

Calculate the FOSM-MV reliability index for roof frame connections on lines 1L - 4L at hour 12:

$$\beta_{rw} := \frac{\mu_{Rg}}{\sigma_{rw}} = 3.676$$

Determine the probability of failure for roof frame connections on lines 1L - 4L at hour 12:

$$P_{f,rw} := \text{pnorm}(-\beta, 0, 1) = 1.184 \times 10^{-4}$$

The reliability index is used as an input in the standard normal distribution.

Determine the contribution to total roof frame connection damage due to damage along lines 1L - 4L at hour 12.

$$A_{AALT} := 234.0625 \cdot \text{ft}^2 \quad \text{Area of region AALT}$$

$$A_T := 53 \text{ft} \cdot 35 \text{ft} = 1855 \cdot \text{ft}^2 \quad \text{Total Roof Area}$$

$$\text{Damage} := P_f \cdot \left(\frac{A_{AALT}}{A_T} \right) = 1.494 \times 10^{-5}$$

Summary: 0.001494% of the total roof area is expected to be damaged as a result of wind acting on frames in Area AALT at hour 12. These calculations are performed at each time step and for each of the 10 roof areas (left and right sides) to determine the total expected degree of roof frame damage, as a ratio of the roof area. If the damage for an individual area at a subsequent time step is lower than that at a previous time step, the previous damage degree is reported.

The following calculations will estimate the degree of damage to WOOD FRAMED SHEAR WALLS that are oriented perpendicular to the roof ridge at hour 13.

$$R(C_1, C_2, L_{sw}, R_{sw}, L_{gp}, R_{gp}) := C_1 \cdot C_2 \cdot (L_{sw} \cdot R_{sw} + L_{gp} \cdot R_{gp})$$

$$Q(K_z, V, G, C_{pw}, A_w, C_{lw}, A_l, C_{wr}, A_{wr}, C_{lr}, A_{lr}, \alpha, \theta) := 0.00256 \cdot K_z \cdot V^2 \cdot G \cdot \cos(\alpha) \cdot \left[\begin{array}{l} C_{pw} \cdot A_w + -C_{lw} \cdot A_l \dots \\ + (C_{wr} \cdot A_{wr} + -C_{lr} \cdot A_{lr}) \cdot \sin(\theta) \end{array} \right]$$

Establish the values of the deterministic variables:

$$A_w := \frac{1}{2} \cdot 53 \cdot 9 = 238.5$$

Half of the windward and leeward wall areas that are parallel to the ridge is tributary to the shear walls oriented perpendicular to the ridge.

$$A_l := \frac{1}{2} \cdot 53 \cdot 9 = 238.5$$

$$\alpha := 96.7 \text{deg} - 90 \text{deg}$$

α is the direction of the wind with respect to the structure axis that is perpendicular to the ridge, AOA - 90 degrees, since AOA is defined with respect to the axis of the roof ridge.

$$\theta := \text{atan}\left(\frac{6}{12}\right) = 26.565 \text{-deg}$$

Roof slope expressed in degrees

$$A_{wr} := \frac{\frac{1}{2} \cdot 35 \cdot 53}{\cos(\theta)} = 1036.977$$

Area of windward roof in square feet

$$A_{lr} := \frac{\frac{1}{2} \cdot 35 \cdot 53}{\cos(\theta)} = 1036.977$$

Area of leeward roof in square feet

Establish the values of the random variables:

μ_{C1} := 0.876	σ_{C1} := 0.0377	Construction variability reduction factor
μ_{C2} := 0.945	σ_{C2} := 0.016	Component resistance reduction factor for shear walls
$\mu_{L_{sw}}$:= 34.78	$\sigma_{L_{sw}}$:= $0.1 \cdot \mu_{L_{sw}} = 3.478$	Required length (feet) of shear wall per WFCM (AWS, 2014b)
$\mu_{R_{sw}}$:= 913	$\sigma_{R_{sw}}$:= 167.08	Shear wall capacity in pounds per foot
$\mu_{L_{gp}}$:= $2.35 - \mu_{L_{sw}} = 35.22$		Length of gypsum board shear wall (feet), taken as the remaining exterior wall after shear walls are subtracted.
$\sigma_{L_{gp}}$:= $0.1 \cdot \mu_{L_{gp}} = 3.522$		
$\mu_{R_{gp}}$:= 216	$\sigma_{R_{gp}}$:= $0.183 \cdot \mu_{R_{gp}} = 39.528$	Shear capacity of gypsum board walls (pounds per foot)
μ_{K_z} := 1.0463	σ_{K_z} := 0.12	Exposure factor
μ_{V} := 100.5	σ_{V} := $0.18 \cdot \mu_V$	Gust wind speed at hour 13
μ_{G} := 0.83	σ_{G} := 0.07	Gust effect factor
$\mu_{C_{ww}}$:= 0.7	$\sigma_{C_{ww}}$:= 0.1	External pressure coefficient for the windward wall
$\mu_{C_{lw}}$:= $0.94 \cdot (-0.39714) = -0.373$		External pressure coefficient for leeward wall, interpolating for L/B = 0.66 (perpendicular to ridge)
$\sigma_{C_{lw}}$:= 0.07		
$\mu_{C_{wr}}$:= $0.986 \cdot 0.247 = 0.244$		Windward roof external pressure coefficient for roof slope = 26.57 degrees and h/L perpendicular to ridge = 0.382
$\sigma_{C_{wr}}$:= 0.14		
$\mu_{C_{lr}}$:= $0.85 \cdot (-0.6) = -0.51$		Leeward roof external pressure coefficient for roof slope = 26.57 degrees and h/L perpendicular to ridge = 0.382
$\sigma_{C_{lr}}$:= 0.05		

Evaluate the performance function using the mean values of the random variables. This is the average reserve capacity of the shear walls in units of pounds.

$$\mu_{R_s} := R(\mu_{C1}, \mu_{C2}, \mu_{L_{sw}}, \mu_{R_{sw}}, \mu_{L_{gp}}, \mu_{R_{gp}}) + -Q(\mu_{K_z}, \mu_V, \mu_G, \mu_{C_{ww}}, A_w, \mu_{C_{lw}}, A_l, \mu_{C_{wr}}, A_{wr}, \mu_{C_{lr}}, A_{lr}, \alpha, \theta) = 19082.269$$

Evaluate the values of the direction cosines, using the mean values of the random variables.

$$\frac{\partial R}{\partial C_1}(C_1, C_2, L_{sw}, R_{sw}, L_{gp}, R_{gp}) := \frac{d}{dC_1} R(C_1, C_2, L_{sw}, R_{sw}, L_{gp}, R_{gp}) \rightarrow C_2 \cdot (L_{gp} \cdot R_{gp} + L_{sw} \cdot R_{sw})$$

$$a_{1_sw} := a_1(\mu_{C1}, \mu_{C2}, \mu_{L_{sw}}, \mu_{R_{sw}}, \mu_{L_{gp}}, \mu_{R_{gp}}) = 3.7197 \times 10^4$$

$$\bar{a}_{2a}(C_1, C_2, L_{sw}, R_{sw}, L_{gp}, R_{gp}) := \frac{d}{dC_2} R(C_1, C_2, L_{sw}, R_{sw}, L_{gp}, R_{gp}) \rightarrow C_1 \cdot (L_{gp} \cdot R_{gp} + L_{sw} \cdot R_{sw})$$

$$a_{2_sw} := a_2(\mu_{C1}, \mu_{C2}, \mu_{L_{sw}}, \mu_{R_{sw}}, \mu_{L_{gp}}, \mu_{R_{gp}}) = 3.448 \times 10^4$$

$$\bar{a}_{2b}(C_1, C_2, L_{sw}, R_{sw}, L_{gp}, R_{gp}) := \frac{d}{dL_{sw}} R(C_1, C_2, L_{sw}, R_{sw}, L_{gp}, R_{gp}) \rightarrow C_1 \cdot C_2 \cdot R_{sw}$$

$$a_{3_sw} := a_3(\mu_{C1}, \mu_{C2}, \mu_{L_{sw}}, \mu_{R_{sw}}, \mu_{L_{gp}}, \mu_{R_{gp}}) = 755.8$$

$$\bar{a}_{3a}(C_1, C_2, L_{sw}, R_{sw}, L_{gp}, R_{gp}) := \frac{d}{dR_{sw}} R(C_1, C_2, L_{sw}, R_{sw}, L_{gp}, R_{gp}) \rightarrow C_1 \cdot C_2 \cdot L_{sw}$$

$$a_{4_sw} := a_4(\mu_{C1}, \mu_{C2}, \mu_{L_{sw}}, \mu_{R_{sw}}, \mu_{L_{gp}}, \mu_{R_{gp}}) = 28.792$$

$$\bar{a}_{4b}(C_1, C_2, L_{sw}, R_{sw}, L_{gp}, R_{gp}) := \frac{d}{dL_{gp}} R(C_1, C_2, L_{sw}, R_{sw}, L_{gp}, R_{gp}) \rightarrow C_1 \cdot C_2 \cdot R_{gp}$$

$$a_{5_sw} := a_5(\mu_{C1}, \mu_{C2}, \mu_{L_{sw}}, \mu_{R_{sw}}, \mu_{L_{gp}}, \mu_{R_{gp}}) = 178.809$$

$$\bar{a}_{5a}(C_1, C_2, L_{sw}, R_{sw}, L_{gp}, R_{gp}) := \frac{d}{dR_{gp}} R(C_1, C_2, L_{sw}, R_{sw}, L_{gp}, R_{gp}) \rightarrow C_1 \cdot C_2 \cdot L_{gp}$$

$$a_{6_sw} := a_6(\mu_{C1}, \mu_{C2}, \mu_{L_{sw}}, \mu_{R_{sw}}, \mu_{L_{gp}}, \mu_{R_{gp}}) = 29.156$$

$$\bar{a}_{6a}(K_z, V, G, C_{ww}, A_w, C_{lw}, A_1, C_{wr}, A_{wr}, C_{lr}, A_{lr}, \alpha, \theta) := \frac{d}{dK_z} Q(K_z, V, G, C_{ww}, A_w, C_{lw}, A_1, C_{wr}, A_{wr}, C_{lr}, A_{lr}, \alpha, \theta)$$

$$a_{7_sw} := a_7(\mu_{K_z}, \mu_V, \mu_G, \mu_{C_{ww}}, \mu_{A_w}, \mu_{C_{lw}}, \mu_{A_1}, \mu_{C_{wr}}, \mu_{A_{wr}}, \mu_{C_{lr}}, \mu_{A_{lr}}, \alpha, \theta) = 12904.617$$

$$\bar{a}_{7b}(K_z, V, G, C_{ww}, A_w, C_{lw}, A_1, C_{wr}, A_{wr}, C_{lr}, A_{lr}, \alpha, \theta) := \frac{d}{dV} Q(K_z, V, G, C_{ww}, A_w, C_{lw}, A_1, C_{wr}, A_{wr}, C_{lr}, A_{lr}, \alpha, \theta)$$

$$a_{8_sw} := a_8(\mu_{K_z}, \mu_V, \mu_G, \mu_{C_{ww}}, \mu_{A_w}, \mu_{C_{lw}}, \mu_{A_1}, \mu_{C_{wr}}, \mu_{A_{wr}}, \mu_{C_{lr}}, \mu_{A_{lr}}, \alpha, \theta) = 268.699$$

$$a_{9}(K_z, V, G, C_{ww}, A_w, C_{lw}, A_1, C_{wr}, A_{wr}, C_{lr}, A_{lr}, \alpha, \theta) := \frac{d}{dG} Q(K_z, V, G, C_{ww}, A_w, C_{lw}, A_1, C_{wr}, A_{wr}, C_{lr}, A_{lr}, \alpha, \theta)$$

$$a_{9_sw} := a_9(\mu_{K_z}, \mu_V, \mu_G, \mu_{C_{ww}}, \mu_{A_w}, \mu_{C_{lw}}, \mu_{A_1}, \mu_{C_{wr}}, \mu_{A_{wr}}, \mu_{C_{lr}}, \mu_{A_{lr}}, \alpha, \theta) = 16267.591$$

$$a_{10}(K_z, V, G, C_{ww}, A_w, C_{lw}, A_1, C_{wr}, A_{wr}, C_{lr}, A_{lr}, \alpha, \theta) := \frac{d}{dC_{ww}} Q(K_z, V, G, C_{ww}, A_w, C_{lw}, A_1, C_{wr}, A_{wr}, C_{lr}, A_{lr}, \alpha, \theta)$$

$$a_{10_sw} := a_{10}(\mu_{K_z}, \mu_V, \mu_G, \mu_{C_{ww}}, \mu_{A_w}, \mu_{C_{lw}}, \mu_{A_1}, \mu_{C_{wr}}, \mu_{A_{wr}}, \mu_{C_{lr}}, \mu_{A_{lr}}, \alpha, \theta) = 5318.861$$

$$a_{11}(K_z, V, G, C_{ww}, A_w, C_{lw}, A_l, C_{wt}, A_{wt}, C_{lr}, A_{lr}, \alpha, \theta) := \frac{d}{dC_{lw}} Q(K_z, V, G, C_{ww}, A_w, C_{lw}, A_l, C_{wt}, A_{wt}, C_{lr}, A_{lr}, \alpha, \theta)$$

$$a_{11_sw} := a_{11}(\mu_{K_z}, \mu_V, \mu_G, \mu_{C_{ww}}, A_w, \mu_{C_{lw}}, A_l, \mu_{C_{wt}}, A_{wt}, \mu_{C_{lr}}, A_{lr}, \alpha, \theta) = -5318.861$$

$$a_{12}(K_z, V, G, C_{ww}, A_w, C_{lw}, A_l, C_{wt}, A_{wt}, C_{lr}, A_{lr}, \alpha, \theta) := \frac{d}{dC_{wt}} Q(K_z, V, G, C_{ww}, A_w, C_{lw}, A_l, C_{wt}, A_{wt}, C_{lr}, A_{lr}, \alpha, \theta)$$

$$a_{12_sw} := a_{12}(\mu_{K_z}, \mu_V, \mu_G, \mu_{C_{ww}}, A_w, \mu_{C_{lw}}, A_l, \mu_{C_{wt}}, A_{wt}, \mu_{C_{lr}}, A_{lr}, \alpha, \theta) = 10342.23$$

$$a_{13}(K_z, V, G, C_{ww}, A_w, C_{lw}, A_l, C_{wt}, A_{wt}, C_{lr}, A_{lr}, \alpha, \theta) := \frac{d}{dC_{lr}} Q(K_z, V, G, C_{ww}, A_w, C_{lw}, A_l, C_{wt}, A_{wt}, C_{lr}, A_{lr}, \alpha, \theta)$$

$$a_{13_sw} := a_{13}(\mu_{K_z}, \mu_V, \mu_G, \mu_{C_{ww}}, A_w, \mu_{C_{lw}}, A_l, \mu_{C_{wt}}, A_{wt}, \mu_{C_{lr}}, A_{lr}, \alpha, \theta) = -10342.23$$

Compute the standard deviation of the performance function at the mean values of the random variables:

$$\sigma_{sw} := \sqrt{a_{1_sw}^2 \cdot \sigma_{C1}^2 + a_{2_sw}^2 \cdot \sigma_{C2}^2 + a_{3_sw}^2 \cdot \sigma_{L5w}^2 + a_{4_sw}^2 \cdot \sigma_{R5w}^2 + a_{5_sw}^2 \cdot \sigma_{Lgp}^2 + a_{6_sw}^2 \cdot \sigma_{Rgp}^2 + a_{7_sw}^2 \cdot \sigma_{Kz}^2 + \dots + a_{8_sw}^2 \cdot \sigma_V^2 + a_{9_sw}^2 \cdot \sigma_G^2 + a_{10_sw}^2 \cdot \sigma_{Cww}^2 + a_{11_sw}^2 \cdot \sigma_{Clw}^2 + a_{12_sw}^2 \cdot \sigma_{Cwt}^2 + a_{13_sw}^2 \cdot \sigma_{Clr}^2}$$

$$\sigma_{sw} = 8009.589$$

Calculate the FOSM-MV reliability index for wood shear walls perpendicular to the roof ridge at hour 13:

$$\beta_{sw} = \frac{\mu_g}{\sigma_{sw}} = 2.382$$

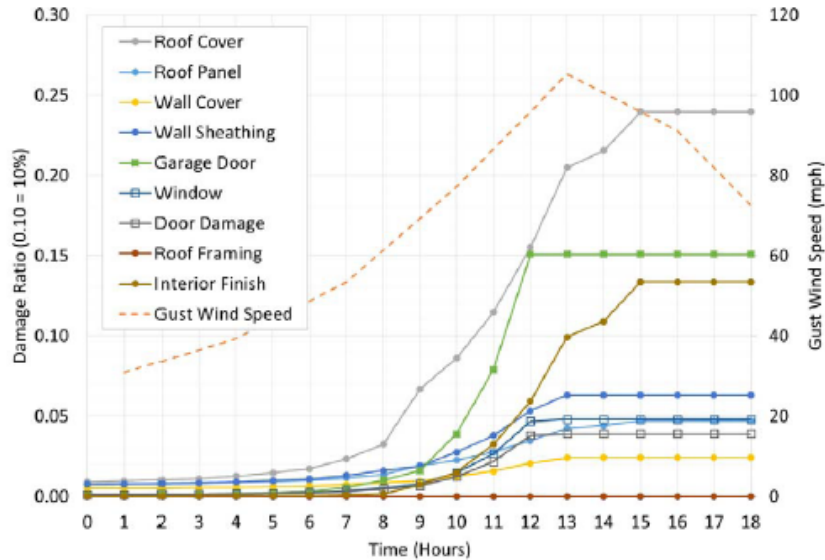
Determine the probability of failure for wood shear walls perpendicular to the roof ridge at hour 13:

$$P_{sw} := \text{pnorm}(-\beta, 0, 1) = 0.009$$

The reliability index is used as an input in the standard normal distribution.

Remark: The shear wall limit state is used as one of the tests for likelihood of structural collapse due to wind. In this case, the probability of shear wall failure perpendicular to the ridge at hour 15 is 0.9%. The maximum probability of failure for the limit states of wall stud bending, stud-to-plate connection, and shear wall failure are used to represent the probability of collapse due to wind.

Performing the Wind Damage Module calculations for all time steps, and adding up the damage to each area on the sample building for all of the considered components yields the following time history of wind damage:



Hour	Roof Cover	Roof Panel	Wall Cover	Wall Panel	Windows	Doors	Garage Door	Roof Frame	Interior	Wind Collapse Probability
0	0.9%	0.8%	0.5%	0.8%	0.1%	0.1%	0.1%	0.0%	0.0%	1.1%
1	1.0%	0.8%	0.5%	0.8%	0.1%	0.1%	0.1%	0.0%	0.0%	1.1%
2	1.0%	0.8%	0.5%	0.8%	0.1%	0.1%	0.1%	0.0%	0.0%	1.1%
3	1.1%	0.8%	0.5%	0.8%	0.1%	0.1%	0.1%	0.0%	0.0%	1.2%
4	1.3%	0.9%	0.6%	0.9%	0.2%	0.2%	0.2%	0.0%	0.0%	1.2%
5	1.5%	0.9%	0.6%	1.0%	0.2%	0.2%	0.2%	0.0%	0.0%	1.3%
6	1.7%	1.0%	0.7%	1.1%	0.2%	0.2%	0.3%	0.0%	0.1%	1.4%
7	2.3%	1.2%	0.7%	1.3%	0.3%	0.3%	0.6%	0.0%	0.1%	1.6%
8	3.3%	1.4%	0.9%	1.6%	0.5%	0.5%	1.0%	0.0%	0.2%	1.8%
9	6.7%	1.9%	0.9%	1.9%	0.8%	0.7%	1.6%	0.0%	0.7%	2.1%
10	8.6%	2.3%	1.2%	2.8%	1.5%	1.2%	3.9%	0.0%	1.5%	2.6%
11	11.5%	2.8%	1.6%	3.8%	2.7%	2.2%	7.9%	0.0%	3.3%	3.3%
12	15.5%	3.5%	2.1%	5.3%	4.7%	3.8%	15.1%	0.0%	5.9%	4.2%
13	20.5%	4.3%	2.4%	6.3%	4.8%	3.9%	15.1%	0.0%	9.9%	3.7%
14	21.5%	4.4%	2.4%	6.3%	4.8%	3.9%	15.1%	0.0%	10.9%	3.3%
15	24.0%	4.7%	2.4%	6.3%	4.8%	3.9%	15.1%	0.0%	13.4%	2.9%
16	24.0%	4.7%	2.4%	6.3%	4.8%	3.9%	15.1%	0.0%	13.4%	2.4%
17	24.0%	4.7%	2.4%	6.3%	4.8%	3.9%	15.1%	0.0%	13.4%	1.9%
18	24.0%	4.7%	2.4%	6.3%	4.8%	3.9%	15.1%	0.0%	13.4%	1.6%

B – Expert Panel CVs



From Left to Right: Douglas A. Smith, Ph.D., P.E., F. ASCE, Texas Tech University; James R. (Bob) Bailey, Ph.D., P.E., F. ASCE, Exponent, Inc. [Chair]; William (Bill) Coulbourne, P.E., F. ASCE, Coulbourne Consulting; Andrew Kennedy, Ph.D., M. ASCE, University of Notre Dame; Samuel D. Amoroso, Ph.D., P.E., S.E., M. ASCE, Forte and Tablada, Inc.

James R. (Bob) Bailey, Ph.D., P.E., F. ASCE [Chair]
Senior Managing Engineer
Houston Office Director
Exponent, Inc.

Professional Profile

Dr. James R. (Bob) Bailey is a licensed Professional Engineer and Fellow of the American Society of Civil Engineers. For over 30 years, Dr. Bailey has served as a technical consultant, project manager, and researcher for private industry, universities, and government. As a Senior Managing Engineer in Exponent's Building & Structures practice, he brings specialized expertise to areas related to wind engineering, construction materials, solid mechanics, dynamics, numerical analysis, structural analysis and design, and materials testing.

Dr. Bailey's primary area of expertise is determining the risk exposure of residential, commercial, and industrial properties to hazards associated with hurricanes, tornadoes, and flooding. He has conducted hurricane risk assessments and developed mitigation programs for various types of health, industrial, educational, and offshore energy facilities. Over the past 15 years he has conducted field surveys to document storm damage in the aftermath of hurricanes Irene (1999), Charley (2004), Francis (2004), Katrina (2005), Rita (2005), Wilma (2005), Ike (2008), and Sandy (2012), Tropical Storm Allison (2001), the Oklahoma City Tornado (1999), and the April-May 2011 Tornado Outbreak.

Dr. Bailey's past work at ExxonMobil included estimating wind loads on drilling structures, developing conceptual designs of gravity-based structures for arctic offshore environments, and conducting research and teaching classes on well cementing. He also has extensive experience working with FEMA under the Public Assistance Program following Tropical Storm Allison (2001–2004), and Hurricane Katrina in Louisiana (2005) and Hurricane Rita in Texas (2005–2006). Dr. Bailey recently conducted an analysis of the storm surge risk posed to the South Texas Project Electric Generating Station using advanced hydrodynamic modeling techniques, and subsequently presented the results to the NRC.

Dr. Bailey has served as a lecturer in the private sector and at the university level on subjects related to wind and petroleum engineering. He also has been responsible for the design of test facilities and the development of test programs related to construction and energy. Dr. Bailey is currently the Presiding Officer of a five member expert panel, appointed by the Texas Department of Insurance in 2013, whose purpose is to develop ways of determining whether a loss to TWIA-insured property was caused by wind, waves, or tidal surges. He is also a member of the ASCE 7-16 Wind Load Subcommittee. He is past Chair of the ASCE Petrochemical Wind Load Task Committee, and served on an API 4F sub-committee assigned to revise specifications and guidelines for determining wind loads on onshore and offshore drilling structures.

Academic Credentials and Professional Honors

Ph.D., Civil Engineering, Texas Tech University, 1989
M.S., Civil Engineering, Texas Tech University, 1984
B.S., Civil Engineering, Texas Tech University, 1982
American Society of Civil Engineers (ASCE)
American Petroleum Institute (API) Spec 4F Wind Engineering Subcommittee
ASCE Wind Loads on Petrochemical Structures Task Committee
ASCE 7-16 Wind Load Subcommittee
Texas Tech University Civil Engineering Advisory Council (2007–2012)

Licenses and Certificates

Professional Engineer, State of Florida, #67773
Professional Engineer, State of Georgia, #PE033027
Professional Engineer, State of Hawaii, #12820
Professional Engineer, State of Louisiana, #33830
Professional Engineer, State of Mississippi, #26488
Professional Engineer, State of South Carolina, #26408
Professional Engineer, State of Tennessee, #114185
Professional Engineer, State of Texas, #74911
Professional Engineer, State of Wisconsin, #42337-6

Patents

Patent No. 5,309,995: Well Treatment Using Ball Sealers, issued May 10, 1994.
Patent No. 5,485,882: Low-density Ball Sealer for Use as a Diverting Agent in Hostile Environment Wells, issued January 23, 1996.
Patent No. 5,582,251: Downhole Mixer, issued December 19, 1996.

Prior Professional Experience

Manager, Extreme Loads and Structural Risk Division, ABS Consulting (formerly EQE International), 2004–2006.
Senior Project Engineer, Extreme Loads and Structural Risk Division, ABS Consulting (formerly EQE International), 2001–2004.
Project Engineer, Extreme Loads and Structural Risk Division, ABS Consulting (formerly EQE International), 1998–2001.
Engineering Specialist, Offshore Division, ExxonMobil Upstream Research Center (formerly Exxon Production Research Company), 1994–1998.
Senior Project Engineer, Drilling and Completions Division, ExxonMobil Upstream Research Center (formerly Exxon Production Research Company), 1992–1994.
Project Engineer, Drilling and Completions Division, ExxonMobil Upstream Research Center (formerly Exxon Production Research Company), 1990–1992.
Lecturer and Research Associate, Civil Engineering Department, Texas Tech University, 1989–1990.

Samuel D. Amoroso, Ph.D., P.E., S.E.
Technical Practice Leader
Forte and Tablada, Inc.

Education

Ph.D. in Civil Engineering – December 2007 (Louisiana State University, Baton Rouge, Louisiana)
B.S. in Civil Engineering – May 1999 (Louisiana State University, Baton Rouge, Louisiana)

Professional Licensure

NCEES 16-hour Structural Engineering Exam – April 2012
Professional Engineering Registration in LA, TX, MS, VA, and FL

Experience

Technical Practice Leader Jun. 2006 – present
Forte and Tablada, Inc., Baton Rouge, LA (Formerly Engensus, LLC)
Experience has included structural design for buildings and civil infrastructure, hurricane and wind risk research and consulting, and the investigation of hurricane and other storm damage.

Adjunct Instructor Aug. 2008 – present
Louisiana State University, Dept. of Civil and Environmental Engineering – Baton Rouge, LA
Part-time instructor CE 2700, “Introduction to Civil Engineering” (current) and CE 3400, “Mechanics of Materials” (prior).

Graduate Fellow Aug. 2003 – Dec. 2006
Louisiana State University, Dept. of Civil and Environmental Engineering – Baton Rouge, LA
Wind tunnel experiments and research related to the wind loading of industrial/petrochemical structures.

Part-Time Structural Engineer May 2005 – Aug. 2005 & Jan. 2006 – Mar. 2006
Gulf Engineers and Consultants, Baton Rouge, LA
Design and detailing of structures supporting variable message signs in high-wind regions and a study of a sign support structure on the I-10 Mississippi River Bridge to determine fatigue damage mechanisms and develop alternative details.

Engineer II May 1999 – July 2003
HNTB Corporation, San Antonio, TX
Structural engineering design on a wide variety of transportation projects.

Selected Publications

Wong, S., Sepaha, A., Swamy, N., Amoroso, S., and Naqvi, D., “Wind loads on non-building structures using ASCE 7-10,” proceedings of the ASCE/SEI 2012 Structures Congress, Chicago, March 2012.

- Amoroso, S. and Levitan, M., "Wind loads for high-solidity open-frame structures," *Wind and Structures, an International Journal*, V. 14, No. 1, 2011.
- Amoroso, S., Hebert, K., Levitan, M., "Wind tunnel tests for mean wind loads on partially clad structures," *Journal of Wind Engineering and Industrial Aerodynamics*, V. 98, No. 12, pp. 689-700, December 2010.
- Amoroso, S., Levitan, M., "Wind Load Analysis Uncertainty for Petrochemical Structures," 11th Americas Conference on Wind Engineering, San Juan, Puerto Rico, June 2009.
- Amoroso, S., "Benefit Cost Analysis for Wind Hazard Mitigation," *Louisiana Civil Engineer, Journal of the Louisiana Section of the American Society of Civil Engineers*, v. 17, no. 3, May 2009.
- Amoroso, S. and Coco, R., "Effective Forensic Engineering Investigations of Hurricane 'Wind vs. Water' Disputes: Techniques and Tools," *Proceedings of the ASCE/SEI 2008 Structures Congress*, Vancouver, B.C., April 2008.
- Amoroso, S. and Levitan, M., "Recent research into wind loads on industrial structures," 12th International Conference on Wind Engineering, Cairns, Australia, July 2007.
- Amoroso, S., Hebert, K., Levitan, M., "Wind tunnel tests on partially clad buildings and structures," 4th European and African Conference on Wind Engineering, Prague, July 2005.
- Amoroso, S. D. and Gurley K. R. "Chapter 5: Response of Structures to Wind, Storm Surge, Flood, and Waves," *Engineering Investigations of Hurricane Damage: Wind versus Water*, edited by Peraza, Coulbourne and Griffith, American Society of Civil Engineers, Reston VA, 2014.
- "Chapter 2: Background," *Wind Loads for Petrochemical and Other Industrial Structures*, American Society of Civil Engineers, Reston, VA, 2011.

Selected Presentations

- Amoroso, S., "Seismic Design Basics for Buildings," Louisiana ASCE Spring Conference, Shreveport, LA, April 2013.
- Amoroso, S., "Recent Updates to the Seismic Design Requirements for Buildings in Louisiana," Louisiana Civil Engineering Conference and Show, Kenner, LA, September 2012.
- Amoroso, S. and VanDreumel, B., "The Development of Insurance Premium Discounts for Wind Hazard Mitigation," Louisiana Civil Engineering Conference and Show, Kenner, LA, September 2009.
- Amoroso, S., "Benefit Cost Analysis for Wind Hazard Mitigation," Louisiana Civil Engineering Conference and Show, Kenner, LA, September 2008.
- Amoroso, S., "Determining Building Wind Loads Using ASCE/SEI 7-05: An Overview," National Hurricane Conference, Orlando, FL, March 2008.

Organizations, Activities, Service

- American Society of Civil Engineers (ASCE) Baton Rouge Branch: Program Director (2012-2013), Education Director (2008 – 2012), and LSU Practitioner Advisor (2007 – 2011).
- Advised a technical committee of the LA State Uniform Construction Code Committee regarding proposed state exceptions to the seismic provisions of the International Building Code (2011 – 2012).
- ASCE Task Committees which published the guide publications, *Wind Loads for Petrochemical Facilities* and *Engineering Investigations of Hurricane Damage*.

William L. Coulbourne, P.E.
Structural Engineering Consultant
Coulbourne Consulting

Mr. Coulbourne has more than 45 years of experience as an engineer and manager. His expertise includes building design, methods, materials, and codes. He is experienced in hazard-related design and construction of wind- and hurricane-resistant structures. He has performed structural inspections and building investigations on thousands of structures to assess past or future performance during a natural hazard event. He has performed structural inspections, and reported on the integrity of major structural elements, conducted risk and vulnerability assessments for education and hospital campuses and written reports and books related to designs for natural hazards. He has participated in or managed the effort of investigations related to ten hurricanes, three major flood events, four major tornadoes and a building collapse caused by terrorists. He develops structural designs for clients located in high wind and storm surge areas.

Mr. Coulbourne has inspected residential and commercial structural failures in foundations and framing systems. Mr. Coulbourne has written articles and given presentations for homebuilders, engineers, architects and homeowners on high wind and flood design and construction issues related to natural hazard design. He has consulted with federal, state and local governments, universities, and other engineering and architectural firms on wind and flood-related issues. He teaches courses for FEMA, ASCE and private education provider organizations on high-wind and flood design. He is a member of the American Society of Civil Engineers standards committees for ASCE 7 Minimum Design Loads for Buildings and Other Structures, ASCE 24 Flood Resistant Design and Construction, and a new ASCE standard on EF Scale Estimation of Tornado Wind Speeds.

Education and Certifications

M.E. / 1999 / Structural Engineering – University of Virginia
B.S. / 1968 / Civil Engineering – Virginia Tech
Certifications in Structural Engineering and Building Inspection Engineering
Registered Professional Engineer: Maryland, Virginia, Delaware

Consulting Projects

- Expert Witness in Floodproofing Case, US Attorney.
- International Masonry Institute, SC. on tornado wind design principles to use for masonry.
- FEMA Coastal Formula Development, Nationwide.
- Elevated Foundation Designs, NJ. Started a Joint Venture providing engineering design services for elevated foundations for residential buildings.
- Peer Review of Tower Wind Speed Analysis, Nationwide.
- Windspeed Web Site development, ATC, Redwood City, CA.
- Floodproofing Industrial Site, NJ. Consultation to a large industrial developer.
- Led Hurricane Sandy Urban Flood Study for ASCE.

- Consulted on Floodproofing Non-Residential Structures guide for FEMA.
- Conducted a Floodwall Failure Investigation in Binghamton, NY.
- Conducted Critical Facility Vulnerability Assessments in Texarkana, TX., Campus-wide Vulnerability Assessment, Eckerd College, St. Petersburg, FL, and a Hospital Vulnerability Assessment, Jacksonville, FL
- Flood proofing and wind engineering consultant, LAHouse, LSU Campus, Baton Rouge, LA.
- Conducted a Sea Level Rise Vulnerability Assessment for Somerset County, MD.
- Developed prescriptive foundations for raised-floor systems for Southern Forest Products Association, Kenner, LA.

Experience and Publications

- Hurricane Katrina Mitigation Assessment Team Report (FEMA 549)
- Recommended Residential Construction for the Gulf Coast: Building on Strong and Safe Foundations (FEMA 550)
- Critical Facilities Design Guide (FEMA 543)
- Hurricane Charley Mitigation Assessment Team Report (FEMA 488)
- Hurricane Ivan Mitigation Assessment Team Report (FEMA 489)
- World Trade Center Building Performance Study (FEMA 403)
- Building Performance Assessment, May 3, 1999 Tornadoes in Oklahoma and Kansas
- Design & Construction Guidance Manual for Community Shelters (FEMA 361)
- Shelter inspection projects in FL, NC, SC, DE, MD, AL, MS
- Tornado Investigations in Tuscaloosa, AL and Joplin. MO 2011
- Coastal Construction Manual (FEMA 55 3rd Edition)
- In-Residence Shelter Design, (FEMA 320)
- Hurricane Sandy Mitigation Assessment Team Report (FEMA P-942)
- ATC Basic Wind Engineering for Low-Rise Buildings (ATC Design Guide 2)
- ASCE Press: Wind Loads: Guide to the Wind Load Provisions of ASCE 7-05
- ASCE Press: Wind Loads: Guide to the Wind Load Provisions of ASCE 7-10
- ASCE Press: Hurricane Damage Investigations: Wind vs. Water
- ASCE Press: Moore, OK Tornado of 2013, Performance of Schools and Critical Facilities

Affiliations

National Society of Professional Engineers, Virginia Society of Professional Engineers, Delaware Society of Professional Engineers, National Academy of Building Inspection Engineers, Fellow – Director and Past President, Association of State Floodplain Managers – Member, American Association of Wind Engineers – Board of Directors, American Society of Civil Engineers – Fellow, Structural Engineering Institute (ASCE), Fellow, ABET, Executive Committee Member for Engineering Accreditation Commission, Florida International University “Wall of Wind” Technical Advisory Committee.

Andrew Kennedy**Department of Civil & Environmental Engineering & Earth Sciences
University of Notre Dame**Professional Preparation

Queen's University, Kingston Civil Engineering, BScE 1991
U. of British Columbia, Vancouver Civil Engineering, MASc 1993
Monash University, Melbourne Mechanical Engineering, PhD 1998
University of Delaware, Newark Civil Engineering, Postdoc 1997-2001

Appointments

Associate Professor, Department of Civil & Environmental Engineering & Earth Sciences,
University of Notre Dame, May 2013-present.
Assistant Professor, Department of Civil & Environmental Engineering & Earth Sciences,
University of Notre Dame, January 2008-May 2013.
Assistant Professor, Department of Civil and Coastal Engineering, University of Florida, August
2001-December 2007.
Postdoctoral Fellow, Ocean Engineering Laboratory, University of Delaware, July 1997-July 2001.
Commonwealth Fellow, Monash University, March 1994-June 1997.

Ten Relevant Journal Papers (of 51)

Kennedy, A.B., Rogers, S., Sallenger, A., Gravois, U., Zachry, B., Dosa, M., and Zarama, F. (2011).
"Building Destruction from Waves and Surge on the Bolivar Peninsula during Hurricane Ike,"
J. Waterway, Port, Coastal and Ocean Eng.-ASCE, 137, 132-141,
doi:10.1061/(ASCE)WW.1943-5460.0000061.

Tomiczek, T., Kennedy, A.B., and Rogers, S.P. (2014). "Collapse limit state fragilities of wood-
framed residences from storm surge and waves during Hurricane Ike", J. Waterway, Port,
Coastal and Ocean Eng.-ASCE, 140(1), 43-55.

Taflanidis, A.A., Kennedy, A.B., Westerink, J.J., Smith, J., Cheung, K.F., Hope, M., and Tanaka, S.
(2013). "Rapid assessment of wave and surge risk during landfalling hurricanes; a
probabilistic approach", J. Waterway, Port, Coastal and Ocean Eng.-ASCE, 139(3), 171-182.

Kennedy, A.B., Chen, Q., Kirby, J.T., and Dalrymple, R.A. (2000). "Boussinesq modeling of wave
transformation, breaking and runup. I: 1D" J. Waterway, Port, Coastal and Ocean Eng.-ASCE,
126, 39-47.

Kennedy, A.B., Westerink, J.J., Smith, J.M., Hope, M.E., Hartman, M., Taflanidis, A.A., Tanaka, S.,
Westerink, H., Cheung, K.F., Smith, T., Hamann, M., Minamide, M., Ota, A., and Dawson, C.
(2012). "Tropical cyclone inundation potential on the Hawaiian Islands of Oahu and Kauai",
Ocean Modelling, 52-53, 54-68. doi:10.1016/j.ocemod.2012.04.009.

Kennedy, A.B., Dietrich, J.C., and Westerink, J.J. (2013). "The surge standard for 'Events of
Katrina Magnitude'". Proc. Nat. Acad. Sci. USA, (Letter to the Editor), 110(29), E2665-E2666,
doi:10.1073/pnas.1305960110.

Hope, M., Westerink, J.J., Kennedy, A.B., Kerr, P., Dietrich, J.C., Dawson, C., Bender, C.J., Smith,
J., Jensen, R., Zijlema, M., Holthuijsen, L., Luettich, R., Powell, M., Cardone, V., 2

- Cox, A.T., Pourtaheri, H., Roberts, H., Atkinson, J., Tanaka, S., Westerink, J., and Westerink, L. (2013). "Hindcast and Validation of Hurricane Ike (2008) Waves, Forerunner, and Storm Surge", *J. Geophys. Res.-Oceans*, 118, 4424-4460, doi:10.1002/jgrc.20314.
- Kennedy, A.B., Gravois, U., Zachry, B., Luettich, R., Whipple, T. Weaver, R., Reynolds-Fleming, J. Chen, Q., and Avissar, R. (2010). "Rapidly installed temporary gauging for waves and surge, and application to Hurricane Gustav", *Continental Shelf Research* 30, 1743-1752.
- Kennedy, A.B., Gravois, U., Zachry, B.C., Westerink, J.J., Hope, M.E., Dietrich, J.C., Powell, M.D., Cox, A.T., Luettich, R.L., and Dean, R.G. (2011). "Origin of the Hurricane Ike forerunner surge", *Geophys. Res. Lett.*, L08805, doi:10.1029/2011GL047090.
- Dietrich, J.C., Westerink, J.J., Kennedy, A.B., Smith, J.M., Jensen, R., Zijlema, M., Holthuijsen, L.H., Dawson, C., Luettich, R.A., Powell, M.D., Cardone, V.J., Cox, A.T., Stone, G.W., Pourtaheri, H., Hope, M.E., Tanaka, S., Westerink, L.G., Westerink, H.J., and Cobell, Z. (2011). "Hurricane Gustav (2008) waves, storm surge, and currents: Hindcast and synoptic analysis in southern Louisiana", *Monthly Weather Review*, 139, 2488-2522.

Synergistic Activities

Reviewer for: 28 journals, funding agencies and publishers
 Assistant Editor: Journal of Waterway, Port, Coastal and Ocean Engineering
 Technical Review Panel: State of Texas Expert Panel
 Recent Conference Organizing/Technical Committees: ATC-SEI Conference, 2012; 3rd International Symposium on Shallow Flows, 2012, AGU Nearshore Processes, 2012; Coastal Structures/Solutions to Coastal Disasters 2015. Board of Directors: Applied Technology Council.

Graduate Advisors (2) and Postdoctoral Sponsors (2)

Michael Isaacson, University of British Columbia; John Fenton, Monash University; James Kirby, University of Delaware, Tony Dalrymple, Johns Hopkins University.

Thesis Advisor (16) and Postgraduate-Scholar Sponsor (1)

David Thomas, unknown; Enrique Guttierrez, unknown; Eileen Czarnecki, Moffatt and Nichol; Kristin Odronic, Taylor Engineering; Yang Zhang, Halcrow; Oleg Mouraenko, Moffat and Nichol; Rumana Arifin, Notre Dame; Brian Hoesman, Taylor Engineering; Weiming Li, Halliburton; Yao Zhang, China; Victoria Tomiczek, Notre Dame; Michael Hartman, Notre Dame; Margaret Owensby, Notre Dame; Mei Huang, Notre Dame; Luning Sun, Notre Dame.

Douglas A. Smith, Ph.D., P.E.

**Department of Civil, Environmental, and Construction Engineering
Texas Tech University**

Education

Texas Tech University, Ph.D. in Civil Engineering, Minor in Statistics, May 1993

Texas Tech University, M.S. in Civil Engineering, August 1979

Texas Tech University, B.S. in Civil Engineering, December 1977

Professional Licensure

Registered Professional Engineer: Texas (#54301), Mississippi (#17663)

Experience

Academic

Associate Professor, Department of Civil Engineering, 9/2003 to present

Assistant Professor, Department of Civil Engineering, 9/1998 to 9/2003

Research Assistant Professor, Wind Engineering Research Center, Department of Civil Engineering, 8/1994 to 9/1998

Non-Academic

Senior Structural Engineer, Utility Engineering Corporation, Amarillo, Texas, 1/1988 to 1/1990

Supervisory Structural Engineer, Southwestern Public Service Company, Amarillo, Texas, 9/1983 to 12/1987

Structural Engineer, Southwestern Public Service Company, Amarillo, Texas, 9/1979 to 8/1983

Research Assistant/Graduate Student, Institute for Disaster Research, Texas Tech University, Lubbock, Texas, 1/1978 to 8/1979

Graduate Faculty Appointments

Texas Tech University, June, 1995 – present

Colorado State University, November, 1995 – 2000

Professional Short Courses and Invited Lectures

Engineering for Extreme Winds, Short Course at TTU (1995, 1996, 1997, 1998, 1999, 2000, 2001, 2002, 2003, 2004, 2005)

ASCE Wind Loads short course, Dallas, TX, 18-19 November 1999, Orlando FL. 22-23 September, 2005; West Palm Beach FL August 17-18, 2006

Wind Effects on Roofing, Corps of Engineers, Belton, TX, May 1997

DOE Natural Phenomena Workshop, Arlington, VA, 1995 (60 participants)

Wind Engineering Research, Short Course at Texas Section ASCE Meeting in Lubbock, TX, 1994

Georgia Emergency Management Agency training sessions for emergency managers on assessing performance of essential facilities in hurricanes, Moultrie, GA; Warner Robbins, GA; Savannah, GA; Augusta, GA; Clarksville, GA; Jasper, GA, August - October 1998; Brunswick, GA, February 2001

Presentation "Application for Wind Damage Prediction." Georgia Emergency Management Agency, Jekyll Island, Georgia. (1998).

Presentation "Variability in design wind loads." Lubbock County National Weather Service. (1999).

Presentation "Application for Wind Damage Prediction." RICOWI, Las Vegas, Nevada. (2004).

Presentation "WISE Facilities & Capabilities, TTU Full Scale Testing." Florida International University. (2007).

Presentation "Application for Wind Damage Prediction." Orange County National Weather Service. (2004).

Keynote Address, Workshop on Wind Disaster Problems-Challenges Ahead, Royal School of Engineering and Technology, Guwahati, Assam, India, "THE ROLE OF FULL SCALE OBSERVATIONS AND TESTING IN MITIGATING WIND DAMAGE," International. (February 22, 2013).

Presentation., Workshop on Wind Disaster Problems - Challenges Ahead, Royal School of Engineering and Technology, Guwahati, Assam, India, "Constructing Probable Wind and Water Damage Sequences from." (February 22, 2013).

Professional Development Activities

ASCE Leadership Conference, 1996

Teaching the Teacher Workshop: Teaching Engineering Faculty to Teach in an Active Learning Environment; A four-day workshop on improving teacher effectiveness, 2000

NATO, Advanced Study Institute, Wind Climate in Cities, 2 week course in Wind Engineering (1993)

Professional Committee Activities

ASCE 7 Task Committee on Wind Loads, 2001-present

Organizing Committee, 10th International Conference on Wind Engineering, 2001- 2003

Publications Committee, 10th International Conference on Wind Engineering, 2001- 2003

American Association of Wind Engineering Organizing Committee, America's Conference on Wind Engineering, 1999-2001

ASCE- Computer-aided Wind Engineering Subcommittee, 1998-1999

ASCE-Wind Effects Committee of ASCE, 1994-1999, Organized Session on Wind Effects on Low Rise Buildings (Structures Congress, 1996)

Texas Section ASCE, Caprock Branch, Vice President/Treasurer (1995-1996), President (1996-1997), Past-President (1997-1998); Board of Directors (1999-2001)

Chairman of the ASCE Texas Section Structural Division, 1988

American Association for Wind Engineering (Board of Directors 2007 - present, Member)

American Society of Civil Engineers (Member)

American Institute for Steel Construction (Member)

Structural Engineers Association of Texas (Member)

C – Sensitivity Analysis of Failure Probability Calculation Techniques

The proposed methodology for the Damage Estimation Module was developed and demonstrated using the First-Order, Second-Moment, Mean Value Reliability Index (FOSM-MV) as the technique for calculating component and structural system failure probabilities. This technique is one of several available techniques for computing failure probabilities once a performance function is formulated and the summary statistics for the contributing random variables have been established. Other available techniques include the Rackwitz-Fiessler Procedure and Monte Carlo Simulation.

The FOSM-MV Reliability Index uses the first-order terms in a Taylor Series expansion of the performance function. It relies only on the mean values and standard deviations of the random variables contributing to the performance function. The Taylor Series approximation of the performance function is expanded about the mean values of the random variables.

The FOSM-MV Reliability Index is easy to use and program. It does not require knowledge of the distribution types for the contributing random variables. However, the accuracy of the method can be affected if the random variable distributions deviate significantly from normal distributions, or if the performance functions are highly non-linear. The results of the method can also vary for different, but apparently equivalent, formulations of the performance function.

The Rackwitz-Fiessler Procedure is an iterative approach to computing the reliability index. It is more complicated to implement than the FOSM-MV Reliability Index, but it has the advantage of better accommodation of non-linear performance functions and random variables with non-normal probability distributions. The technique is also insensitive to the formulation of the performance function.

Monte Carlo Simulation (MCS) is the most versatile technique, but executing it requires much more computational effort and resources. In this technique, a value of each of the random variables in the performance function is randomly sampled according to its particular probability distribution. The performance function is evaluated using the sampled values. This step constitutes one simulation. The process is repeated many

times until a stable rate of failure is established (i.e. how often the value of the performance function is less than or equal to zero).

The number of repetitions required using MCS depends on the desired resolution of the resulting failure probability, and the acceptable variance between the estimate provided by the technique and the true value. It is common for tens of thousands of individual simulations to be conducted for a simple structural reliability analysis. However, the technique can accommodate performance functions of arbitrary complexity and can handle any type of probability distribution.

Regarding the proposed methodology as presented in Section 6, a sensitivity analysis was conducted to determine whether the limitations associated with the FOSM-MV technique will have appreciable practical impacts on the results of the failure probability calculations. Roof cover damage results using the FOSM-MV technique were compared to results using MCS for a variety of wind speeds and structure characteristics, as follows:

- Three different time histories of wind speed were used, with the difference being the magnitude of the peak wind speed (85 mph, 100 mph, and 115 mph). The variation of wind direction with time was not changed. The time history for a peak wind speed of 85 mph is shown in Figure C-1.
- Four different structure scenarios were analyzed: a base case, plus three more cases in which roof slope, terrain exposure, and structure primary axis were varied. Figure C-2a through Figure C-2d show the structure characteristics for the four scenarios.

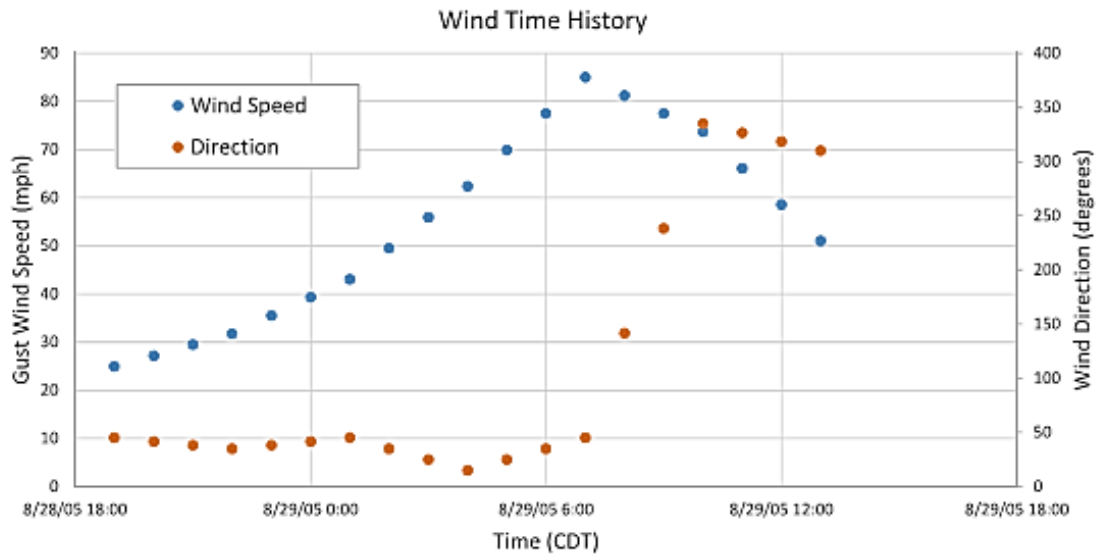


Figure C-1: Wind Speed and Direction Time History shown for a peak wind speed of 85 mph.

Structure Input	Scenario 1 Characteristics		
Roof Shape	Gable		
Length	60	feet	(parallel to ridge)
Width	35	feet	(perpendicular to ridge)
Plate Height	8	feet	
Eave Height	20	feet	
Roof Slope	6	:12	26.56505 degrees
Roof Height	24.38	feet	28.75 ridge height
Number of Stories	1		Living Space, not including area under elevated first floor
Structure Primary Axis	0	degrees	(orientation of ridge with respect to North = 0 degrees)
Terrain Exposure	B		ASCE 7 Category
Overhead Garage Door Type	Roll-Up		
Roof Cover Type	Asphalt Shingle (Unknown Classification)		
Roof Cover Age	10	years	
Wall Cover Type	Vinyl Siding		
Direction of Garage Door	90	degrees	90 Garage Relative Angle, Degrees
Garage Panel Door Width	Single		
Garage Attached?	Yes		
Window Type	Non-Impact Resistant		
Percent Window Area	25-50	Percent	0.375
Door Type	Non-Impact Resistant		
Opening Protection	No		
Age of Structure	10	years	

Figure C-2a: Structure Scenario 1

Structure Input	Scenario 2 Characteristics		
Roof Shape	Gable		
Length	60	feet	(parallel to ridge)
Width	35	feet	(perpendicular to ridge)
Plate Height	8	feet	
Eave Height	20	feet	
Roof Slope	4	:12	18.43495 degrees
Roof Height	22.92	feet	25.83333 ridge height
Number of Stories	1		Living Space, not including area under elevated first floor
Structure Primary Axis	0	degrees	(orientation of ridge with respect to North = 0 degrees)
Terrain Exposure	C		ASCE 7 Category
Overhead Garage Door Type	Roll-Up		
Roof Cover Type	Asphalt Shingle (Unknown Classification)		
Roof Cover Age	10	years	
Wall Cover Type	Vinyl Siding		
Direction of Garage Door	90	degrees	90 Garage Relative Angle, Degrees
Garage Panel Door Width	Single		
Garage Attached?	Yes		
Window Type	Non-Impact Resistant		
Percent Window Area	25-50	Percent	0.375
Door Type	Non-Impact Resistant		
Opening Protection	No		
Age of Structure	10	years	

Figure C-2b: Structure Scenario 2

Structure Input	Scenario 3 Characteristics		
Roof Shape	Gable		
Length	60	feet	(parallel to ridge)
Width	35	feet	(perpendicular to ridge)
Plate Height	8	feet	
Eave Height	20	feet	
Roof Slope	4	:12	18.43495 degrees
Roof Height	22.92	feet	25.83333 ridge height
Number of Stories	1		Living Space, not including area under elevated first floor
Structure Primary Axis	0	degrees	(orientation of ridge with respect to North = 0 degrees)
Terrain Exposure	D		ASCE 7 Category
Overhead Garage Door Type	Roll-Up		
Roof Cover Type	Asphalt Shingle (Unknown Classification)		
Roof Cover Age	10	years	
Wall Cover Type	Vinyl Siding		
Direction of Garage Door	90	degrees	90 Garage Relative Angle, Degrees
Garage Panel Door Width	Single		
Garage Attached?	Yes		
Window Type	Non-Impact Resistant		
Percent Window Area	25-50	Percent	0.375
Door Type	Non-Impact Resistant		
Opening Protection	No		
Age of Structure	10	years	

Figure C-2c: Structure Scenario 3

Structure Input	Scenario 4 Characteristics		
Roof Shape	Gable		
Length	60	feet	(parallel to ridge)
Width	35	feet	(perpendicular to ridge)
Plate Height	8	feet	
Eave Height	20	feet	
Roof Slope	4	:12	18.43495 degrees
Roof Height	22.92	feet	25.83333 ridge height
Number of Stories	1		Living Space, not including area under elevated first floor
Structure Primary Axis	45	degrees	(orientation of ridge with respect to North = 0 degrees)
Terrain Exposure	D		ASCE 7 Category
Overhead Garage Door Type	Roll-Up		
Roof Cover Type	Asphalt Shingle (Unknown Classification)		
Roof Cover Age	10	years	
Wall Cover Type	Vinyl Siding		
Direction of Garage Door	135	degrees	90 Garage Relative Angle, Degrees
Garage Panel Door Width	Single		
Garage Attached?	Yes		
Window Type	Non-Impact Resistant		
Percent Window Area	25-50	Percent	0.375
Door Type	Non-Impact Resistant		
Opening Protection	No		
Age of Structure	10	years	

Figure C-2d: Structure Scenario 4

For each of the four structure scenarios and each of the three wind speed time histories, the total roof cover damage was estimated using FOSM-MV; MCS with all random variables treated as normal (or Gaussian); and MCS with the GC_p variable treated as an Extreme Value Type I distribution. With the exception of the GC_p variable, all random variable statistics were as documented in Section 6. Each MCS analysis consisted of 20,000 simulations.

Comparing the FOSM-MV results to MCS simulations with all normal random variables should reveal whether performance function non-linearity has an appreciable effect on the FOSM-MV results. This comparison should also reveal whether there is an invariance problem associated with the formulation of the performance function for the FOSM-MV method.

Comparing the FOSM-MV results to the MCS simulation treating the GC_p variable as an Extreme Value Type I random variable should reveal whether neglecting to consider non-normal distributions has an appreciable effect of the FOSM-MV results. The parameters for the Extreme Value Type I distribution were established from the statistics tabulated in Section 6 using the following formulas:

$$\alpha \approx \frac{1.282}{\sigma_x} \quad (\text{Eq. C-1})$$

$$u \approx \mu_x - 0.45\sigma_x \quad (\text{Eq. C-2})$$

The maximum total roof cover damage ratios for each of the wind speed and direction time histories, for each of the structure scenarios, and for each technique are summarized in Table C-1. It is apparent from the table that only slight variations appear among results from the three methods. The results from all three methods are quite similar, and the FOSM-MV results are between the results from the two MCS simulations. For this case, little practical consequence results from the theoretical limitations associated with the FOSM-MV technique. A few reasons for this outcome are as follow.

**TABLE C-1: SENSITIVITY ANALYSIS RESULTS
ROOF COVER DAMAGE RATIOS**

Wind 85			
Scenario	FOSM-MV	MCS All Gaussian	MCS GCp - EV I
1	0.0572	0.0580	0.0515
2	0.0830	0.0842	0.0798
3	0.1180	0.1232	0.1125
4	0.0984	0.1006	0.0916

Wind 100			
Scenario	FOSM-MV	MCS All Gaussian	MCS GCp - EV I
1	0.1082	0.1111	0.1006
2	0.1589	0.1700	0.1526
3	0.2219	0.2310	0.2151
4	0.1907	0.1955	0.1840

Wind 115			
Scenario	FOSM-MV	MCS All Gaussian	MCS GCp - EV I
1	0.1875	0.1905	0.1816
2	0.2664	0.2720	0.2598
3	0.3543	0.3652	0.3466
4	0.3191	0.3267	0.3085

In general, structural reliability calculations incorporating wind loading are dominated by the influence of the wind speed variable. The wind speed variable is squared in the performance function. The probability distributions of annual extreme wind speeds are often characterized by Extreme Value Distributions of either Type I or Type III, where the mean values might be on the order of 40-50 mph, and the 100-500 year events might be on the order of 100-150 mph. However, the current application is not a general case.

The mean value of the wind speed will have been established in the hazard module. The randomness associated with the wind speed reflects only the variation between modeled and measured values, which may well be characterized by a normal distribution, rather than an extreme value distribution. Furthermore, the range of likely values for the wind speed is much smaller in the Damage Estimation Module than it would be in a general structural reliability calculation. In summary, the influence of the

wind speed variable is very much constrained in the current application, which reduces the variation among the three methods represented in the sensitivity analysis.

The FOSM-MV method relies on a first-order Taylor Series expansion of the performance function about the mean values of the random variables. Since only one of the variables in the roof cover performance function is non-linear (wind speed, which is a second order term), little accuracy is lost with this approximation. As such, it is not expected that the mild non-linearity of the roof cover performance function will have a great effect on the accuracy of the FOSM-MV results.

An Extreme Value Type I distribution for the GC_p variable has a mean value that is greater than the median or the mode, whereas the mean, median, and mode of corresponding normal distribution all have the same value. The Extreme Value Type I distribution must have a greater number of occurrences of low values to balance the influence of the small number of extremes. The practical impact of this difference is that the MCS results actually show a lower damage rate when the Extreme Value Type I distribution is used for the GC_p variable.

In conclusion, the results of this sensitivity analysis show that the theoretical limitations associated with the FOSM-MV technique for calculating component and structural system failure probabilities have little practical significance for the methodology as currently proposed.